Remote Sensing of *Phragmites australis* with the EO-1 Hyperion Sensor

By

Bruce W. Pengra

A thesis submitted in partial fulfillment of the requirements for the

Master of Science

Major in Geography

South Dakota State University

2005

Remote Sensing of *Phragmites australis* with the EO-1 Hyperion Sensor

This thesis is approved as a creditable and independent investigation by a candidate for the Master of Science degree and is acceptable for meeting the thesis requirements for this degree. Acceptance of this thesis does not imply that the conclusions reached by the candidate are necessarily the conclusions of the major department.

Dr. Thomas Loveland
Thesis Advisor November 9, 2005

Dr. Roger Sandness
Head, Geography November 9, 2005

ACKNOWLEDGMENTS

Thanks to Carol Johnston and the Center for BioComplexity Studies for financial and moral support as well as for the good humor and friendship during the tenure of my research assistantship.

Thanks to Tom Loveland and EROS data center for generously supplying the Hyperion image and for just as generously showing faith in my abilities.

Thanks to Mirela Tulbure and Jiyul Chang for providing good humor, friendship and encouragement as well as your invaluable help in the field.

Thanks to Dad for teaching me the value of learning.

A special Thanks to my wonderful wife Ellen and to my wonderful kids Daniel and Maggie for being patient as I have gone back to school.

This material is based upon work supported by the National Science Foundation/EPSCoR Grant No. 0091948 and by the State of South Dakota. Any opinions, findings, and conclusions or recommendations expressed in this material are those of the author(s) and do not necessarily reflect the views of the National Science Foundation.

Although the research described in this thesis has been funded in part by the United States Environmental Protection Agency through cooperative agreement EPA/R-82867501 to the Great Lakes Environmental Indicators (GLEI) Project, it has not been subjected to the Agency's required peer and policy review and therefore does not necessarily reflect the views of the Agency and no official endorsement should be inferred. Additional funding from NASA Grant No. NAG5-11262.

ABSTRACT

Remote Sensing of *Phragmites australis* with the EO-1 Hyperion Sensor

Bruce W. Pengra

November 9, 2005

Phragmites australis is an invasive wetland plant that is recognized as a cause and a symptom of wetland degradation. This study evaluates the utility of Hyperion hyperspectral remote sensing imagery and common image analysis software for detecting large monodominant stands of *Phragmites* in coastal wetlands. Two approaches to hyperspectral image classification—unsupervised classification and target detection—are evaluated. The target detection approach achieved 68.3 percent overall accuracy with 41.2 percent user's accuracy. These results suggests that with further refinement of analysis techniques and the evolution of sensor technology, Hyperion and other space platform hyperspectral sensors may provide wetland scientists and resource managers with an efficient and effective monitoring tool.

Key words: *Phragmites*, remote sensing, hyperspectral, Hyperion, invasive species, wetlands, Great Lakes, Green Bay

Table of Contents

CHAPTER 1: INTRODUCTION AND BACKGROUND 1

1-1: Introduction 1

1-2: The Problem of Invasive Species 2

1-3: Phragmites australis in North America..... 4

1-4: Phragmites impact on North American Wetlands 7

1-5: The Need for Better Data 9

1-6: Remote Sensing as a Source of Species Level Data..... 9

1-7: The Hyperion Sensor 10

CHAPTER 2: RESEARCH OBJECTIVES 12

2-1: Can Hyperion Predict *Phragmites*? 12

2-2: Are *Phragmites* and *Typha* Training samples spectrally distinct? 12

2-3: Change since the Wisconsin Wetlands Inventory 13

CHAPTER 3: LITERATURE REVIEW 14

3-1: Overview 14

3-2: Non-imaging spectrometer multi-spectral scanner simulations 14

3-3: Satellite and Airborne Multi-spectral Remote Sensing Studies 15

3-4: Non-imaging Spectrometer Studies for Hyperspectral Applications 18

3-5: Airborne Hyperspectral Remote Sensing 20

3-6: Hyperspectral Remote Sensing of Phragmites 22

3-7: Application of Hyperion Data 23

3-8: Conclusions 25

CHAPTER 4: METHODOLOGY – Study Design 26

4-1: Overview 26

4-2: Study Site..... 26

4-3: Choice of Training Data 29

4-4: Field Data Collection..... 30

4-5: Data Preprocessing 35

4-6: Vertical Striping 35

4-7: Image Rectification 38

4-8: Bad Bands..... 39

4-9: Minimum Noise Fraction 40

CHAPTER 5: METHODOLOGY - Image Analysis..... 42

5-1: Overview 42

5-2: Target Detection 42

5-3: Unsupervised Classification 47

5-4: Accuracy Assessment..... 49

CHAPTER 6: RESULTS..... 55

6-1: Target Detection 55

6-2: Unsupervised Classification 59

6-3: Spectral Separabilty of Typha and Phragmites Training Samples 63

6-4: Change since the Wisconsin Wetlands Inventory 66

CHAPTER 7: DISCUSSION AND CONCLUSIONS 70

7-1: Was Phragmites successfully predicted?..... 70

7-2: Is Phragmites spectrally distinct from other wetland species? 73

7-3: Change Since the Wisconsin Wetlands Inventory 75

7-4: Hyperion data 76

7-5: Future Research 77

7-6: Final Words 78

REFERENCES: 79

Appendix A-1: Target Detection Classification 90

Appendix B-1: Unsupervised Classification 94

Appendix C-1: Unsupervised Classification – Merged Emergent Classes 98

Appendix D- 1: Accuracy assessment points 102

List of Tables

Table 1: Vegetation Classes Defined. 31

Table 2: Phragmites Training Samples. 46

Table 3: Error matrix – Target Detection 55

Table 4: Error matrix – Target Detection Over All Reference Classes. 57

Table 5: Accuracy Point Details – Target Detection Errors 57

Table 6: Error Matrix – Unsupervised Classification 60

Table 7: Accuracy Point Details – Unsupervised Classification. 61

Table 8: Error Matrix – Merged Emergent Classes 69

List of Figures

Figure 1: Spread of the Invasive Genotype of *Phragmites australis* 5

Figure 2: Dense Monotypic stand of *Phragmites* 7

Figure 3: Image Footprint and Study Site Location..... 27

Figure 4: Data Collection Sheet 34

Figure 5: Identification of Columns with Miscalibrated Detectors 37

Figure 6: Before and After Stripe Removal 38

Figure 7: SAM/SCM Algorithm 43

Figure 8: Accuracy Point Selection 52

Figure 9: Location of Predicted *Phragmites* 56

Figure 10: Variation in *Phragmites* Training Spectra..... 63

Figure 11: *Phragmites* and *Typha* training Spectra at Red Edge..... 64

Figure 12: Mean *Phragmites* and *Typha* Training Spectra..... 64

Figure 13: *Phragmites* and *Typha* training spectra 65

Figure 14: Shoreline Change WWI to 2004 66

Figure 15: Change in Location of Emergent Wetlands 68

Figure 16: Misclassified Points at Pensaukee River Mouth 72

Figure 17: Spectral Separability of Training Samples..... 74

CHAPTER 1: INTRODUCTION AND BACKGROUND

1-1: Introduction

Phragmites australis (hereafter *Phragmites*) is a species of wetland grass native to every continent but Antarctica (Blossey et al., 2002). An invasive *Phragmites* genotype, thought to have arrived with European settlement, has expanded its range across North America over the last 150 years—particularly the last few decades (Saltonstall, 2002). Domination of wetlands by large dense stands of *Phragmites* alters the natural functioning of these ecosystems (Marks et al., 1994; Benoit and Askins, 1999; Meyerson et al., 2000) and is considered an indicator of wetland disturbance and decline (Saltonstall, 2002; Marks et al., 1994).

Airborne remote sensing of *Phragmites* has been pursued as a means locating and studying these invasions (Lopez et al., 2004). In fact, many studies using airborne sensors have had good success in identifying or mapping invasive species (Williams and Hunt, 2002; Underwood et al., 2003; Bachman et al., 2002). However, the cost and limited spatial and temporal coverage of airborne remote sensors is a barrier to their use for ongoing study and wetland management. For that reason, this study evaluates the facility of Hyperion, a hyperspectral sensor aboard the EO-1 satellite, for distinguishing *Phragmites* from its wetland surroundings.

Phragmites is not the only species invading the Great Lakes coastal wetlands. *Lythrum salicaria*, *Typha x glauca*, *Phalaris arundinacea*, and *Myriophyllum spicatum* are among the other invasive wetland species that are currently of great concern (Galatowitsch et al., 1999). In addition, *Lythrum*, *Typha* and *Phalaris* also met the

requirement of occurring in large monodominant stands that could potentially be resolved with the 30 m resolution of Hyperion. However, the fact that other hyperspectral remote sensing studies have had some success in species level identification of *Phragmites* (Bachmann, 2002; Lopez et al., 2004) and thus provided a methodological starting point, made *Phragmites* a logical choice of subject for this investigation.

1-2: The Problem of Invasive Species

Geographical barriers and biological limitations have historically maintained the rate of plant species dispersal. This state of relative equilibrium has been tied to the rates of climate change, evolution, occurrence of major disturbance, and even plate tectonics. It is in the context of this geological rate of change that the planet's species and ecosystems have evolved.

These historical rates of dispersion and disturbance have been accelerated by orders of magnitude by humans (Vitousek et al., 1997). Species which had been largely isolated for millions of years are now dispersed throughout the biosphere (Mooney and Cleland, 2001). Many species were deliberately transported for human use. Many more were inadvertently transported with livestock, humans, agricultural products, ships' ballast and so on.

Whether deliberately or accidentally introduced, many of these plants have become successful colonizers of their new environments. In many continental environments 20 percent or more of the plant species are non-native (Vitousek et al., 1997). On many islands, invasive species account for over 50 percent of the total species (Vitousek et al., 1997). In the United States it is estimated that approximately 5,000 non-

native plant species have become established in the natural environment compared to 17,000 native plant species (Pimentel et al., 2000). In U.S. National Parks and nature reserves, areas assumed by many to be pristine, 5 percent to 25 percent of vascular plants are non-native species (Vitousek et al., 1996). Many of these invasive species become dominant in the environments they colonize. In most cases, once established, these invaders are practically impossible to eradicate (Shigesada and Kawasaki, 1997).

There are many reasons to be concerned about the rapid and increasing rate of non-native species introductions. One of the most compelling reasons is that this unprecedented rate of introduction constitutes an experiment with our environment which we have little prospect of reversing (Mooney and Hobbs, 2000). Furthermore, the complexity of the interactions between invasive species and the environments that they colonize makes prediction of probable invaders and probable environmental impacts extremely difficult (Schwartz et al., 1996). It seems almost certain the rate of change in the global ecosystem will exceed the pace at which we advance our understanding of that change.

More concretely, evidence is accumulating that ties invasive species to increased extinction and loss of biodiversity (Schwartz et al., 1996; Pimentel et al., 2000; Pimm et al., 1995; Novacek and Cleland, 2001). In an analysis of the factors responsible for the current global extinction event, Wilcove and others (1998) said that, of the plants at risk of extinction in the United States, 57 percent were at risk in part due to pressure from invasive species. The only factor that Wilcove's study ranked higher was "habitat degradation/loss"—relevant for 81 percent of plants at risk (Wilcove et al., 1998). Pimm

suggests that the number of extinctions attributed to invasive species may be underestimated, pointing out that the predation, competition, disease, and habitat modification, most frequently blamed for extinctions in biodiversity hotspots, are often caused by introduced species (Pimm et al., 1995).

Within these areas of invasion non-native species can dramatically reduce plant species diversity and in turn reduce habitat and species diversity of native fauna as well (Vitousek et al., 1996). Zedler and Kercher (2004) propose that wetlands are particularly susceptible to invasion due to their landscape position which subjects them to increased nutrients, moisture, and disturbance.

1-3: Phragmites australis in North America

Phragmites (common reed) is a widespread perennial wetland grass species. Its name is derived from the Greek word for fence due to the narrow fencelike stands that it forms along streams and coastlines (Marks et al., 1994). Evidence of its pre-settlement presence in North America suggests that is was somewhat more regional and much less common than it is now (Chambers et al., 1999; Lynch and Saltonstall, 2002).

Since European settlement *Phragmites* has increased in distribution and relative abundance in wetlands in northeastern states and to a lesser extent throughout the eastern half of North America and the Gulf Coast. This pattern has been documented in several locations including the Great Lakes Basin since about 1960 (Chambers et al., 1999; Galatowitsch et al., 1999).

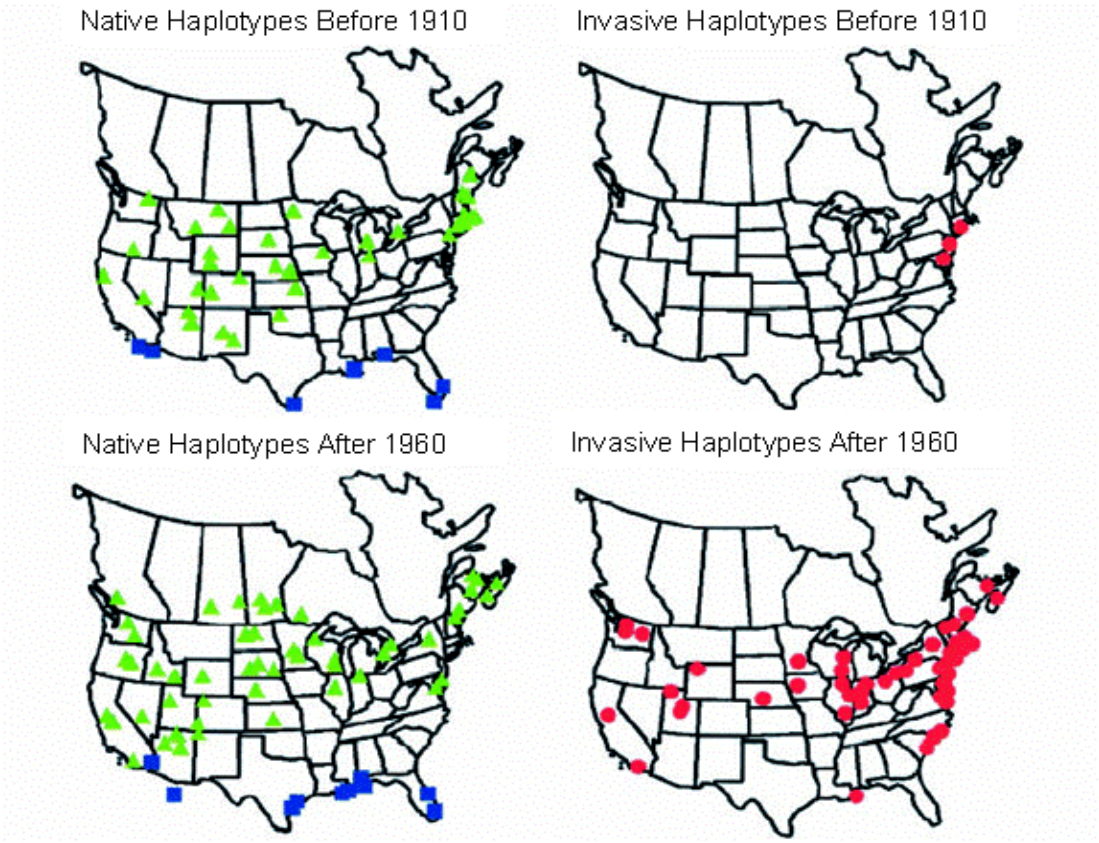

Figure 1: The invasive *Phragmites* haplotype or genotype (right) has dramatically increased in range in the last 100 years. (from Saltonstall, 2002)

The expansion of *Phragmites'* range and abundance in the last several decades (figure 1) has led to speculation that a non-native variant of *Phragmites* may have been introduced into the North American environment following European settlement (Marks et al., 1994). This was confirmed by DNA analysis in 2002 (Saltonstall, 2002). This same study suggests that in the areas of invasion the native genotype has been displaced by the more aggressive invasive one.

Some of the expanded range and abundance of *Phragmites* may be explained by this non-native genotype, nevertheless there is good reason to believe that environmental factors play a significant role as well. Seed propagation by *Phragmites* and other

opportunistic invaders is favored by unvegetated, moist soil (Chambers et al., 1999; Ailstock et al. 2001; Galatowitsch et al., 1999; Havens et al., 1997). Human population expansion in the 1800s was accompanied by the agricultural conversion of many of the naturally occurring wetlands. This resulted in massive areas of substrate disturbance for ditching, installation of drainage tile, road building and farming (Dahl and Allord, 1997). Natural means of seed dispersal were aided by the intense traffic in people, livestock, and goods, increasing the probability that the opportunity of open, wet soil would be exploited. The fact that non-native species correlate with road density (Zedler and Kercher, 2004) is at least consistent with the theory that anthropogenic disturbance has contributed to the spread of *Phragmites*. Many of these wetlands were forested prior to agricultural conversion (Dahl and Allord, 1997). Clearing of these forests provided further environmental disturbance which again may have favored *Phragmites*.

Phragmites tends to grow at or above the mean water level (Ailstock et al., 2001). It is classified as a facultative wetland species and can occasionally be found in upland areas (Reed, 1988). Reduced tidal action, lowered water table and decreased salinity may favor *Phragmites* within salt marsh settings (Marks et al., 1994). While *Phragmites* favors a landscape position that is higher relative to the water table than many wetland species, it is relatively tolerant of hydrological variability and can survive conditions that many competitors cannot (Marks et al., 1994).

Figure 2: Dense monodominant stands of *Phragmites* are common in the Atlantic Northeast; this one is on the west shore of Green Bay.

1-4: Phragmites impact on North American Wetlands

Large, nearly monospecific clonal stands of *Phragmites* are a common occurrence in tidal marshes of the Atlantic coast (Chambers et al., 1999). *Phragmites* population is increasing in the Midwest (Blossey et al., 2002) with many reports of dramatically increasing populations across the Great Lakes Basin (Marks et al., 1994; Galatowitsch et al., 1999; Wilcox et al., 2003).

Native *Phragmites* can exist in stable relationship within wetland plant communities. However, when *Phragmites* stands are aggressively expanding and displacing other native species (figure 2) they are considered a problem (Marks et al.,

1994). The primary concern relative to *Phragmites* invasion is the loss of species richness and consequent potential for extinction and loss of biodiversity (Havens et al., 1997, Chambers et al., 1999).

Although seed propagation may be important for colonization of new areas, (Blossey et al., 2002) in most cases once *Phragmites* is established in a wetland it propagates vegetatively (Chambers et al., 1999). Established plants form buds that grow into horizontal rhizomes during the summer. These rhizomes can extend up to 10 m from the plant of origin, terminating with an upward apex (Marks et al., 1994). The following spring this apex forms a new ramet which can again send out horizontal rhizomes. These clonal stands are typically monodominant (Marks et al., 1994) with culms growing as tall as 4 m. (Haslam, 1969) and very high stem density and above ground biomass (Meyerson et al., 2000).

It is broadly accepted that *Phragmites* invasion reduces the plant species richness of an area (Meyerson et al., 2000; Chambers et al., 1999; Amsberry et al., 2000; Blossey et al., 2002; Ailstock et al., 2001; Zedler and Kercher, 2004). This decrease in species richness is greater in more diverse freshwater marshes, such as the wetlands in the Great Lakes Basin, than it is in less diverse brackish systems (Meyerson et al., 2000). It is also suspected that reduced plant diversity increases susceptibility to invasion, possibly creating a positive feedback to wetland decline (Zedler and Kercher, 2004).

The impact of this loss of plant diversity on fauna seems to be variable, (Chambers et al., 1999) favoring some species and excluding others (Meyerson et al., 2000; Marks et al., 1994). Ailstock and co-authors (2001) report that the diversity of

macroinvertebrates is not affected by the displacement of native species and loss of plant species diversity. For migratory waterfowl, however, there is a loss of resting, feeding and breeding habitat (Chambers et al., 1999). Species of large wading birds are excluded, bird species diversity declines and marsh specialists lose out to generalist species (Benoit and Askins, 1999; Chambers et al., 1999).

1-5: The Need for Better Data

In spite of rapid increase in *Phragmites* abundance and expansion of its range, quantitative data as to the extent and rate of *Phragmites* spread are fragmented and inadequate, often based on anecdotal evidence (Ailstock et al., 2001; Chambers et al., 1999; Blossey, 1999). The call for more research, especially research that will yield quantitative data, is almost universal in the literature of invasive species, including *Phragmites* (Marks et al., 1994; Blossey, 1999; Meyerson et al., 2000; Ailstock et al., 2001). The appropriate scale, uniformity, and timeliness required of these data are all but impossible to acquire with only field assessment and monitoring (Heywood, 1995).

1-6: Remote Sensing as a Source of Species Level Data

With the launch of Landsat in the early 1970s, remote sensing began to provide synoptic data for ecological studies on a broad scale. In some cases, studies of individual species have been possible with these data. Generally, however, inadequate spatial and spectral resolution has limited the utility of remote sensing in species specific ecological studies (Williams and Hunt, 2002). Nevertheless, the repeatable, synoptic character of remote sensing has made it attractive to ecologists studying invasive species (Mooney and Hobbs, 2000).

The advent of hyperspectral remote sensing such as the Airborne Visible and Infrared Imaging System (AVIRIS) has reinvigorated the hope that remote sensing will be able to provide ecologists with broad scale, species level data. Several studies have confirmed the utility of AVIRIS (Martin et al., 1998; Hirano et al., 2003; Underwood et al., 2003; Williams and Hunt, 2002) and other hyperspectral sensor data (Schmidt and Skidmore, 2001; Bachmann et al., 2002) for species level studies.

Remote sensing of *Phragmites* has been investigated (Lopez et al., 2004) using the PROBE-1 airborne hyperspectral sensor. Flown at an altitude of 2170 m, the PROBE-1 data produced a nominal spatial resolution of 5 m. The sensor collects data in 128 bands from 440 to 2490 nm—104 bands were determined to be usable for image analysis. Spectra drawn from the image were used along with the Spectral Angle Mapper algorithm to map dense *Phragmites* stands. The investigation achieved 91 percent accuracy for the presence or absence of *Phragmites*.

Success in species level remote sensing with AVIRIS and other airborne sensors has been mixed but encouraging. As airborne systems, however, these systems lack the broad scale coverage and cost efficiency that satellite remote sensing provides.

1-7: The Hyperion Sensor

The Hyperion sensor aboard the EO-1 satellite is an experimental technology designed to provide the spectral detail of AVIRIS with the breadth of scale and cost efficiency of a satellite system. Hyperion has 242 continuous spectral channels from 357 nm to 2576 nm with approximately 10 nm bandwidths. Seventy bands fall in the visible and near infrared range (VNIR) and 172 bands in the short wave infrared (SWIR) range

(USGS, 2001). Hyperion's spatial resolution is approximately 30 m for the entire spectrum—comparable to Landsat and several other space platform multispectral sensors, and approximately 36 times coarser than the two airborne sensors used in previous attempts at remote sensing of *Phragmites* (Bachman et al., 2002; Lopez et al., 2004).

In its design, Hyperion's spectral resolution exceeds AVIRIS which has 224 bands across approximately the same spectral range (Williams and Hunt, 2002). In reality many of Hyperion's 242 bands are not usable because of the increased signal to noise ratio of Hyperion data. This increased noise relative to signal is the consequence of Hyperion's greater distance from the reflecting surface of the target and the increased atmospheric scattering and absorption that comes with space platform remote sensing (Lillesand and Kiefer, 2000).

Hyperion's lowest signal to noise ratio occurs in the SWIR range where it is 50:1, compared to 500:1 for airborne sensors (Kruse et al., 2002). This was shown to reduce Hyperion's capacity to resolve minerals (Kruse et al., 2002). This may be less problematic for vegetation studies where much more of the discriminative information is found in the visible red, red edge, and near infrared parts of the spectrum (Datt et al., 2003; Schmidt and Skidmore 2003).

Investigators with the NASA EO-1 Science Validation Team (Datt et al., 2003) discuss recommended noise reduction steps for Hyperion prior to use with vegetation indexes. The article recommends removing bands with the worst noise levels, correcting vertical striping and managing residual and introduced noise using Minimum Noise Fraction smoothing.

CHAPTER 2: RESEARCH OBJECTIVES

2-1: The primary objective of this investigation will be to answer the question: Can Hyperion imagery and georeferenced training data be used to predict the presence of large stands of *Phragmites*? Because *Phragmites* is a cause of wetland degradation and an indicator of wetland condition, this would provide a valuable tool for wetland study and management. The design of this study is focused on answering this question.

Two benchmarks of success for remote sensing of *Phragmites* are the 68 percent user's accuracy of Bachman et al.'s study (2002) using the HyMap airborne hyperspectral sensor with 4.5 m resolution and 91 percent accuracy for Lopez et al. (2004) using the PROBE-1 airborne hyperspectral sensor with 5 m resolution. Both sensors share finer spatial resolution and, being airborne sensors, have much better signal to noise ratios than a space platform sensor such as Hyperion. Furthermore, Hyperion is a first generation instrument with some data anomalies such as the "spectral smile" (Jupp and Datt, 2004) and vertical striping (Han et al., 2002). A more reasonable standard of success, considering these differences and considering the small proportion of the study area covered with the material of interest, might be a user's accuracy of 50 percent or better. Accuracy in this range could almost certainly be improved on as techniques and technology evolve.

2-2: A second related objective is to look at the spectral separability of *Typha* vs. *Phragmites*. **Is spectral variation greater between *Phragmites* and *Typha* training samples than it is among the samples of each species?** Monodominant stands of these

two species manifest in similar and often adjacent locations in the landscape making them difficult to distinguish in 30 meter resolution remote sensing imagery. While these two species have some spectral differences they have proven difficult to distinguish with automated remote sensing techniques (Lopez et al., 2004).

2-3: Finally, what changes can be seen in the study area from the time of the data used for the Wisconsin Wetlands Inventory (WWI) until the time of the Hyperion image acquisition? These two data sets are not similar enough to use for a detailed change analysis, however, some broad changes can be observed.

CHAPTER 3: LITERATURE REVIEW

3-1: Overview

Through the three decades that remote sensing studies have been conducted from space platforms a large body of literature on vegetation studies has been generated. While the majority of these studies have been with multispectral data and only a minority have attempted species level classification, they provide the fundamental lessons for any remote sensing of vegetation. Airborne remote sensing, both multi-spectral and hyperspectral, provides data more suited to species level studies, albeit at a much higher cost. Several techniques relevant to use of Hyperion data for vegetation studies may be drawn from airborne hyperspectral studies, especially AVIRIS, which shares many data characteristics with Hyperion. Many studies designed to inform multispectral and hyperspectral remote sensing of vegetation have been done with non-imaging spectrometers. These studies provide laboratory type control and can inexpensively answer important questions about the reflectance characteristics of remote sensing targets. Finally, while the Hyperion sensor is quite new, studies using Hyperion data have been published. These can provide the some of the most specific guidance for further use of Hyperion data; however, they are few and relate to a limited number of applications.

3-2: Non-imaging spectrometer multi-spectral scanner simulations

To distinguish species within remote sensing images on the basis of spectral characteristics there must be greater spectral variation between those species than there is within each species (Schmidt and Skidmore, 2003). Furthermore, these differences must

be resolvable at the spectral resolution of the sensor. Much of the research aimed at this question has been done with non-imaging spectroscopy.

Ernst-Dottavio and others (1981) used a spectrometer mounted on the strut of a helicopter to collect spectral data from an Indiana wetland. The spectrometer averaged wavelengths within the ranges of the four Landsat MSS bands to roughly simulate Landsat data. Discriminant analysis determined that samples taken over six different wetland classes could be separated by spectral characteristics alone. While the study did not discriminate individual species, studies with similar design have been used to evaluate increasingly finer spectral and spatial resolutions and to develop more successful image analysis techniques.

Ramsey and Jensen (1996) used field gathered spectrometer data to investigate spectral separability of three mangrove species. The study was limited to simulated visible and near infrared multi-spectral bands (e.g. SPOT, TM and AVHRR) as well as a set of narrower bands designed to capture the maximum amount of information and variation within corresponding multi-spectral bands. The study found considerably more spectral variation within each of the three mangrove species than existed between these three species. From this they concluded that species discrimination between these three mangrove species was not possible with multi spectral remote sensing.

3-3: Satellite and Airborne Multi-spectral Remote Sensing Studies

In a 1999 article, Rutchey and Vilchek (1999) use a previously clustered SPOT image which they reclassify for the purpose of accuracy comparison with air photos in a study of cattail coverage. When the original 20 classes including several mixed classes

were merged into 12 more general classes, they achieved overall accuracy of approximately 81 percent. Classification included only two species based classes; otherwise classes were more generic—e.g. slough, open water, etc. However, for the purpose of the study, they showed that the species of interest could be quantified for inventory and change detection.

Two other TM studies used subpixel classification techniques to successfully detect tree species. Oki and colleagues (2002) used unmixing techniques to detect alder in a Japanese mire. The technique assumes that the reflectance of each cover class within a pixel varies linearly with the proportion of the pixel occupied by that cover class. No accuracy numbers are published in the article; however Oki concludes that the unmixing method of estimating alder tree coverage was more accurate than maximum-likelihood classification of the TM image. They also concluded that the accuracy of the unmixing method's estimates varied with the quality of the data used to create the spectral signature or endmember for alder.

In a similar study also using TM imagery, Huguenin and others (1997) were able to detect bald cypress and tupelo gum trees at the subpixel level. The spectra of the endmembers were derived from pixels at known locations of relatively homogeneous stands within the TM image. Accuracy was assessed on the basis of presence or absence of the material of interest in the ground site relative to image detection or non-detection of the species. On this basis, cypress had an overall accuracy of 89 percent and tupelo had an overall accuracy of 91 percent.

Thomas Bernthal and Kevin Willis (2004) used Landsat 7 ETM+ data in a study of *Phalaris arundinacea*, a wetland grass species, with very similar goals to those of this paper. Clustering the ETM+ data with the ISODATA algorithm and using an unsupervised classification they accomplished a remarkable 89 percent accuracy for the "heavy dominant" class. The high accuracy rate must be considered against the fact that the classification scheme only recognized three classes—"heavy dominant," co-dominant, and "absent to sub-dominant." Furthermore, the study masked out all non-wetland areas based on the Wisconsin Wetland Inventory classes. This reduced the number of vegetation species from which *Phalaris* had to be distinguished.

Malthus and George (1997) used field spectrometer data and Daedalus Airborne Thematic Mapper data to determine the separability of spectra for wetland plant species in a U.K reservoir. Airborne imagery was collected at 800m above ground level resulting in approximately 2m spatial resolution. Stepwise discrimintant analysis of the field spectrometer data determined that four wavelengths (626nm, 673nm, 912nm, and 1000nm) could discriminate 19 of 20 spectra correctly. Similar results were achieved with spectra derived from the Daedalus ATM image. Forty of 48 spectra were judged to be separable based on the same stepwise discriminant analysis. Much of the separability was attributed to the canopy structure of the various species. Two genera, (*Eleocharis* and *Equisetum*), could not be separated based on their image spectra or field spectrometer spectra. The signature for *Phragmites* appeared to be the most distinct of the species analyzed.

3-4: Non-imaging Spectrometer Studies for Hyperspectral Applications

Van Aardt and Wynne (2001) compared the performance of simulated AVIRIS and TM data for discriminating six southern tree species. Field spectrometer samples were gathered from a boom truck in late summer. The simulated TM data demonstrated almost equal facility to the simulated AVIRIS hyperspectral data in determining broader classes—deciduous and conifer. The hyperspectral data discriminated between the two classes approximately 99 percent of the time, the simulated TM data about 94 percent of the time. The simulated AVIRIS data discriminated species within the conifer class at 62 percent to 84 percent accuracy and species within the hardwood class at 78 percent to 93 percent accuracy. The within class discrimination of the TM simulation data dropped to a little above 50 percent accuracy.

Cochrane (2000) studied the spectral separability of tropical rainforest canopy vegetation sampled with a non-imaging spectrometer. The first derivative of the red edge was calculated from the slope of the difference between the visible red absorption minimum and the near infrared reflection maximum in vegetation. Cochrane found that the value of maximum inflection and the wavelength where maximum inflection of the red edge occurs contain useful information for species discrimination (Cochrane, 2000). Plotting histograms for the distribution of the maximum inflection of the red edge derivative, Cochrane shows that distributions are different for the different species in the study, suggesting that there is a basis for discriminating between species.

In another study, also using non-imaging spectroscopy, Yamano and co-workers (2003) were able to discriminate between four grass species in an arid to semi-arid area

of northern China. Two of the grass species were dominant in healthy grasslands. The other two species were opportunistic invaders indicative of degraded grasslands.

Field recordings of leaf specimen and canopy spectra for the four species were taken between 300 and 1100 nm. The data were converted to fourth order derivatives to create the spectral peaks from which the researchers could discriminate between the four species. The locations of local maxima and minima between 670 nm and 720 nm were able to discriminate between the leaf specimen samples. When canopy spectrometer data were used, peaks for three of the four species shifted by 2 nm. This left only one of the species as distinguishable with canopy spectral data. This was still judged to be useful as an indicator of grassland condition.

Spanglet and colleagues (1998) utilized portable spectrometer data to study the effect of canopy architecture on a list of vegetation indices. Leaf spectra of three wetland species were recorded with an active spectrometer. *In situ* canopy spectra were measured with a passive spectrometer. Hardstem bulrush, an extremely vertical plant, had the least canopy coverage of the three plants studied and the least photosynthetic surface oriented toward the sensor. Spanglet credits these architectural characteristics for the much lower NDVI of the bulrush canopy reflectance compared to its leaf measured NDVI. At the other extreme, the most horizontally oriented of the three species—the yellow water lily, has large flat foliage almost entirely oriented toward the sensor which, in both leaf and canopy measures, was one leaf thick. Thus, canopy and leaf measures of NDVI were very similar for yellow water lily. Finally, the spherical canopy of the beaked sedge caused an intermediate difference in NDVI from leaf measurements to canopy

measurements. This research suggests that differences in species architecture may be as important an element in the spectral signatures of *in situ* vegetation canopies as is individual leaf reflectance.

Schmidt and Skidmore (2003) directly address the question of spectral separability among wetland plant species in a Netherlands saltmarsh. The species in the study reflect local Dutch varieties; however, species belonging to several of the genera listed occur in temperate North American wetlands as well. Reflectance profiles of 27 vegetation associations were statistically analyzed to determine if there was greater spectral variability within or between groups. Wavelengths at which each vegetation association's median reflectance was statistically different from all other vegetation associations were determined. Schmidt and Skidmore claim that these wavelengths can "potentially be used for identifying vegetation types." Following continuum removal for all the spectra, the same radiometric comparison and statistical significance tests were applied. Continuum removal increased the number of wavelengths that were statistically different in the visible range but decreased the number in NIR. Thus, some species were distinguishable at fewer wavelengths with continuum removal, e.g. *Phragmites*. Schmidt and Skidmore conclude that the majority of the saltmarsh species are spectrally distinct. They suggest that with adequate calibration hyperspectral remote sensing may be able to identify many vegetation species.

3-5: Airborne Hyperspectral Remote Sensing

Martin and colleagues (1998) attempt to establish a link between hyperspectral image data—AVIRIS—and foliar chemistry of tree species for the purpose of species

level classification. Lignin and nitrogen ratios associated with specific tree species can be used as markers that indirectly identify those species. Nine AVIRIS bands previously determined to be useful in measuring canopy nitrogen and lignin were classified using a standard maximum likelihood algorithm for classification. The accuracy matrix showed three of 11 classes to have low producer's accuracy (red maple 33 percent, white pine 38 percent, and hemlock 17 percent). The deciduous/conifer mix was mapped with 60 percent producer's accuracy. Two classes were accurate at 80 percent plus producer's accuracy and the remaining four at 100 percent producer's accuracy.

Williams and Hunt (2002) applied a subpixel technique called mixture tuned matched filtering (MTMF) to AVIRIS to estimate fractional leafy spurge cover. MTMF is a partial unmixing technique that finds the abundance of one spectral endmember and does not require that the spectra of the background be determined or estimated. Pixel purity index (PPI) was used to find candidate pixels in the image and these were used to define the endmember spectrum for the MTMF analysis. Two surfaces are output from the MTMF analysis. One shows relative abundance per pixel of the spectral endmember of interest, the other is an infeasibility grid showing the degree to which the estimated spectral components explain the pixel's spectrum. Pixels with a high infeasibility value were not classified as leafy spurge. The MTMF process performed best in the prairie areas ($r^2 = 0.79$) and worst in forested areas ($r^2 = 0.57$).

Schmidt and Skidmore (2001) analyze signatures from laboratory spectrometer data and the Compact Airborne Spectrographic Imager (CASI) to determine the best wavelengths for discriminating among eight African grass species. The visible red

wavelengths (550-680 nm) showed the greatest potential for discriminating grass species. The red edge and near infra-red also showed very large reflectance differences between grass species, however, within-species variation of NIR meant that reflectance in this range was not significantly different between species samples.

Hirano and colleagues (2003) applied AVIRIS for discrimination of wetland species and species associations in the Florida everglades. A supervised classification using Spectral Angle Mapper (SAM) with all 224 bands produced a species level map which was judged against a map from the Everglades Vegetation Database. The producer's accuracy achieved varied from 41.9 percent for button wood forest to 100 percent for spike rush and leatherleaf. The authors attribute the low accuracy in some classes to the mixed pixels resulting from the 20 meter resolution of AVIRIRS and specifically caution that the 30 meter resolution of the Hyperion sensor will present similar limitations.

3-6: Hyperspectral Remote Sensing of Phragmites

Charles Bachman and others (2002) investigated the use of HyMAP airborne hyperspectral images for automated classification of a saltwater wetland on Smith Island off the coast of Virginia. The study used data processed with a feature extraction algorithm called "projection pursuit." This algorithm was described as serving the same purpose as Principal Component Analysis—to reduce data dimensionality. Supervised and unsupervised classifications were utilized. The article points out two specific difficulties in discriminating *Phragmites australis* in its natural environment. The first is the tendency for the stands of *Phragmites* to occur with the dimension perpendicular to

the shoreline being much narrower than the dimension which is parallel to it. This often means that large contiguous areas of *Phragmites* present as highly mixed pixels. A second problem is that *Phragmites* has spectral characteristics that are similar to other wetland plants. The authors say its "unlikely that systems with a few broad spectral channels would be able to discriminate it," in the midst of other similar species. Their results supported this statement. *Phragmites* was one of the four most confused of the 19 cover types in the classification.

Ricardo Lopez and others (2004) used data collected with the PROBE-1 airborne sensor to detect *Phragmites* in a Lake Erie wetland. The PROBE-1 data had very similar spectral and spatial resolution to the HyMap data used by Bachman et al. (2002). This investigation also used endmembers selected from within the image data. Homogenous *Phragmites* endmembers were selected using ground referenced GPS points. Those were used as training data in a supervised classification using the Spectral Angle Mapper (SAM). Based on the very simple accuracy matrix of predicted presence or absence of *Phragmites* versus reference data presence or absence of *Phragmites*, the study predicted the presence or absence of *Phragmites* with 91 percent accuracy.

3-7: Application of Hyperion Data

Hyperion was shown to be more effective in classifying different floristically based classes of rainforest vegetation than were 3 space-based multi-spectral sensors (Thenkabail, 2004). The study compared IKONOS, ETM+, ALI, and Hyperion. The study used classes defined by general attributes that were well suited to Hyperion's 30 m spatial resolution. Classes included, fallow, mixed secondary forest, mature secondary

forest, young secondary forest and so on. The overall accuracy in classifying the nine broad classes was 96 percent for Hyperion compared to 48 percent for IKONOS, 42 percent for ETM+, and 51 percent for ALI.

Apan and others (2004) used discriminant analysis to determine which narrow-band indexes based on Hyperion data were the best indicators of plant stress caused by the "orange rust" disease in sugarcane. They found that indices taken from the red edge spectra were poor indicators of disease. Indices using only NIR wavelengths performed moderately better. The best indices were those using the 1600 nm short wave infrared band in a ratio with either an 800 nm NIR band or 550 nm green band.

A forestry study in British Columbia was successful in classifying a Canadian forest to 10 classes—most of them to species level (Goodenough et al., 2002). Classification to eleven classes, most of them defined by a dominant tree species, was 92.9 percent accurate. This success was described as "operational" accuracy for forest classification. This accuracy was compared to 84.8 percent for ALI and 75 percent for ETM+ classifications of the same area.

In a study attempting to quantify and map wildfire fuel potential in a California forest, Ustin and colleagues (2002) found that in general Hyperion "produced maps of abundances similar to AVIRIS in quality." This was in spite of the fact that "Hyperion performs more poorly in producing maps based on specific narrow band features due to the lower SNR." In fact, Ustin et al. were unable to use the bandwidths usually used to calculate moisture indices at around 980 nm due to poor signal to noise ratios and instead used the signal from around 1200 nm.

3-8: Conclusions

The literature shows some success with species level classification of multispectral data (Bernthal and Willis, 2004; Oki et al., 2002; Huguenin et al., 1997). However, for many species there seem to be no reliable spectral differences at the spatial and spectral resolution of space platform multispectral scanners (Ramsey and Jensen, 1996). Tightly controlled non-imaging spectrometer studies, using spectral resolutions comparable to hyperspectral scanners, have been able to find spectral differences adequate to distinguish species of grasses, trees and wetland plants including *Phragmites* (Yamano et al, 2003; Schmidt and Skidmore, 2003). Some of these spectral differences have been successfully exploited in species level classifications of airborne hyperspectral images from AVIRS, HyMap and PROBE-1 sensors (Williams and Hunt, 2002; Bachman et al., 2002; Lopez et al., 2004). Bachman et al. (2002) and Lopez et al. (2004) predicted *Phragmites* in airborne hyperspectral images with 68 percent and 91 percent accuracy respectively. Comparison of airborne hyperspectral data with Hyperion suggests that even with coarser spatial resolution and a decreased signal to noise level species level distinctions can be made (Ustin et al., 2002; Goodenough et al., 2002). This study will draw on the lessons and techniques in the preceding literature as it tests Hyperion's facility for distinguishing *Phragmites* from its wetland surroundings.

CHAPTER 4: METHODOLOGY – Study Design

4-1: Overview

Methodology has been divided into two chapters. This chapter describes steps leading up to actual image analysis, the logic of those steps and some of the objectives served. The study site is described and the reasons for choosing it explained. The decision to use training signatures extracted from the image is explained and the collection of GPS locations used to extract those signatures is described. Then, preprocessing of the image prior to image analysis including georectifying, removal of bad bands and addressing vertical striping anomalies is detailed.

The next chapter covers the image analysis and accuracy assessment. The two approaches to image classification are explained. Finally the accuracy assessment design and the collection of accuracy assessment field data are described.

4-2: Study Site

This study received its primary funding from the Great Lakes Environmental Indicators (GLEI) research project which is aimed at developing indicators of wetland condition for the coastal wetlands of the Laurentian Great Lakes. The choice of where along the Great Lakes coast to locate the study site was based on a variety of considerations.

Monospecific stands of *Phragmites* that would be resolvable with the 30m spatial resolution of Hyperion was the primary criterion. Large stands of *Phragmites* were observed in the Green Bay area in July of 2004 at Point AuSable, Little Tail Point, and the extreme SW corner of Green Bay. Comparison with sample data from the GLEI

study (Johnston et al, in review) and aerial photos showed that in some cases these large stands of *Phragmites* had dramatically increased in area in only a few years. This met the criteria for the presence of large stands of *Phragmites* and further suggested that these stands were recent invaders.

A second criterion for site selection was orientation of the shoreline. The Hyperion sensor collects images in 7.5 km wide swaths along its near-polar, sun-synchronous orbit. This makes the Hyperion images very narrow and oriented at a northeast to southwest angle. A study site oriented along a north to south stretch of coast allows a much longer segment coastline to be captured in a single image than a more east west oriented study site would. This made both the east and west coasts of Green Bay good targets for the sensor.

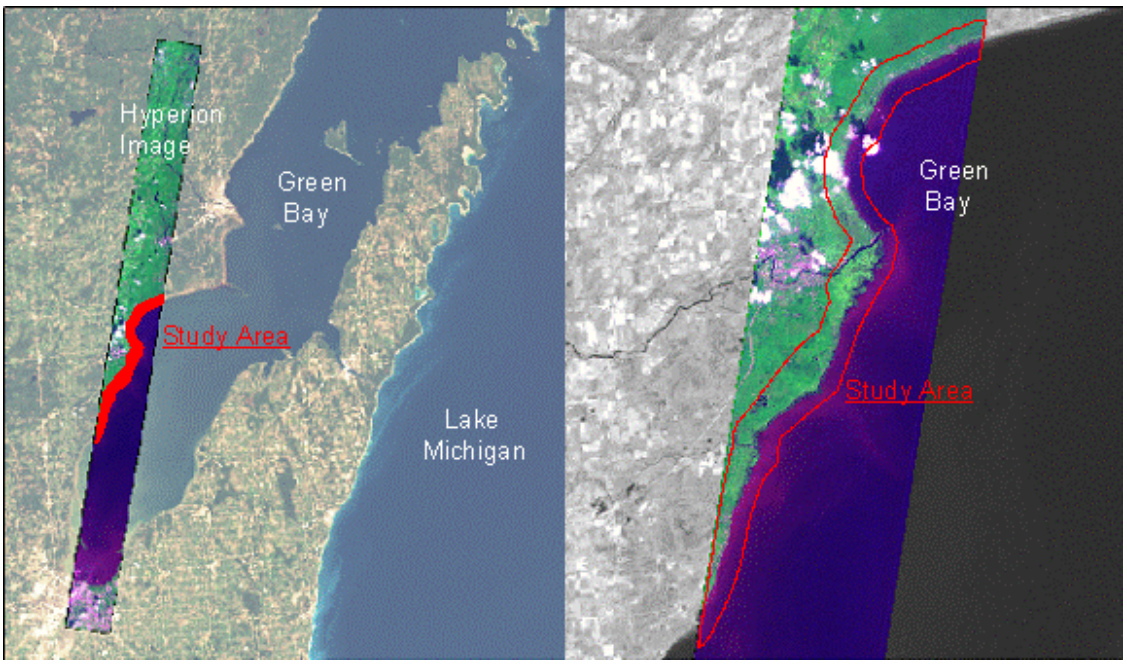

Figure 3: A study site (solid red, left; red outline, right) was chosen on the west shore of Green Bay. This maximized several considerations, one of which was matching the northeast to southwest orientation of the Hyperion image to a similarly oriented shoreline.

The WWI (Johnston, 1984) showed that the west coast of Green Bay had several areas of emergent wetlands—probable areas of *Phragmites* invasion. These wetland areas coincided with two areas of public land and a private preserve: the Pensaukee Public Hunting Ground, the Oconto Marsh State Game Refuge, and Oconto Marsh—a private hunting preserve. Public land was preferable for ease of access issues. Additionally, hunting grounds and game refuges were assumed to be in a more natural state than most private land in the area.

The decision was made to center the study site around the Oconto Marsh area on the west coast of Green Bay (figure 3). Image acquisition was scheduled during early fall when spectral differences between *Phragmites* and other wetland species are most pronounced (Bachman et al., 2002; Bernthal and Willis, 2004; Wolter, personal communication). Weather and availability of student help for carrying out field work were also judged to be optimal during the early fall. The data acquisition request was made for between the first week of September and the second week of October. Actual data acquisition took place on September 4, 2004 at 11:23:53 a.m. CDT. Conditions were fair to good yielding an image with less than 25 percent cloud cover. While some clouds fell within the study area they were outside of the public land and the private hunting preserve.

To focus on GLEI's aim of developing an indicator of wetland condition for the coastal wetlands of the Great Lakes, the study area was limited to the coastal area of the image. To do this a buffer extending 750 meters either side of the shoreline was created along the stretch of the Green Bay shoreline that passed through the image. The National

Oceanic and Atmospheric Administration's (NOAA) "medium resolution digital vector shoreline", (NOAA, 1992) was used to define the shoreline for this purpose. The buffer was adjusted to include an area of dense *Typha* which was used a training data. The adjusted study site covered 4734 hectares. Approximately 39 percent of this was open water.

4-3: Choice of Training Data

Classification of remote sensing images relies on some form of reference data to relate spectrally or visually identified features within the image to ground cover features. Hyperspectral remote sensing emphasizes the use of spectral signatures of land cover classes or materials of interest. These spectral signatures can be collected with spectrometers and compiled in spectral libraries or extracted from within remote sensing images by identifying one or several pixels that are the collected reflectance of the ground cover or material of interest. The later approach is more practical and therefore more common.

Use of image derived spectra was determined to be appropriate for this investigation and better fit the available resources of the study. Field collected spectra or spectral library signatures would have required atmospheric correction of the image to surface reflectance (ERDAS, 2002b; Schmidt and Skidmore, 2001). Because atmospheric correction of Hyperion data is still technically problematic (Jupp and Datt, 2004) and at the time of the image analysis, no software package designed for atmospheric correction of Hyperion data was available on the SDSU campus, atmospheric correction was determined to be impractical.

Furthermore, spectral variation in vegetation caused by phenological and environmental conditions makes it difficult to collect field spectrometer signatures that match the vegetation in any given image from any source other than that image. Finally, the literature of species level remote sensing showed that image derived spectral signatures were widely used (Malthus and George, 1997; Lopez et al., 2004; Bachman et al., 2002) and generally preferred (deLange et al., 2004) for vegetation studies.

4-4: Field Data Collection

To extract spectral signatures from within the Hyperion image, GPS points were collected for large stands of *Phragmites* and representative examples of the other vegetation classes from within the study area at as near to the date of image collection as possible. An initial investigation of the study area was made on August 31, 2004. Several GPS points were collected and photographs and notes were taken in preparation for later field work. Three of the points collected at this time would later be used as reference points for image derived *Phragmites* spectra (dp1n1w1, dp3, and R13, table 2). The vegetation classes to be used for image classification (table 1) were developed from observations made during this initial trip.

On September 24 and 25, 2004 field data were collected for 19 points. Prospective locations of large *Phragmites* stands as well as 6 classes of non-target vegetation were pre-selected based on aerial photography, the WWI, United States Geological Survey (USGS) quadrangle maps, and the Hyperion image itself. Additional or alternative collection points were selected in the field when pre-selected ones proved inadequate and as better sites were encountered. Collection was made by two teams of

two persons each. Data collection included GPS points, digital photographs, a sketched map of a 60m square surrounding the point, a list of the most prevalent species of vegetation, descriptions of the sample point area, and samples of plant species which could not be identified in the field. Points for deep water (water1), shallow water (water2), or impervious surface were not field collected because they could reliably be taken from available aerial photography and image signatures.

Table 1: Field description of vegetation classes used.

Vegetation Class	Description
Impervious surface	Area is dominated by road, parking lot, sidewalk, roof tops, bare soil
Meadow	More than 50% of the area is dominated by upland and/or wetland grass species; or grass species account for more than 50% of the canopy of the area
Water 2	predominantly shallow standing water (generally <1 m) with few floating plants, SAV, or emergent plants;
Forest Deciduous	The 30 x 30 quadrat surrounding the sample point is predominantly broadleaf species. Understory is relevant only where canopy gaps would allow it to receive full light and be visible from above. Include mixed conifer/deciduous areas that are not clearly dominated by needle leaf species
Forest Conifer	Clearly dominated by with needle leaf species. Understory is relevant only where canopy gaps would allow it to receive full light and be visible from above
Scrub/shrub	Area surrounding the sample point is populated with willow, dogwood, and other woody shrub species such that during leaf-on season they would account for more than 50% of the canopy. Trees more than 4 meters account for less than one third of the canopy.
Typha	*Typha* dominant in more than 50% of area surrounding sample point; or *Typha* mixed thoughout & accounts for 50% of the canopy surrounding the sample point.
Phragmites	*Phragmites* dominant in more than 50% of the area surrounding the sample point; or *Phragmites* mixed throughout & accounts for 50% of the canopy surrounding the sample point.
Mixed emergent wetland	The area surrounding the sample point is not dominated by any one species, it is predominantly a mixture of non-woody non grass emergent wetland vegetation; if *Phragmites* or *Typha* are present neither of them alone accounts for more than 50% of the canopy.

Field data were georeferenced using two Garmin MAP76 consumer model GPS units. One unit was held at approximately 3.5 meters above the ground by a "holster" on a pole attached to the top of an 8 ft. aluminum ladder. The other unit used an external antenna on a tripod at about the same elevation above ground. For each GPS point approximately 300 points were collected in the averaging mode. At all times the Wide Angle Augmentation System (WAAS) was used for realtime differential correction.

Both arrangements had been tested for accuracy prior to the field trip, using the units' own estimated accuracy. The GPS unit using the ladder mounted "holster" on a pole typically achieved accuracy just over 1 meter. The unit using the external antenna did slightly better—occasionally registering accuracy to less than .8 meters.

Two series of digital photographs were taken for each sample point. The first was four shots in the directions of the four compass points from the top of an 8 ft. ladder. This was intended to capture the degree of homogeneity of the vegetation in the 60 m x 60 m sample area. It also provided some additional information about the composition and layout of that vegetation.

The second series of digital photographs was taken along a transect running through the sample site. The photographs were spaced at 0 m, 7.5 m, 15 m, and 25 m in opposite directions from the GPS points. The distances were determined by using a measuring tape attached to the ladder at the point where the GPS point was taken. The orientation of each of these transects was adjusted to a 90 degree angle from the path taken into the center of the study site by the field workers. This had the dual function of

avoiding pictures of trampled vegetation and ensuring that more of the area within the study site was visually observed by field workers.

A map of the vegetation in a 60 m square area surrounding the point was sketched from the top of the aluminum ladder at the GPS collection point (figure 4). This only included vegetation constituting a significant portion of the canopy. The observer sketching the map used a parallax optical rangefinder to fix distances for delineation of different vegetation patterns. They were also able to obtain distances from the other worker taking transect photographs. A second, smaller map was sketched of any standing water or wet soil beneath the vegetation canopy.

A list was made of the most significant vegetation associations in the sample site area in descending order of prevalence. Each of these sites had been selected as training data for one of the 6 vegetation classes. Therefore, the first association listed on each data sheet was from among the study defined classes (table 1). Each species or association listed was associated with areas delineated on the sketched map. This allowed for a rough estimate of the proportions of various plants or associations captured by the pixels overlaying each sample site. The density of the vegetation association within the delineated areas of the sketched map was recorded as a value from 1 to 6, with 6 being the densest. Specimens were collected for species which could not be identified in the field if they made up a significant fraction of the sample area.

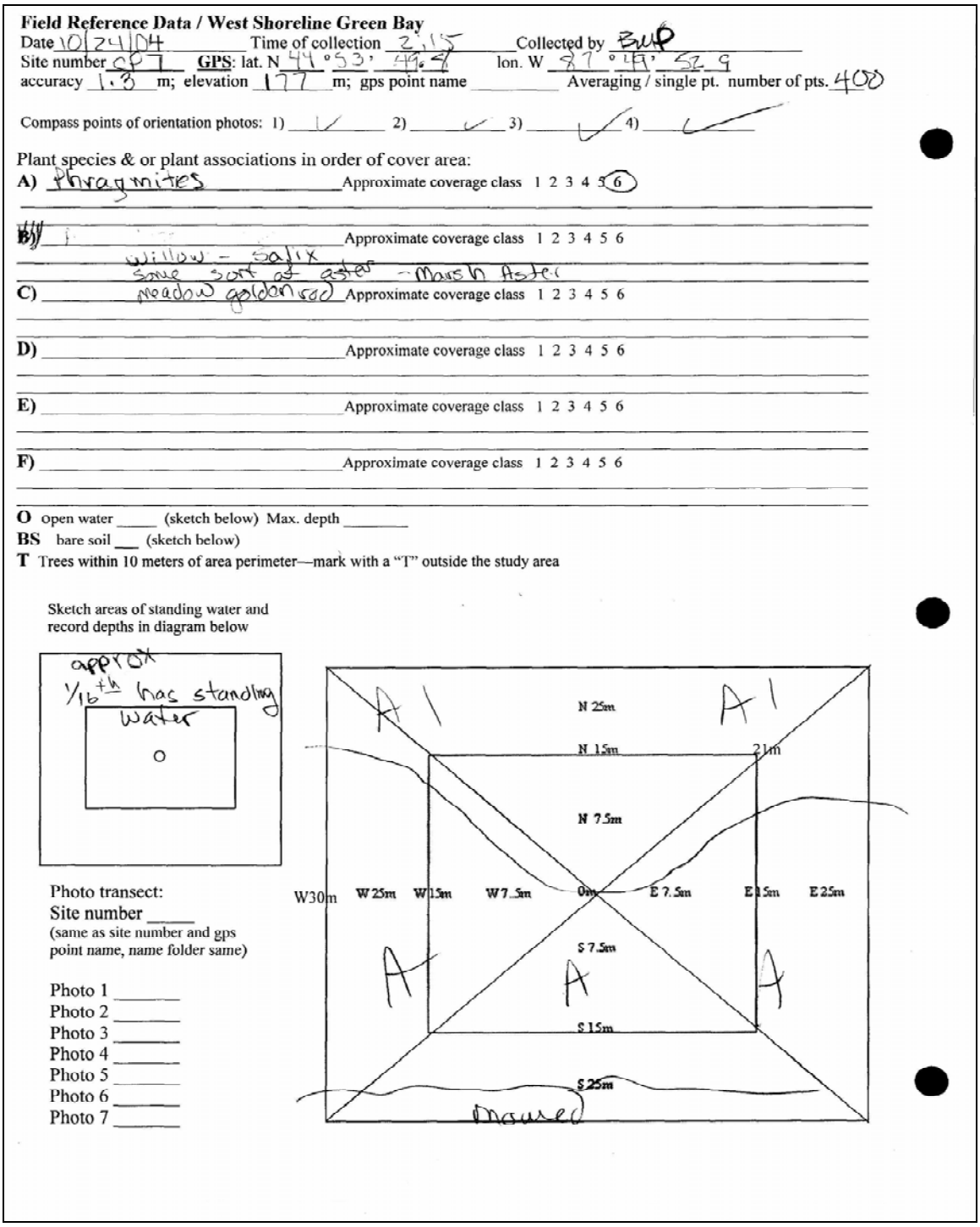

Field Reference Data / West Shoreline Green Bay

Date 10/24/04 Time of collection 2:15 Collected by BWP

Site number SP7 **GPS**: lat. N 44° 53' 49.8 lon. W 87° 49' 52.9

accuracy 1.3 m; elevation 177 m; gps point name _____ Averaging / single pt. number of pts. 400

Compass points of orientation photos: 1) ✓ 2) ✓ 3) ✓ 4) ✓

Plant species & or plant associations in order of cover area:

A) Phragmites Approximate coverage class 1 2 3 4 5 (6)

B) Approximate coverage class 1 2 3 4 5 6

willow - Salix

some sort of aster - Marsh Aster

C) meadow golden rod Approximate coverage class 1 2 3 4 5 6

D) Approximate coverage class 1 2 3 4 5 6

E) Approximate coverage class 1 2 3 4 5 6

F) Approximate coverage class 1 2 3 4 5 6

O open water _____ (sketch below) Max. depth _____

BS bare soil ___ (sketch below)

T Trees within 10 meters of area perimeter—mark with a "T" outside the study area

Sketch areas of standing water and record depths in diagram below

approx 1/16th has standing water

Photo transect:

Site number _____

(same as site number and gps point name, name folder same)

Photo 1 _____

Photo 2 _____

Photo 3 _____

Photo 4 _____

Photo 5 _____

Photo 6 _____

Photo 7 _____

Figure 4: Data sheets recorded and mapped the dominant vegetation at each sample site as well as exposed soil, standing water and open water. GPS coordinates were recorded as a back up the GPS unit's memory.

Notes were also made on data collection sheets with respect to GPS accuracy, time of collection, number of points collected and the latitude and longitude of the collection point. Additional notes were made when anomalies in the sampling process occurred. An example of this would be when transect photographs were taken out of sequence.

4-5: Data Preprocessing

Hyperion level 1R data delivered by the USGS is radiometrically corrected. It is not geometrically corrected or georeferenced. It is in the Hierarchical Data Format (HDF) version 4.1r5 (USGS, 2005). Delivered data includes 44 bands which are not calibrated and have data values set to 0. Prior to classification outlier values and vertical striping of the image were addressed, the image was georectified, bands with high levels of noise were removed and a strategy for applying Minimum Noise Fraction (MNF) noise removal was determined.

4-6: Vertical Striping

Dark vertical striping is visually apparent in several of the Hyperion bands. These visible stripes are caused by miscalibrated, dead and stuck detectors in the pushbroom sensor of Hyperion. Uncorrected, these anomalous values can appear as extreme values to automated classification algorithms and introduce noise into the classification process. The problem is significant enough that Australian scientists working on the evaluation and validation studies for EO-1 all made corrections to address the stripes before using the data (Jupp and Datt, 2004). An article addressing these abnormal pixels (Han et al., 2002) separated them into four distinct classes. These divisions did not correspond

directly to the anomalies found in the data for the Green Bay study site. However, the general strategies described by the Han team and by Bisun Datt and others (2003) to address the stripping anomalies were adapted to address the most affected bands.

Striping anomalies in the Green Bay Hyperion image could be put into three classes: 1) Columns with intermittent dark pixels. 2) Columns that were consistently darker than the columns on either side but that generally tracked the changes in digital number of those two adjacent columns. 3) Columns that were darker than their two adjacent columns but do not track with the changes in digital number of those columns.

The first class of striping was not addressed unless the number of dark pixels was well over half of the pixels in the column. When that threshold was met the stripe was addressed by using a convolution filter to average the pixels to the right and left of the affected column and substitute that value for the pixel in the stripped column. The fix was applied to the entire length of the affected column.

The second class of stripe is described as arising from miscalibrated detectors (Datt et al., 2003). Except in the more extreme instances these columns contain valid data but their digital numbers are offset from the data of the well calibrated detectors by a fairly constant value. These columns could be identified by graphing the values of dark column and its two adjacent columns for comparison (figure 5). When the dark or stripped column's values roughly paralleled the values of the two adjacent columns but at a consistently lower level it was judged to be the result of miscalibration.

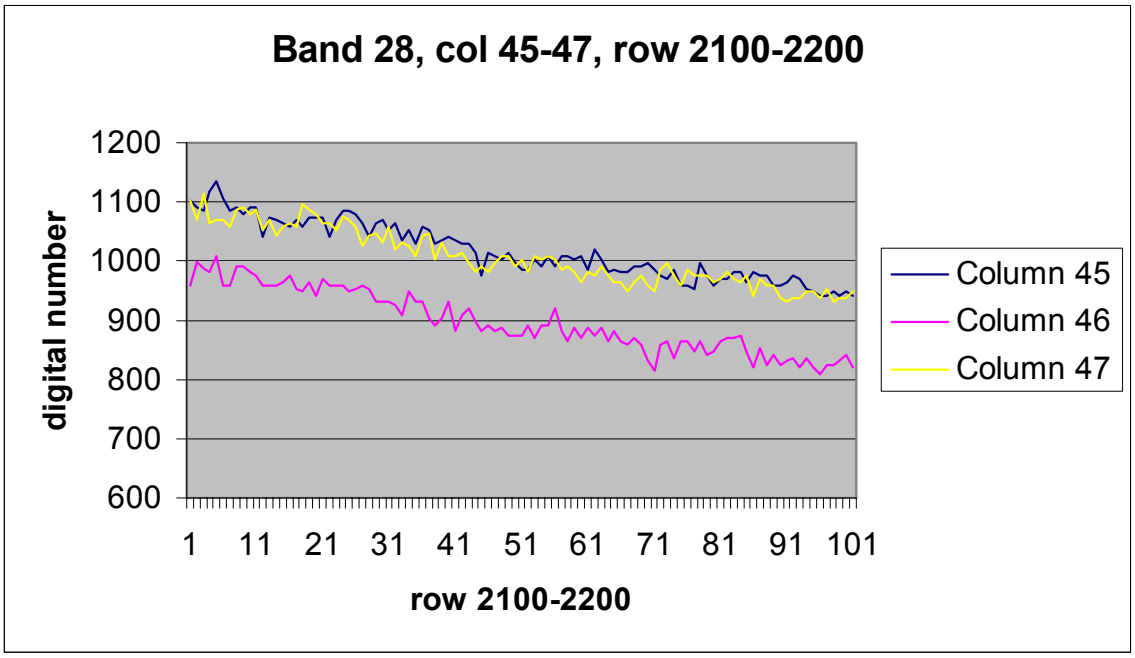

Figure 5: Columns where the dn followed the changes in ground reflectance by generally paralleling the values of the adjacent columns were identified as resulting from miscalibrated detectors. These columns were normalized to the two immediately adjacent columns

A simple offset added a fixed value to each pixel such that the means of columns would be normalized. This would not address the difference in variability that could be caused by the lower gain of the miscalibrated detectors of the dark columns. Variability statistics were taken from the columns to the right and left of the dark columns. The standard deviations of pixels in the normal columns were compared to the standard deviations of pixels in the striped columns with a Tukey's Studentized Range (HSD) Test. The test showed that standard deviations in the striped columns were not statistically different from standard deviations in the normal columns. On this basis it was decided that addressing the variability of pixel values in striped columns was not necessary.

Offsets were calculated by averaging the mean pixel value of the columns to the right and left of the striped columns and subtracting the mean pixel value of the dark

column from that average. By selecting the affected column and applying a single offset value to every pixel in the column the striped columns were normalized to the local mean (figure 6).

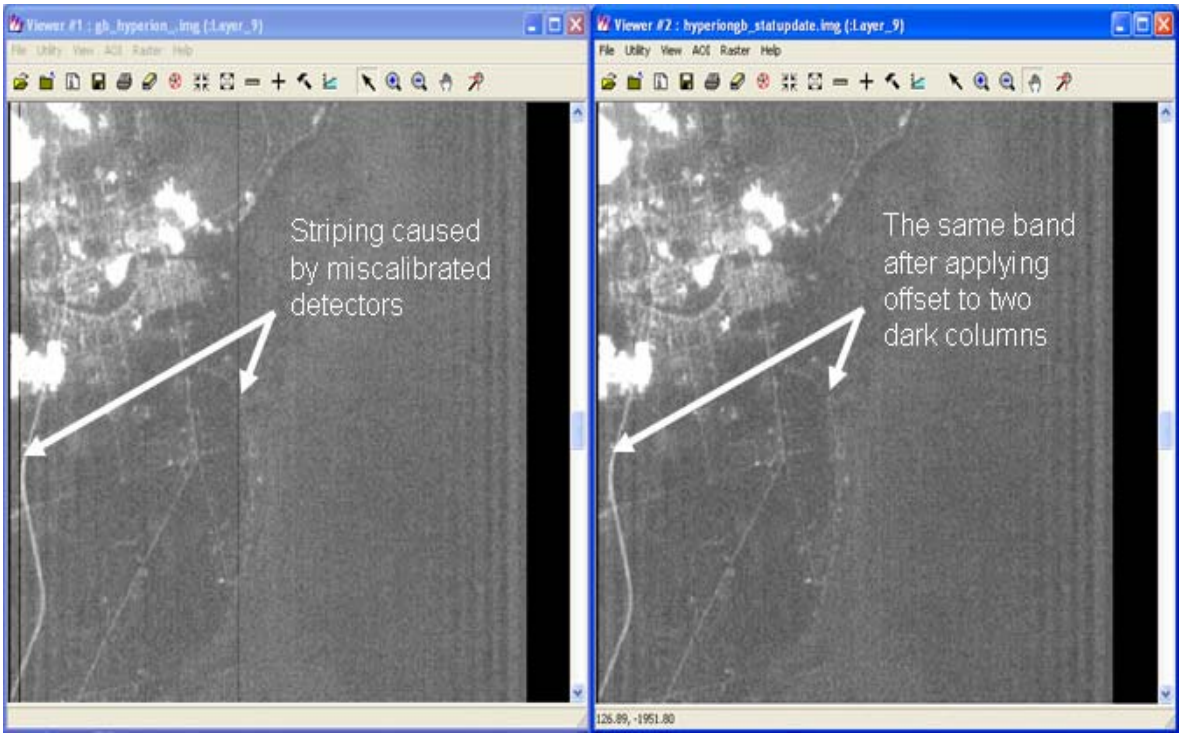

Figure 6: Offsets were applied to pixels of the dark columns caused by miscalibrated detectors, normalizing them to the mean of pixels in the two adjacent columns.

4-7: Image Rectification

The panchromatic band of a Landsat 7, ETM+ orthorectified image projected to Albers, NAD 83 was used as a base map for georectification. The Albers projection is standard for the GLEI project from which the ETM+ image was acquired. The 15 meter cell size provided adequate resolution and the terrain correction insured that the geographic fidelity was consistent throughout the image.

Twelve control points were selected from throughout the entire Hyperion image. The 3 of these with the largest residuals were rejected. The remaining 9 were used for a 2nd order polynomial transformation. The resulting transformation had an estimated total RMS error of .2962 pixels or about 4.443 meters. Nearest neighbor resampling was used to retain as much spectral fidelity as possible. Visual analysis of the rectified image overlaid on the ETM+ image confirmed that rectification was successful.

4-8: Bad Bands

While the Hyperion sensor was designed with 242 bands, the level 1R data is delivered with 44 of those bands set to zero. The data in these bands were judged to have too low a signal to noise ratio to be usable. Among the remaining bands there are several that contain enough noise that they are often removed before image analysis. Bands with excessive noise can be identified visually and are generally found in the spectral ranges where atmospheric water vapor absorbs most of the incident and reflected light (Datt et al., 2003). There is also spectral overlap between the SWIR and VNIR sensors making two pairs of bands redundant.

Visual inspection showed that an additional 51 of the SWIR bands had very poor signal to noise ratios. These bands were removed from image analysis. No additional bands from the VNIR sensor were removed from the data. This left a total of 147 bands for spectral analysis—50 from the VNIR sensor and 97 from the SWIR sensor. The bad bands were removed from the image analysis.

4-9: Minimum Noise Fraction

Minimum Noise Fraction (MNF) is a modified Principal Component transform which can be used with hyperspectral imagery. It can be used to generate a transformed image where the systematically occurring noise is segregated into progressively noisier bands and, conversely, meaningful image information is concentrated into fewer bands (ERDAS, 2002a). The noisiest bands can be eliminated from further processing. This reduced dimensionality has the further advantage of reduced computational demands during processing.

Classification can be performed on the MNF bands with the least noise or the transformation can be reversed to reconstruct an image with the original number of layers minus some of the noise. Alternatively, the MNF transform can be calculated with each iteration of the analysis algorithm without outputing an MNF image. The later approach was used.

The MNF transform can be based on the entire image or a subset of the image. Using a homogenous area of the image to calculate the transformation helps to isolate systematic noise from meaningful image information (ERDAS, 2002a). An area of open water was used to calculate the transform that was then applied to analysis of the study area of the image.

In part, the decision to use the MNF transformation was based on trials with the Spectral Correlation Mapper and the target detection routine where it improved the selectivity of the training samples. Training samples extracted from the best of the field-identified *Phragmites* sites were run with and without the MNF transformation. The

MNF transform trials identified fewer pixels overall and more often identified pixels relating to known areas of *Phragmites*. In addition, MNF is widely used with hyperspectral data (Apan et al., 2004; Hirano et al., 2003; Kruse et al., 2003). Finally, Datt et al. (2003) demonstrated that when MNF is applied to Hyperion data with the striping anomalies corrected the resulting noise reduction compares favorably with the noise reduction achieved in HyMap airborne hyperspectral sensor data.

CHAPTER 5: METHODOLOGY - Image Analysis

5-1: Overview

The primary focus of image analysis was use of the spatially referenced training data to produce a classification that would show the locations of large monodominat stands of *Phragmites*. Two strategies were used to accomplish this. First, a target detection routine was applied to the Hyperion image to produce a "yes/no" map of predicted areas of dense *Phragmites*. Second, an unsupervised classification assigned 200 spectrally distinct classes from the Hyperion data to ground cover classes, including *Phragmites*, based on the spatially referenced training data. In addition, classes in the unsupervised classification were merged to broader classes to show the pattern of lakeward expansion of the emergent wetlands relative to the Wisconsin Wetlands Inventory and 1998 Ortho Photos.

5-2: Target Detection

Spectral Angle Mapper (SAM) is an analysis algorithm which treats spectra as n-dimensional vectors where n is the number of bands in the image and in the training data (figure 7). The theory is that difference in angle between vectors of two different spectra is a measure of the similarity (or dissimilarity) of the materials reflecting the light (Kruse et al., 1993). Spectral Correlation Mapper (SCM) is a refinement of the SAM algorithm. Where SAM cannot distinguish between positive and negative correlation, the SCM algorithm standardizes vectors prior to calculating the spectral angles such that positive and negative correlations between samples can be distinguished (Lumme, 2004).

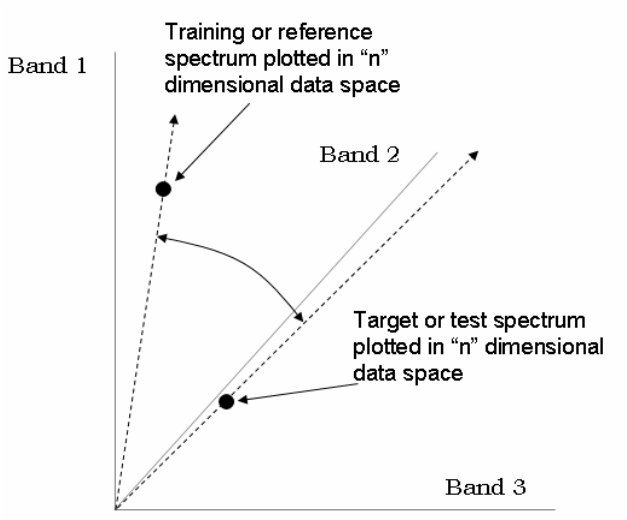

Figure 7: The SAM algorithm calculates a vector passing through a point plotted in "n" dimensional data space based on the values for each band of data used. The angle between the vector of a reference spectrum and a test spectrum quantifies the two points' spectral similarity or dissimilarity.

(Based on Kruse et al., 1993)

Several factors were considered in deciding to use the Spectral Correlation Mapper algorithm. The Spectral Correlation Mapper is presented as a refinement of SAM which has broad application in hyperspectral remote sensing of vegetation (Artigas and Yang, 2004; deLange et al., 2004; Lumme, 2004; Ustin et al., 2004; Eckert and Kneubühler, 2004). SAM and by inference SCM are designed for use primarily with hyperspectral data (Kruse et al., 1993). An additional practical advantage was that SAM and SCM are supported in ERDAS Imagine 8.7 Spectral Analysis Workstation (ERDAS, 2002b) which was the software being used for all other steps of the image processing and analysis.

Training data spectra (described in a previous section) were extracted from the Hyperion image using the tools in the Spectral Analysis Workstation. An overlay of the GPS points where *Phragmites* had been identified in the field was used to locate the pixels associated with those sample sites in the image. Spectra were extracted from these single pixels and compiled in "Spectral Library" files. In some cases field-located *Phragmites* GPS points fell near the boundaries of pixels. In these cases the spectrum of

the pixel adjacent to the sample pixel was extracted and labeled as well. After examination of the digital photos taken at these sites, the maps drawn of these sites at the time of data collection, aerial photographs and graphs of the spectra, some of these adjacent pixels were judged to more probably contain a majority of reflectance from *Phragmites* than the pixel in which the sample site GPS point fell. These adjacent pixels were further tested against the GPS-point pixels in target detection trials and, when judged superior in selecting known *Phragmites* sites, were retained as the training data for the associated sample site.

The target detection dialog box allows generation of either a continuous value or a yes/no output. The continuous value option yields a raster with a range of values corresponding to the degree to which the image pixels match the target spectrum. The yes/no option yields a two class thematic raster showing pixels that meet a user defined threshold for matching the target spectrum. This threshold is defined in radians of separation between the target vector and the image pixel vector as defined by the SCM algorithm.

Initial iterations were done with the yes/no output option which required a user defined threshold. Several trials with different spectra revealed that different targets gave very different results with the same threshold. For example a threshold of 5 radians may yield no pixels within the angle of the threshold for sample A—clearly too small a threshold for that sample. Sample B might yield more than 2,000 pixels which could be seen to fall in several different types of land cover—clearly too large a threshold. The process of trial and error to determine a threshold that produced a selective enough match

to each target spectrum took many trials, each of them taking several minutes of processing time for the computer to generate output.

An alternative approach was devised to decrease processing time. The "continuous" option was used in the target detection dialog box to create a raster with a range of values from 0 to 1. A value of 0 was a match with the SCM vector for the target material. A value of 1 would be the maximum angle of separation from the target vector and presumable the most dissimilar target spectrum. This continuous value raster was then imported into ArcGis 8.3 where it was displayed as a classified raster with two manually defined classes. The class between 0 and the manually defined boundary could then be adjusted to include pixels with greater or lesser angles of difference between the target spectra and the image pixel spectra.

This process was carried out for each of the pixels selected as *Phragmites* training data. The boundary or threshold was repeatedly adjusted until the "low SCM angle" class (between 0 and the user defined threshold) overlaid known *Phragmites* locations and probable *Phragmites* locations but did not overlay areas known not to contain significant *Phragmites* populations. The target spectra from some training samples produced output that corresponded well with the location of other known stands of *Phragmites*. The thresholds for these samples were adjusted to include many pixels in the presumed *Phragmites* class. Other training samples produced layers that seemed to have less relationship with known and probable *Phragmites* locations. For these samples the threshold was lowered until they included only a small number of pixels which could not be ruled out as *Phragmites* locations.

This approach relied considerably on reference data to determine the degree to which each training sample would contribute to the final classification. If a training sample's SCM output was selective of other known *Phragmites* locations from the training samples, this was a basis for expanding its threshold and in turn its contribution to the classification. On the other hand if a training sample's SCM output was selective of areas shown to be improbable locations of *Phragmites* that was a basis for constricting the sample's threshold and in turn decreasing its contribution to the classification. Reference data used included digital photographs taken during field data collection, aerial photographs from April 1998, digitized USGS 1:24,000 quadrangle maps, USGS Digital Elevation Models, and the Wisconsin Wetlands Inventory in digital format.

Table 2: Thirteen training samples collected during August, September and October of 2004 were used for the target detection classification.

sample point id	number of pixels	Percentage of total pixels mapped as *Phragmites*
bp3	61	9.53%
bp2	16	2.50%
bp1	32	5.00%
ap3b	16	2.50%
dp1n1w1	20	3.13%
dp3	42	6.56%
cp7	21	3.28%
cp6e1	67	10.47%
cp5e1	62	9.69%
cp4w1	99	15.47%
cp2	60	9.38%
r13	126	19.69%
cp1e1	18	2.81%
total	640	100.00%

Thirteen training samples were included in the final classification. The number of pixels that each sample contributed to the classification ranged from 16 pixels for point

bp2 to 126 pixels for r13 (table 2). In many cases the pixels selected by one training sample overlapped the pixels selected by other training samples. However, the majority of pixels in the final classification were unique to the layer of only one training pixel.

The 13 layers generated by this process were combined to create one thematic layer with only two classes—a *Phragmites* dominant class ("*Phragmites*") and a *Phragmites* subdominant class ("not-*Phragmites*"). The "*Phragmites*" class was defined as where dense *Phragmites* (coverage class 5 or 6) covered more than half of the sample site or where less dense *Phragmites* (cover class 3 or 4) covered all or nearly all of the sample site or some combination of dense and less dense *Phragmites* that resulted in *Phragmites* being the majority vegetation in the canopy. In the final thematic map (appendix A) the "*Phragmites*" class was the union of the "*Phragmites*" layers from all 13 training samples. The "not *Phragmites*" class of the final thematic map was any pixel not classified as "*Phragmites*" in any of the 13 layers.

5-3: Unsupervised Classification

The second strategy tested to identify dense stands of *Phragmites* was unsupervised classification. The same study area was used for the both target detection and the unsupervised classification. The same 147 bands used in the target detection routine classification were used in the unsupervised classification. The bands set to zero prior to distribution of the data and the bands determined to be too noisy by visual inspection were removed and a new 147 band image file was created. Preprocessing of the data was the same as for the target detection routine with the exclusion of the MNF transform.

The ISODATA algorithm sorts pixels into clusters by determining the "minimum spectral distance" from a user defined number of mean cluster locations in n-dimensional data space. In the initial iteration the means are established automatically or provided by the user. The initial set of clusters is used to recalculate new mean locations for the next iteration. Pixels are then regrouped by minimum spectral distance to this new set of means. This process repeats either a user defined number of iterations or until iterations produce a user defined minimum amount of pixel regrouping. (ERDAS, 2002a) These pixel groupings are output as a classified image and associated signature file. This process creates a thematic map of pixels with similar spectral characteristics as defined by the ISODATA algorithm. It is the assumption of spectrally based remote sensing that these spectrally defined classes correlate with land cover classes. The corresponding land cover classes must be assigned by an analyst based on some form of reference data.

Initial clustering trials generated 77 and 150 spectral classes. Comparison of these classifications to the field data showed that many of the spectrally defined classes clearly overlapped 2 or more of the 11 land cover classes defined by the study. The increase from 77 to 150 classes or clusters decreased this overlap somewhat. However, in many cases the new subclasses were within classes that were not of primary interest to the study rather than subclasses within the wetland vegetation areas. The decision to use 200 classes was based on this diminishing return of adding classes versus the additional time required to assign those spectral classes to land cover classes. Additionally, as the number of spectral classes was increased the likelihood of any reference data being

associated with a given class decreased. Without reference data the additional spectral classes could not be associated with ground cover classes.

Each spectral class or cluster was assigned to one of 11 classes of land cover. Two of those classes—clouds and open water—were masked out of the accuracy assessment. The remaining 9 classes are the same as for field data collection (table 1). Class assignments were made based on GPS locations of known vegetation and digital photographs from field data collection. Digital Ortho Photos, digitized USGS quadrangle maps, and digital elevation model maps were used as well. For the final map (appendix B), "forestD," "forestC" and "scrub/shrub" were merged into a single class, "woody vegetation."

5-4: Accuracy Assessment

The number of sample points required for a statistically sound estimate of remote sensing accuracy varies with the purpose, scale and location. In most cases, however, meeting ideal statistical standards exceeds the resources of the study. Congalton (1991) points out that a one-half percent sample of a Landsat Thematic Mapper scene would be 300,000 pixels. It is necessary then to make concessions to practicality, and the rule of thumb of 50 samples for each land cover class was used as a guide for this study (Congalton, 1991).

Collecting data for 450 sample points (50 points per class for all 9 vegetation classes of the unsupervised classification) would be beyond the resources of this investigation. Congalton endorses the practice of adjusting the number of points collected per class based on the objectives of the study and the importance of the class

(Congalton, 1991). The primary objective of this study was to determine the feasibility of detecting *Phragmites* within Hyperion imagery. Fifty points were collected within the "*Phragmites* dominant class" of the target detection routine and 50 points were selected for the "*Phragmites*" class of the unsupervised classification. An additional 50 points were selected from the "*Phragmites* sub-dominant or absent" class of the target detection routine. These points would be randomly distributed across the 8 non- *Phragmites* vegetation classes of the unsupervised classification and would serve as the sample points for those classes as well.

Quantitative assessment of the two classifications required that a probabilistic sampling scheme be used to locate accuracy assessment sample points. Because *Phragmites* only occurs in a small proportion of the study area, a simple random sampling scheme would almost certainly under-sample *Phragmites*. This made it necessary to use some form of stratified sampling that would place an adequate number of sample points in areas of actual *Phragmites* and in areas of predicted *Phragmites*.

Phragmites culms from one season's growth generally remain standing into the next growing season and in some cases may persist for as long as 4 years (Windham, 2001). This allowed field work for accuracy assessment to be carried out the following spring. Because of this it was possible to use the classified images as the basis for strata in the sampling scheme.

Allocating sample points on the basis of the classified image presents some statistical problems. For example, if the classification is quite inaccurate, the sample points-per-class may measure the errors of commission (predicted material of interest

which is not actually the material of interest) but do not measure the errors of omission (the proportion of the material of interest that went unpredicted by the classification). This arises from the fact that if the samples are not simply random within the study area and if the allocation of sample points is based on a largely errant classification, then it is not possible to infer the actual distribution of the classes within the study area. Without knowledge of the actual land cover proportions it is then not possible to determine the errors of omission, (how much of the target material was missed) or how much better than random the classification is.

All of these shortcomings were balanced against the need to design a sampling scheme which would provide information about the *Phragmites* class and still be within the resources of this study. In the end a scheme based on what Stehman and Czaplewski (1998) describe as two-stage cluster sampling was used. In this type of scheme "primary sampling units" or clusters are randomly selected and then further selection of secondary sampling units is made within those larger units (Edwards et al., 1998).

A vector layer of the unsupervised classification was created in ArcGis 8.3. The area of the Water1 (open water) and cloud classes were removed from the layer. This did not completely remove cloud compromised pixels from the layer so a mask was created that eliminated the cloud affected areas from selection for accuracy assessment. Within the remaining area of the layer, 12 random points were selected by using an add-on extension (Hawth's Analysis Tools, 2002) in ArcGis. Around these twelve points 11-pixel by 11-pixel primary sampling units were created. For points near the edge of the study area or near the excluded cloud and open water areas, adjustments were made so

that each primary sampling unit included the same area and the same number of pixels (figure 8). The total area of these 12 windows was the sampling frame.

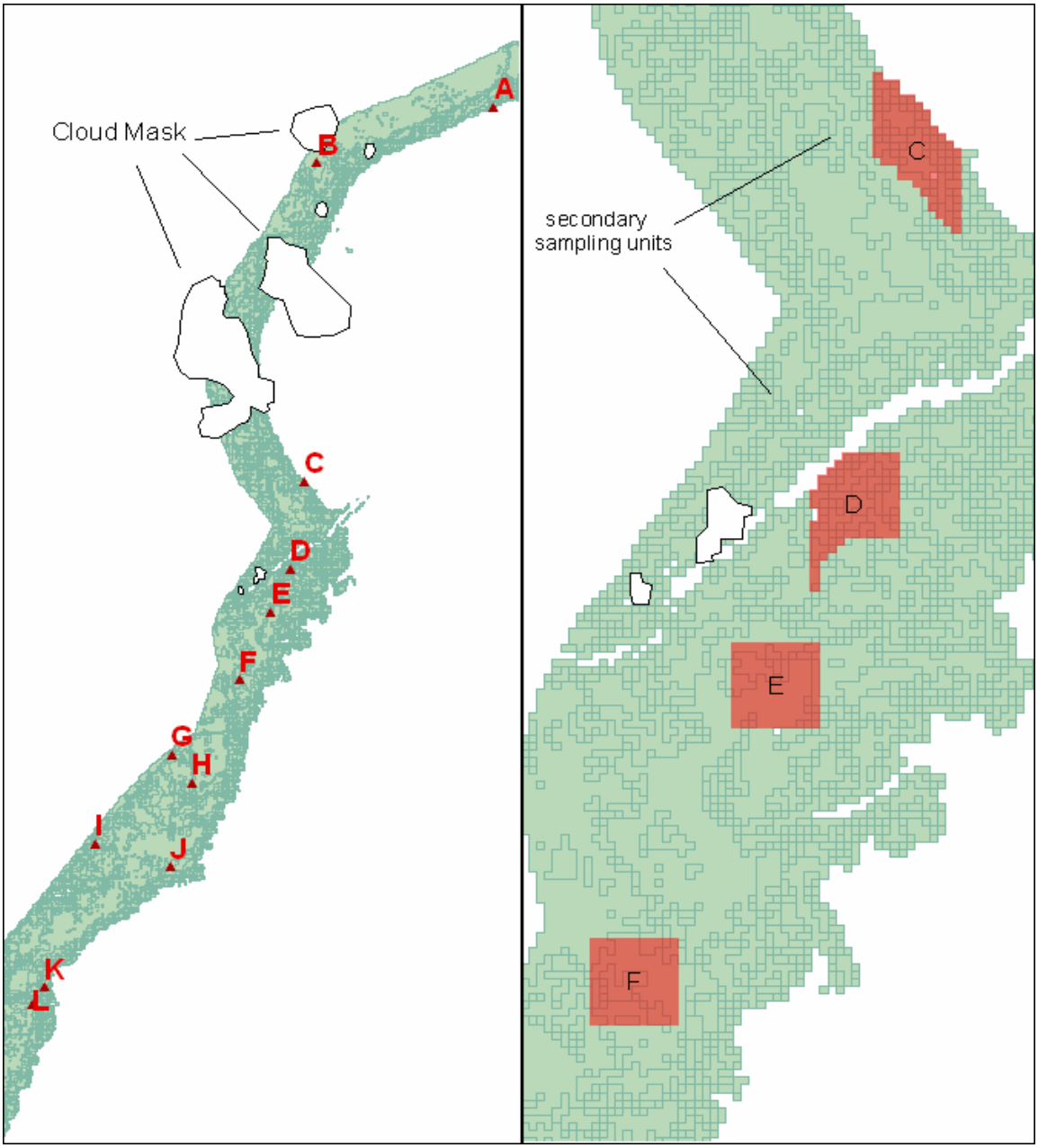

Figure 8: Secondary sampling units were located by 12 points randomly selected within the study area.

Sixty-seven of the 1452 pixels within the sampling frame were classified as *Phragmites* in the unsupervised classification. Approximately 50 of these would need to be verified by field collected ground truth for accuracy assessment. To randomly reduce the 67 pixels to 50 pixels, 16 points were randomly selected within the area of the 67 pixels. The 16 pixels selected by these points were eliminated from the original 67 pixels. When more than one point fell in a pixel, the nearest pixel where no points fell was selected for elimination. This left 51 *Phragmites* pixels for accuracy assessment field data collection.

In the target detection routine classification, only 35 of the "*Phragmites*" class pixels fell within the 1452 pixels of the primary sampling units. To bring the number of accuracy assessment field data collection points to 50 for the target detection classification, the sampling frame was expanded to include pixels within 60 m (two pixels) of the primary sampling unit boundaries. This produced 50 pixels in the "*Phragmites*" class of the target detection classification to be used as accuracy assessment sample points.

The 50 accuracy points for the non- *Phragmites* classes of both classifications were chosen by random selection from all of the area within the primary sampling units that was not classified as *Phragmites* in the unsupervised classification. At least two significant compromises arise from this shortcut. First, 2.75 percent of the sampling frame, concentrated in areas with a high likelihood of having *Phragmites*, was excluded from the target detection routine classification's "not *Phragmites*" class point selection. Second, this relied on chance to allocate sample points among the 8 non-*Phragmites*

classes of the unsupervised classification. While some classes were clearly underrepresented in this sample, the distribution did generally follow the distribution of the classification.

These compromises were a trade off for having the same 50 "not *Phragmites"* points serve the accuracy check of both classifications. This and the overlap of points in the *Phragmites* classes of both classifications, allowed 200 points (50 *Phragmites* and 50 non- *Phragmites* for each classification) to be compressed into only 131 actual field collection sites. This was judged to be close to the maximum number of sites that could be collected by the three person sampling team in the three days available for field work.

CHAPTER 6: RESULTS

6-1: Target Detection

The target detection approach produced the best map of monodominant stands of *Phragmites* (appendix A). The overall accuracy of the target detection classification was 68.3 percent (table 3). Producer's accuracy for the "*Phragmites*" class was 91 percent with 21 of the 23 ground truth samples dominated by *Phragmites* having been predicted. For the "not-*Phragmites"* class, 48 of the 78 *Phragmites* samples were correctly predicted for a producer's accuracy of 62 percent. For the "*Phragmites"* class, errors of commission were higher. Twenty-one of the 51 predicted *Phragmites* samples were actually *Phragmites*—a user's accuracy of 41 percent. However, for the "not-*Phragmites*" class, the target detection classification correctly predicted 48 of the 50 samples—a user's accuracy of 96 percent. Much of the *Phragmites* mapped by the target detection classification occurred on the newly exposed soil and associated shallow water created by lower water levels (figure 9).

Table 3: Error matrix for the target detection classification.

Target Detection Classification		Reference Classification		Target Detection totals	User's Accuracy
		Phragmites	Not *Phragmites*		
	Phragmites	**21**	30	51	41%
	Not *Phragmites*	**2**	**48**	50	96%
	Reference total	23	78	101	
	Producer's Accuracy	91%	62%		Overall Accuracy 68.3%

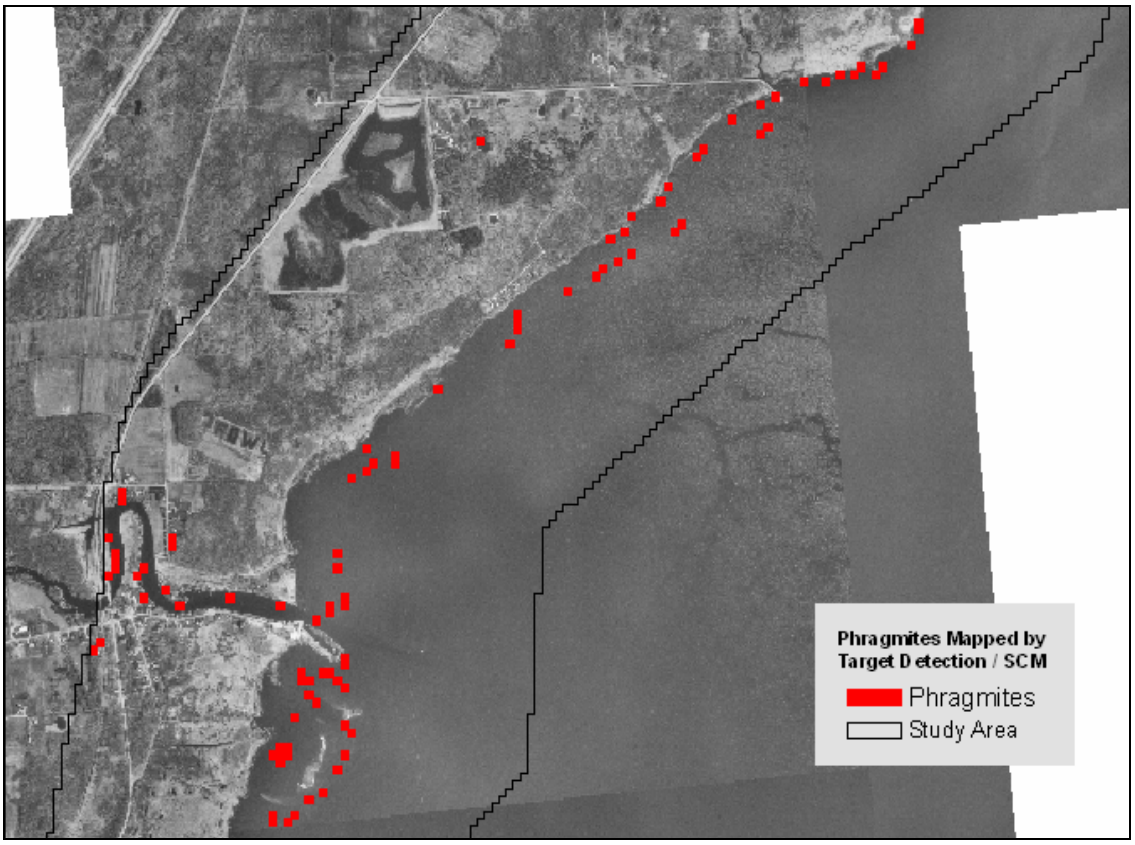

Figure 9: The majority of *Phragmites* was mapped on the newly exposed mudflat and the associated shallows created by the lowered water levels.

An error matrix distributing the target detection classification's errors across all of the reference data classes shows the types of land cover where the errors occurred (table 4). The largest category of errors (n = 7) in the target detection classification was of samples predicted to be *Phragmites,* but found to be "meadow." Six of these 7 errors resulted from a single training sample, Dp1n1e1. This training sample was taken from a typically long narrow stand of *Phragmites* in a drier location, atypical of the majority of training samples. It was bounded by mix of vegetation on the east side that included forbs (thistles and goldenrod) and by an area with some exposed wet soil on the west edge which appeared to have been driven on during the 2004 growing season.

Table 4: Error matrix for the target detection classification over all reference data classes.

Target Detection Classes	Target Detection (over all reference classes)	Reference Classes											
		ForestC	ForestD	Impervious	Meadow	MixedEm	other	*Phragmites*	Scrub	*Typha*	Water2	Target Detection	User's Accuracy
	Phragmites	2	2		7	5	1	21	3	5	5	51	41.2%
	Not *Phragmites*	4	5	2	12	9		2	10	3	3	50	96.0%
	Reference Classification Totals	6	7	2	19	14	1	23	13	8	8	101	
	Producer's Accuracy	67%	71%	100%	63%	64%	0%	91%	77%	38%	38%	Overall Accuracy 68.3%	

Three classes which typically occur in the same context as *Phragmites* and are often intermixed—"mixed emergent," "*Typha*," and "water2"—account for much of the remaining error. There were 5 errors of commission associated with each of these classes (tables 4 and 5). Four of the 5 mixed-emergent ground truth samples which had been misclassified as "*Phragmites"* were found to contain some *Phragmites* in the field, but it was not the dominant cover type. Three of these 5 samples were mixed pixels containing significant proportions of more than three cover type classes. Two of the sample units had open water and one other had approximately 4 cm of standing water.

Table 5: **Accuracy sample points for errors in target detection classification**

Reference class	Point ID	Sample Point Description
ForestC	G02	Tree farm, tall pines with very little understory vegetation, small area of short (<5M) deciduous
ForestC	H04	Tree farm, tall pines with very little understory vegetation, somewhat open canopy
ForestD	D01	Quite mixed pixel at the end of line of trees, also area of grasses, forbs, emergent & shrubs and some open water
ForestD	D14	Deciduous canopy, semi open, shrub understory sparse, river at edge of pixel

Meadow	D04	Mostly mixed grasses/meadow, transition as water's edge includes some *Phragmites,* open water small portion of sample unit
Meadow	D07	Dominated by *Calamagrostis,* some *Typha* no standing water, *Typha* litter
Meadow	D09	Predominantly grasses, meadow, with some *Typha* mixed in a the center of the sampling unit, soggy ground
Meadow	D10	Equally divided between grasses with a few goldenrod and *Typha,* no standing water or bare soil.
Meadow	D12	More than 1/2 grasses, *Typha* area and mixed emergant areas make up rest of pixel
Meadow	E02	Grassy meadow mix, plowed land at edge, trees, and some sparse *Phragmites,* originally called "other"
Meadow	E06	Predominantly grasses with isolated areas of *Typha, Phragmites,* and corn, soggy throughout.
MixedEm	C25	Center of pixel scirpus, *Typha,* and sedges. / *Phragmites* to the north, sparse phrag to the southeast, sparse *Phragmites* to the sw
MixedEm	D03	Few *Phragmites, Typha,* sedges, mixed emergent, about 1/2 open water
MixedEm	D19	Mixed emergent with only edges of open water on one side and shrubs/trees on the other
MixedEm	J04	Mixed emergent with a sparse mix of *Phragmites* to the northwest
MixedEm	J06	Mixed emergent with a lot of exposed soil 3 or 4 cm of water, sparse *Phragmites* shoots and litter from last year
other	G07	1/3 road & gravelly sholder, 1/3 ditch with some water, 1/3 shrubs at edge of trees, shadows from trees
Scrub	D15	mixed pixel with meadow with shrubs at center, water at north edge and trees at edges east and west
Scrub	D17	Sparse *Phragmites* in north third, shrubs in center and trees to the south, water at north edge
Scrub	D18	shrubs, water at very north edge
Typha	C15	Typha in standing water at edge of shore, lots of severed *Typha,* data sheet shows *Phragmites* to north, south and east
Typha	K08	Very mixed pixel, *Typha* dominant in at least the center 1/2 of the pixel, dense *Phragmites* to the west, open water to east
Typha	K13	*Typha* dominant in center of pixel some open water the east, an area of *Phragmites* to the north center of the pixel
Typha	K14	*Typha* dominant, open water to the northeast corner of pixel, *Phragmites* to the northwest, probably out of the pixel
Typha	L14	*Typha* and open water, standing water 30 cm
Water2	C06	*Typha* in standing water at edge of shore, lots of severed typha, data sheet and digital photos show *Phragmites* to the west
Water2	C22	About 1/3 of the pixel is *Phragmites* in standing water, about 1/2 open water, remainder is *Typha*
Water2	L01	Open water in the middle of the Pensaukee river.
Water2	L06	Open water in the middle of the Pensaukee river.
Water2	L10	Open water in the middle of the Pensaukee river.

Of the 5 samples predicted to be "*Phragmites*" which were actually "*Typha,*" 4 did contain some *Phragmites*. None of these sample sites was dominated by any single vegetation or land cover class. All five of these sample units contained some open water.

Three of the 5 sampling units misclassified as "*Phragmites*" but found to be "water2" were in the open water of the Pensaukee River mouth (see discussion). The other two samples contained some "*Phragmites*." All five sample units had some open water or standing water.

6-2: Unsupervised Classification

For the unsupervised classification, two-hundred spectral classes were defined using the ISODATA algorithm. The clusters with the largest membership tended to be outside the wetland areas and were predominantly assigned to the "forest," "meadow," "scrub" and "water1" classes. The clusters in the wetland areas tended to have smaller membership and were consequently more numerous. Class assignment for the larger membership clusters ("forestD" and "meadow") was straightforward. There was greater ambiguity among the smaller more numerous clusters located in the wetland areas. Spectral classes that corresponded to *Phragmites* sample points generally did not overlap multiple areas of known *Phragmites*. This was consistent with the visual comparison of *Phragmites* training samples' spectra (figure 14) which shows greater variability within the *Phragmites* samples as a group than between that group and *Typha*.

While some of the woody vegetation classes (forestD, forestC and scrub) include areas of forested wetland, the objective of this study was to distinguish *Phragmites*. With only 3 of 51 predicted *Phragmites* sites falling in areas that were found to be "scrub" and

none in either of the forest classes, these three classes were merged into a single "woody vegetation" class for the thematic map of the unsupervised classification (appendix B) as well as in the error matrix.

Table 6: Error matrix for unsupervised classification.

		Reference Classification									
Unsupervised Classification	Unsupervised Classification Woody Classes Merged	Impervious	Meadow	MixedEm	other	*Phragmites*	*Typha*	Water2	Woody Vegetation	Unsupervised Classification totals	User's accuracy
	Imperv	**1**	2							3	33.3%
	Meadow		**6**	2						8	75.0%
	MixedE		1	**3**					1	5	60.0%
	Phrag		1	8	2	**19**	8	10	3	51	37.3%
	Typha		1	2		1		1		5	0.0%
	Water2							**2**		2	100.0%
	Woody	1	2	2		1	3		**18**	27	66.7%
	Reference totals	2	13	17	2	21	11	13	22	101	
	Producer's Accuracy	50.0%	46.2%	17.6%	0	90.5%	0.0%	15.4%	81.8%		Overall Accuracy 46%

The error matrix (table 6) shows that out of the 21 ground-truth points that were found to be "*Phragmites*," 19 were classified as *Phragmites* by the unsupervised classification—a producer's accuracy of 90.5 percent. This translates to very few errors of omission in the "*Phragmites*" class. However, errors of commission were high for the unsupervised classification *Phragmites* class. Of 51 points selected from the "*Phragmites*" class, only 19 were shown to meet the "*Phragmites"* class criteria by the ground-truth data—a user's accuracy of only 37.3 percent.

Eight of the pixels classified as "*Phragmites*" were found in the field to be "mixed emergent." Six of these 8 were verified to contain some *Phragmites* and the other two

had been mown, making it difficult to determine dominant land cover at the time of image collection (table 7).

Eight of the sample points classified as *Phragmites* were found in the field to be *Typha* (table 7). Of these, 5 contained some *Phragmites*. Six of these sample points also included either standing or open water.

Table 7: Accuracy sample points for errors in unsupervised classification.

Reference classification	POINT ID	Sample Point Description
Meadow	D04	2/3 mixed *Calamagrostis, Phalaris,* very sparse *Typha;* remaining 1/3 grasses, goldenrod, *Phragmites* & open water
MixedEm	C01	mostly mixed emergent, western 3/5 mown; eastern edge stands of *Spartina* & *Phragmites* open water
MixedEm	C20	mixed emergents including *Phragmites, Typha*, and sedges; Large stand of *Phragmites* at the eastern edge
MixedEm	C26	southern 1/2 is a backyard with large broadleaf trees; northern 1/2 is mown emergents
MixedEm	D03	Few *Phragmites Typha,* sedges, mixed emergent, 1/2 open water
MixedEm	D19	Mixed emergent with only edges of open water on one side and shrubs/trees on the other
MixedEm	J07	mixed emergent vegetation including *Scirpus, Carex* and very sparse *Phragmites*
MixedEm	J08	Mixed emergent including *Scirpus,* other sedges, also *Salix* and some very sparse *Phragmites*
MixedEm	L17	Mixed emergent including *Scirpus,* sparse *Typha* and *Salix,* stand of *Phragmites* at north edge
other	G06	1/3 road & gravelly sholder, 1/3 ditch with some water, 1/3 shrubs at edge of trees, shadows from trees
other	G07	1/3 road & gravelly sholder, 1/3 ditch with some water, 1/3 shrubs at edge of trees, shadows from trees
Scrub	D15	Mixed pixel with meadow with shrubs at center, water at north edge and trees at edges east and west
Scrub	D17	Sparse *Phragmites* in north third, shrubs in center and trees to the south, water at north edge
Scrub	D18	Shrubs, water at very north edge
Typha	C02	Center (1/2) of pixel *Typha* in 30+cm of water, med density *Phragmites* in west & sw 1/3 of pixel; open water in east fraction

Typha	C08	*Typha* in standing water, sheared off stems, nw 1/3 open water
Typha	K07	2/3 *Typha* in standing water, far right edge open water, *Phragmites* to nw just less than 1/4 of pixel, to west and south edges of pixel
Typha	K08	Very mixed pixel, *Typha* dominant in at least the center 1/2 of the pixel, dense *Phragmites* to the west, open water to east
Typha	K12	*Typha,* open water to the ne edge
Typha	K13	*Typha* dominant in center of pixel some open water the east, an area of *Phragmites* to the north center of the pixel
Typha	L13	*Typha* and *Typha* litter, shallow standing water 10cm+/-
Typha	L14	*Typha* in shallow standing water, *Phragmites* at extreme sw edge
Water2	C06	Center 1/5 of pixel *Typha* in standing water, mostly open water, moderate to low density *Phragmites* to the west edge
Water2	D06	Western 3/5 of pixel shallow open water, narrow band of *Scirpus* at waters edge and 1/5 of pixel grasses
Water2	L01	Open water
Water2	L02	Open water
Water2	L03	Open water with sliver of bank *(Salix,* trees, shrubs, some rushes)
Water2	L04	open water with 1/5 pixel bank *(Salix,* sparse *Phragmites)*
Water2	L05	1/2 open water, 1/2 someone's yard and house, road at so edge.
Water2	L06	Open water in the mouth of the Pensaukee river
Water2	L07	Open water with tree and rocks in nw corner
Water2	L08	Open water

Ten of the 51 ground truth points predicted to be *Phragmites* were found to be "Water2" (tables 6 and 7). This was the most common error in the unsupervised classification. Eight of these 10 errors were in the mouth of the Pensaukee River, in shallow water and within approximately 30 m of the bank (see discussion). Four of these eight sample points contained only open water (L1, L2, L6 and L8; table 7), while the remaining four sample points contained as much as one third land. The other two sample points where predicted *Phragmites* was found to be "Water2" were both mixed pixels containing open water and vegetation which included but was not limited to *Phragmites*.

The *Typha* class was the least successful from both the producer's and user's accuracy perspectives. Of 11 ground truth samples that were found to be *Typha*, none

were predicted by the unsupervised classification. The 5 pixels predicted to be *Typha* all turned out to be other classes: "mixed emergent," "meadow," "*Phragmites*" and "water2."

6-3: Spectral Separabilty of Typha and Phragmites Training Samples

Visual comparison of spectra from pixels selected as *Phragmites* training data showed considerable variation among samples (figure 10). This variation is of particular importance in the red edge portion of the spectrum (figure 11) between the red absorption minimum (approximately 670 nm) and the near infrared maximum (between 700 and 800 nm) (Lillesand and Kiefer, 2000). This portion of the spectrum is of primary importance in vegetation studies (Datt et al., 2003; Schmidt and Skidmore, 2003).

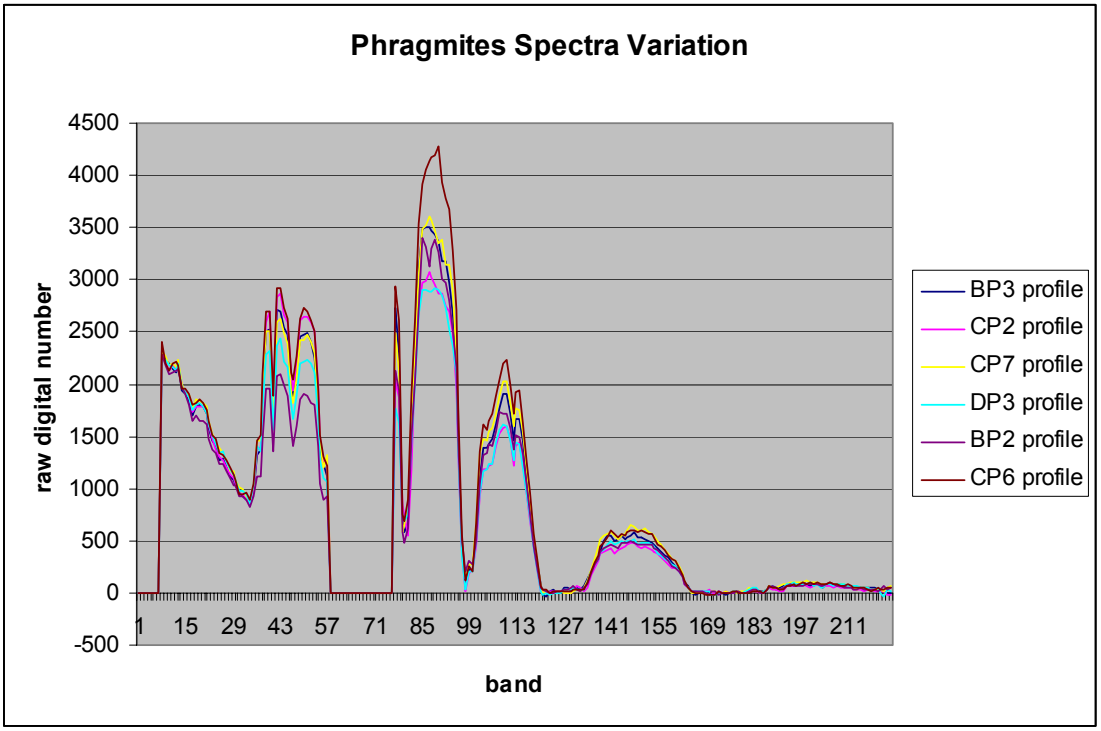

Figure 10: Variation among *Phragmites* training spectra across all Hyperion bands.

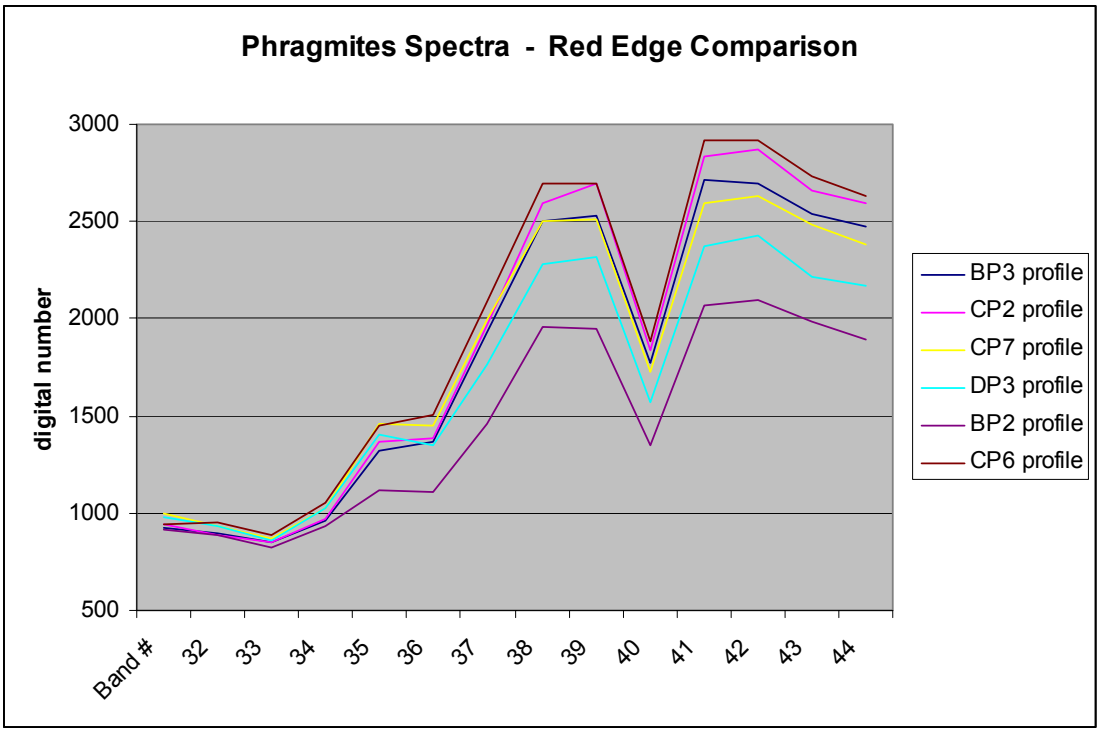

Figure 11: Variation among *Phragmites* training spectra across red and infrared bands.

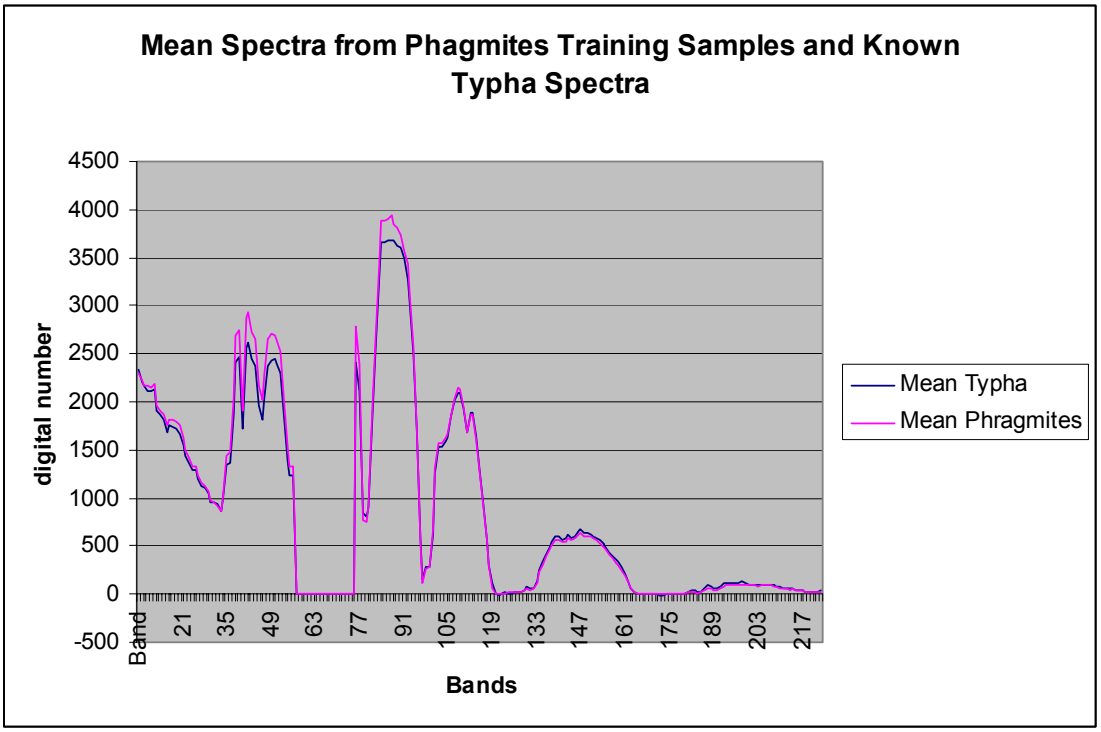

Figure 12: Comparison of mean *Phragmites* spectra to mean *Typha* spectra across all Hyperion bands.

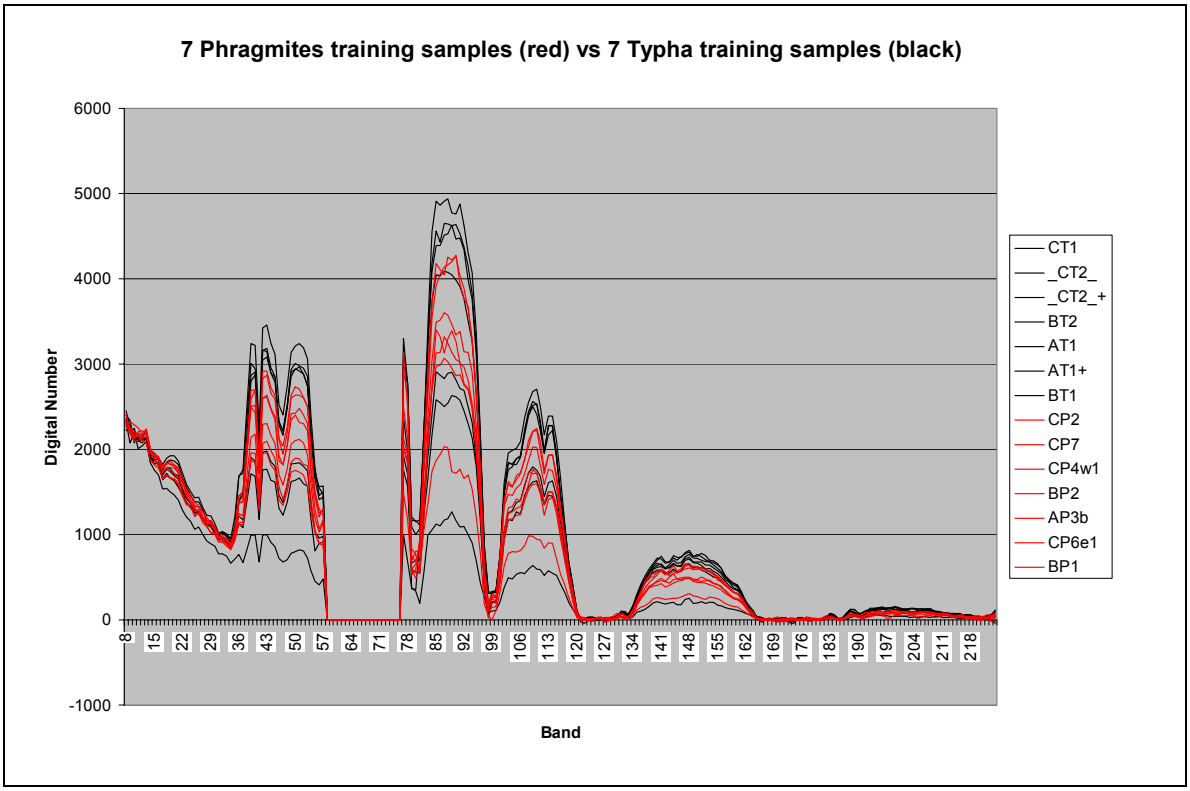

Figure 13: Comparsion of 7 *Phragmites* training samples (red) vs. 7 *Typha* training samples (black).

Simple visual comparison of the mean spectra of the Phragmites training samples with the mean spectra of the Typha training samples shows that they are quite similar (figure 12). More importantly, display of several examples of Typha and Phragmites training samples together shows that the variation in each set of spectra overlaps much of the other set (figure 13). The majority variation in the training sample spectra within these two classes was assumed to result from the various proportions of land cover contributing reflectance to the training pixels, not from variation in the target vegetation itself.

6-4: Change since the Wisconsin Wetlands Inventory

Water levels in Green Bay rise and fall following the historic pattern of broad water level fluctuations in the Great Lakes over periods of 10 to 30 years (NOAA, 2005). The mean water level in Lake Michigan during September of 2004 when the Hyperion image was acquired was 176.29 m (IGLD, 1985) up 35 cm from a 39 year low of 175.94 m the September before (USACE, 2005). Only 18 years earlier Lake Michigan had been at 177.38 m, higher than any year between 1918 and 2004. Comparison of aerial photographs from April of 1998 when water levels were at 176.95 with the Hyperion image taken in September 2004 when water levels were at 176.29, shows the effect that changes in water level have on the shoreline (figure 14). A drop of 37.5 cm has shifted the shoreline between 75 m and 100 m lakeward.

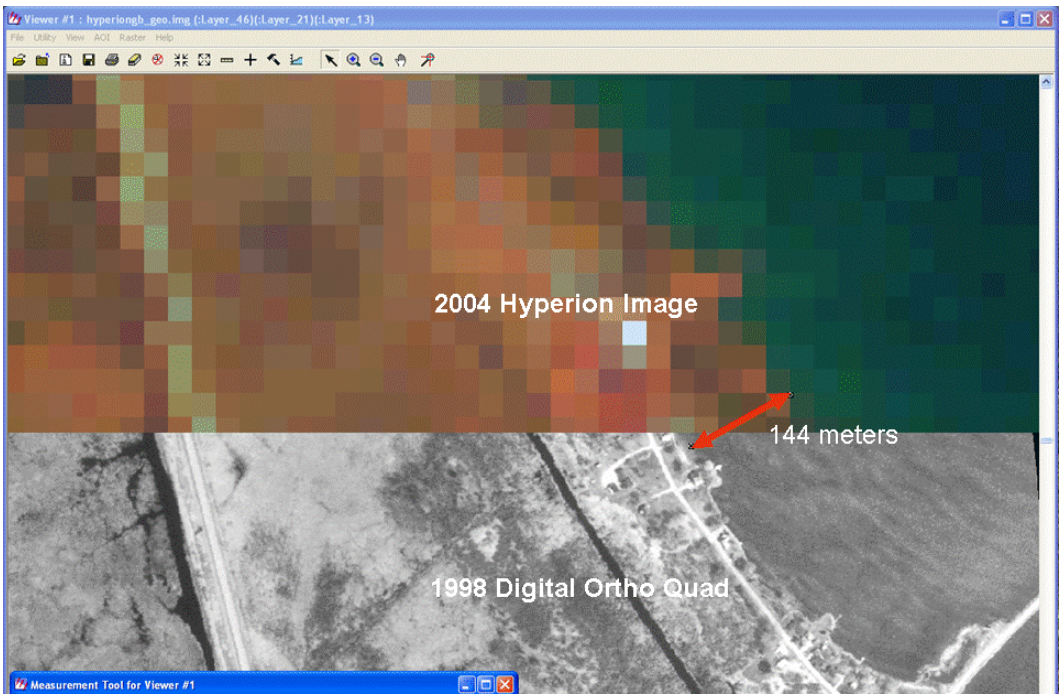

Figure 14: Water levels in 2004 were approximately 37.5 cm. below levels in 1998, (NOAA, 2005) and are reflected in the shoreline change between the 1998 Ortho Quad Photos and the 2004 Hyperion image.

Historically, when the water level and shoreline have changed so have extent and location of wetlands along the coastal margins of Green Bay (Hallett et al., 1977). The lakebed exposed by the relatively low water levels of September of 2004 has been colonized by a variety of emergent wetland vegetation. To map this new emergent wetland area, classes in the unsupervised classification were generalized to combine the two forest classes (forestC and forestD) into a single "Forest" class, and the three emergent vegetation classes (*Typha*, mixed emergent, and *Phragmites*) into a single "Emergent" class. Other classes remained the same (water, impervious, scrub and meadow). Deep water, (water1) and cloud areas were recoded to "unclassified" and are not displayed in the map. Clouds and deep water were also masked for selection of accuracy assessment samples and so are not a part of the error matrix. The "Water2" class is shallow water and was retained to prevent masking out areas of emergent vegetation in standing water. The resulting map (appendix C) shows that the emergent wetlands in the study area have expanded lakeward relative to the 1978 and 1979 aerial photos used to create the Wisconsin Wetlands Inventory (figure 15).

Direct comparison of the areal extent of the emergent wetlands is not possible because of differences in definition of "emergent" by the two maps: the Wisconsin Wetlands Inventory included wetland meadow vegetation in its "emergent" class (Johnston and Meysembourg 2002), whereas this study included it in "meadow," a class which contained both upland and wetland meadows. The lakeward expansion of emergents is real, however. These areas of emergent vegetation that have developed tens of meters lakeward of the 1978 shoreline are new emergent wetland not accounted for in

the original release of the WWI. This illustrates the ephemeral nature of these wetlands and the value that periodically updated remote sensing provides to their study and management.

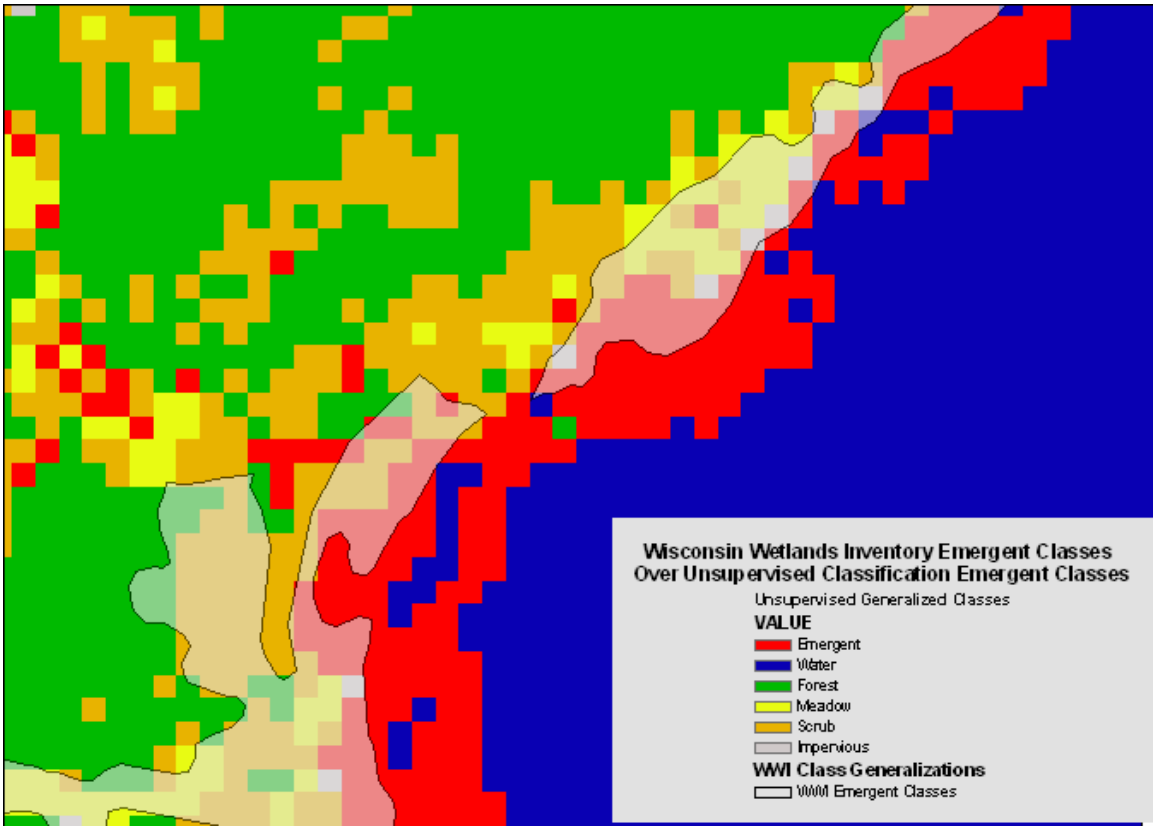

Figure 15: The merged emergent wetland classes from the 2004 unsupervised classification extend tens of meters lakeward, beyond the WWI boundary.

Producer's accuracy for the mixed emergent class was high at 83.7 percent with most of the confusion occurring between the "mixed emergent" and "water2" classes (table 8). Once again the concentration of errors at the mouth of the Pensaukee River accounts for a large proportion of the error—8 of the 20 errors of commission. With the inclusion of these 8 points the user's accuracy for the merged "emergent" class was 67.2

percent. Excluding these 8 points the user's accuracy would be 41 points correctly predicted of 53 emergent wetland accuracy points or 77 percent user's accuracy.

Table 8: Error matrix comparing unsupervised classification with reference classification using merged emergent and forest classes.

		Reference Classification								
		Emergent	Forest	Impervious	Meadow	no data	Scrub	Water2	Classification Totals	User's Accuracy
Unsupervised Classification	Emergent	41			3	2	4	11	61	67%
	Forest	3	6				4		13	46%
	Imperv			1	2				3	33%
	Meadow	2			6				8	75%
	Scrub	3	3	1	2		5		14	36%
	Water2							2	2	100%
	Reference Classification Totals	49	9	2	13	2	13	13	101	
	Producer's Accuracy	84%	67%	50%	46%	0%	38%	15%	Overall Accuracy 60.4%	

CHAPTER 7: DISCUSSION AND CONCLUSIONS

7-1: Was Phragmites successfully predicted?

The two previous attempts at distinguishing *Phragmites* with hyperspectral remote sensing that were found in the literature used airborne sensors with spatial resolutions of 4.5 m (Bachmann et al., 2002) and 5m (Lopez et al., 2004). Hyperion's 30 m x 30 m pixels capture approximately 36 times as much area as the data in either of these studies. However, even at 4.5 m resolution, Bachmann et al. (2002) found that *Phragmites*' tendency to form long linear stands that were in some instances only one pixel in width was problematic. Using several image analysis algorithms and approaches, accuracy for their *Phragmites* class ranged from approximately 27 percent to a high of 68 percent (Bachman et al., 2002). The stands of *Phragmites* at the Green Bay study site were similarly narrow and, with the coarser spatial resolution of Hyperion, likely posed the greatest obstacle to accuracy in this investigation.

It was clear from early in the investigation that the size of the features of interest (dense stands of *Phragmites*) only rarely reached the size of the Hyperion sensor's spatial resolution—30 m x 30 m—within the study area. With very few stands of *Phragmites* reaching the spatial resolution of the sensor, training samples drawn from within the image inevitably included mixed pixels. Logically, if the spectra from these mixed pixels were to be used as training data for supervised classification or target detection, the optimum result would be identification of similarly mixed pixels.

The typical occurrence of *Phragmites* in the study area was a linear stand parallel to the shoreline that seldom exceeded 20 m in the dimension perpendicular to the

shoreline. Most stands were surrounded by and often mixed with other wetland species, such as *Typha*, *Salix*, *Scirpus*, and *Carex*. In most cases some part of the stand had standing water in the understory and often there was open water adjacent to the stand. The training samples were made up of varying combinations of these land cover components.

Considering those obstacles the 68.3 percent overall accuracy and 41.2 percent user's accuracy of the target detection classification are a reasonable success. Approximately 1 percent of the study area was classified as *Phragmites* by the target detection routine. If this is within an order of magnitude of being correct the actual proportion of the study area that met the *Phragmites* class criteria was between 0.1 percent and 10 percent. Assuming this, the 68 percent overall accuracy and 41 percent users accuracy for the *Phragmites* class detection, suggest that the *Phragmites* training data could identify pixels that were considerably more probable than random to include dense stands of *Phragmites*.

No conclusive explanation was found for the concentration of error at the mouth of the Pensaukee River. However, the close proximity of 8 identical errors and all 8 of these points being similarly situated in shallow water near the riverbank (figure 16) suggest two possible explanations. The first possibility is misregistration, of the image. Comparison of the Hyperion image with aerial photographs and the orthorectified ETM+ panchromatic layer used for georeferencing show that the Hyperion image may be shifted approximately half a pixel or fifteen meters to the south, relative to the ETM+ image. The presence one of the errors on the south bank of the river (L05) is some evidence

against this explanation—this sample would be made more anomalous by adjusting the Hyperion image half a pixel to the north. However, this is a single sample point compared to seven errors near the north bank; therefore, georeferencing error remains a likely contributor to the 8 misclassified samples.

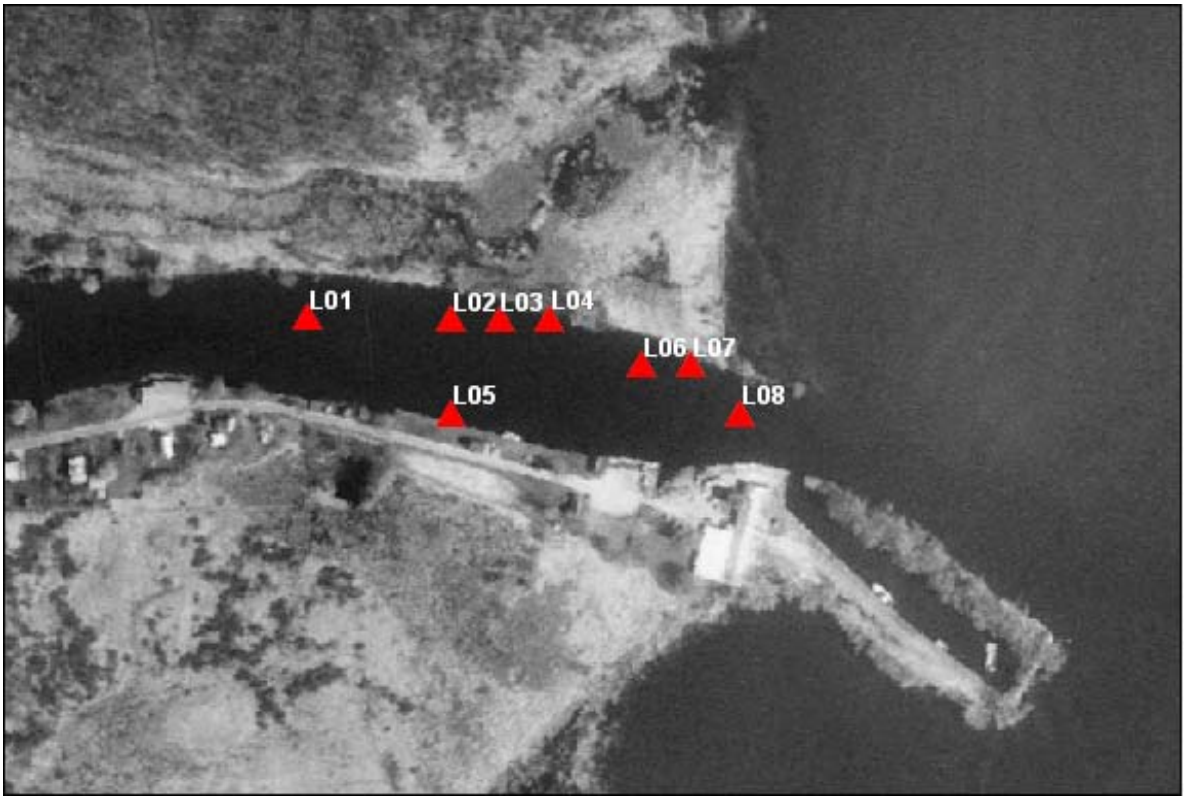

Figure 16: 8 points classified as *Phragmites* were shown to be open shallow water in the mouth of the Pensaukee River.

A second possible contributor to these errors may have been the delay between image acquisition and collection of accuracy data. For the accuracy assessment of the two classifications it was assumed that the persistent nature of *Phragmites* would allow accuracy data to be collected in the spring, 8 months after image acquisition. This delay introduced some uncertainty about whether vegetation was the same in May as it had been in September, when the image was acquired. Specifically, the 8 sample points

classified as *Phragmites* that were found to be open water in the mouth of the Pensaukee River suggest the possibility that ice or heavy spring runoff may have scoured stands of *Phragmites* that were detected in the Fall image. There were also *Typha* stems sheared off 15 to 30 cm above the spring water level (sample points C02, C06, C08, C10, C13, C15, C18, and C22), apparently by ice and wave action over the winter. In this case the remaining stems provide some evidence of the previous fall's vegetation. They also raise the possibility that other emergent vegetation may have been lost over the winter, affecting the accuracy of the reference data.

7-2: Is Phragmites spectrally distinct from other wetland species?

By treating each of the training samples in the target detection classification as a separate material of interest, (figure 17) the final classification is, in theory, a composite of 13 maps of different combinations of *Phragmites* and other land cover. Similarly, the unsupervised classification's 200 spectrally distinct clusters, in theory, included a subset of clusters composed of various combinations *Phragmites* and other land cover. The clusters that overlapped known areas of *Phragmites* were assumed to belong to that subset and were assigned to the "*Phragmites*" class.

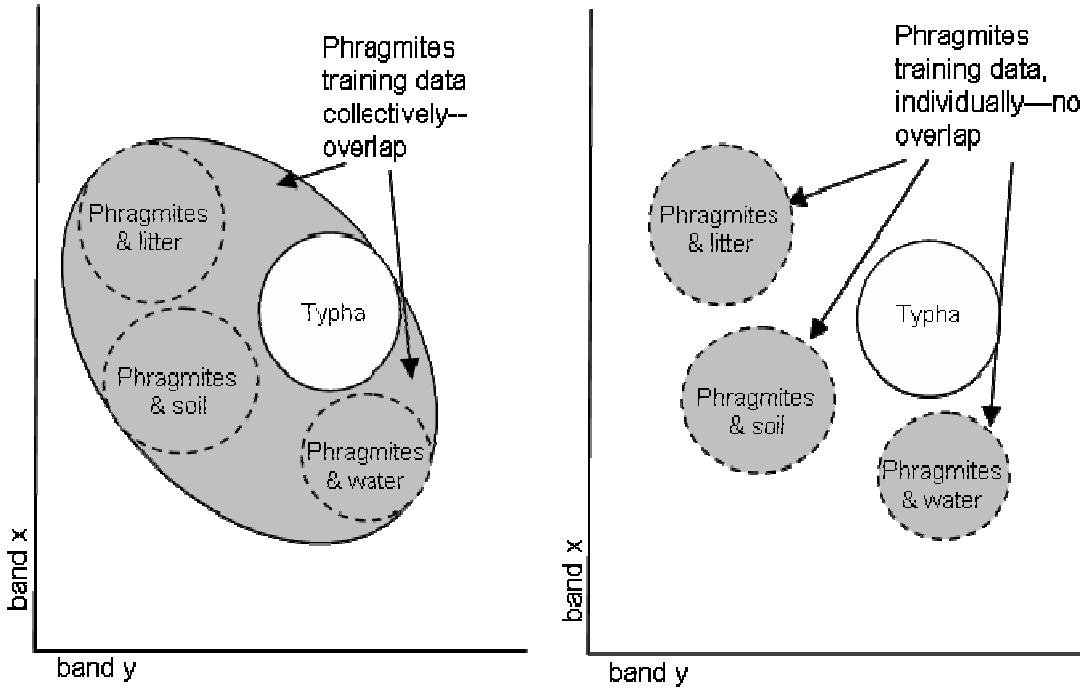

Figure 17: This simplified representation of spectral clusters in data space illustrates that the variation in the mixed *Phragmites* training samples collectively may have prevented them being spectrally distinct. Using each mixed sample point separately was intended to avoid this overlap.

Realizing this, it is important to remember that the accuracy numbers are for *Phragmites*-plus-context rather than for just *Phragmites*. Furthermore, by treating each sample as an individual material of interest and utilizing ancillary data, the accuracy assessment is of the entire classification process rather than the spectral detection of *Phragmites* in Hyperion data alone. This may not be an area of direct concern from the standpoint of operational use if the process predicts the presence of *Phragmites*. However, it means that the accuracy numbers do not necessarily indicate that *Phragmites* itself is spectrally distinct from any of the other wetland species in the error matrix. In reality, it is possible that other combinations of water, soil, litter and vegetation with similar reflectance characteristics were indistinguishable from the reflectance of water, soil, litter and *Phragmites*. This would likely become more of a problem as the fraction

the sampling unit covered by *Phragmites* decreased and the fraction of reflectance coming from soil, water and litter increased. Again, it is important to keep in mind that the mixed pixels used for training data limit conclusions about the spectral distinctness of *Phragmites* itself within the Hyperion image. It is quite possible that some of the positive relationship between the mapped *Phragmites* locations and the reference *Phragmites* locations is a product of the spectral similarity of elements correlated with *Phragmites* occurrence rather than *Phragmites* itself; for example shallow water, bare soil and shadows.

7-3: Change Since the Wisconsin Wetlands Inventory

The classifications scheme used in this study was not the same as used for the WWI. The most problematic difference, for the purpose of comparing the emergent wetlands areal extent within the study area, was the merging of wetland and upland meadow into a single class in this study where they were distinguished in the WWI. This was done because the two were found to be spectrally indistinguishable in the image. Because of this the emergent wetlands classes of this study should underestimate the extent of emergent wetlands by some fraction of the meadow class. In spite of this, the total area of emergent wetland in this study's wetland classes is 58.6 hectares more than in the WWI, (551 h compared to 492 h). While this gives no precise measure of the increase in emergent wetlands, it confirms the visually apparent increase in emergent wetlands in the study area and illustrates the constant change in the ecosystem of Great Lakes coastal wetlands.

7-4: Hyperion data

The narrow stands of *Phragmites* found in the study area provided few if any pure pixels for training data at the 30 m resolution of the sensor. The design of Hyperion trades finer spatial resolution for finer spectral resolution, and in doing so likely provides as much or more information for species level remote sensing applications. However, accessing this information requires more sophisticated sub-pixel classification techniques and a higher level of data processing than this study used. Alternatively, this study's approach likely would have produced better results with a spatial resolution of 10 m or 15 m, which would have allowed pure training pixels to be used. The best trade off between spatial and spectral resolution seems likely to be different for different applications and different image analysis techniques. If Hyperion type sensors are to serve a variety of applications, their design will require a compromise in balance of spatial and spectral resolution ideal to any one application. In addition, design must anticipate the development of techniques and technologies that would change that ideal balance for different applications. Nevertheless, in the case of this study it seems that sacrificing some spectral resolution for greater spatial resolution would have been beneficial.

Solutions to the problems of signal to noise, vertical striping and "spectral smile" would seem to be key to application oriented users on two levels. The information that can be extracted from the data and the confidence in that information are naturally of primary importance to users applying the data to real world problems. In addition, many users may be unwilling to approach data that requires excessive preprocessing, for which there are not yet clearly defined techniques or specifically designed software applications.

7-5: Future Research

The most limiting factor in successfully distinguishing monodominant *Phragmites* seems to have been the spatial resolution of the sensor relative to the size and shape of the stands of *Phragmites* in the study area. Two possibilities to consider in further attempts to use Hyperion to distinguish *Phragmites*: 1) The use of sub-pixel algorithms and techniques in the image analysis; and 2) Image acquisitions that include one or more *Phragmites* stands that are several pixels in size in both dimensions.

Use of subpixel algorithms such as the MTMF have been successfully used to map vegetation as a percentage of land cover per pixel (Williams and Hunt, 2002). Williams and Hunt used the MTMF with AVIRIS data flown at high altitude which gave it similar spatial resolution (20 m x 20 m) to Hyperion (30 m x 30 m). The MTMF algorithm has the further advantage of not requiring *a priori* knowledge of spectra for other materials within the image (Boardman et at., 1995).

Site location that includes larger *Phragmites* stands from which to draw training samples may also improve results. Bachman et al. (2002) state that accuracy and specificity of supervised classification was highly dependant on the size of training samples and the accuracy of georeferencing. With 5 m resolution and image derived spectra, Lopez et al., (2004) achieved 91 percent accuracy. The success of Lopez et al. (2004), using relatively large training samples and essentially the same spatial resolution, reinforces Bachman et al.'s conclusions about sample size.

Stands of *Phragmites* that significantly exceed the 30 m x 30 m resolution of Hyperion were observed in at least two locations in the Green Bay area; the extreme

southwest corner of the bay and at the end of Little Tail Point. Location of the Hyperion image was based on a center point of the study area given to EROS for image acquisition. In retrospect, it would have been a worthwhile risk to have located that point to the southwest of the study area, moving the study area to the right edge of the image, but including these known large stands of *Phragmites*. Future studies would benefit from making inclusion of such stands within the study area a priority.

7-6: Final Words

Airborne hyperspectral remote sensing has the technical advantage for species level studies with its finer spatial resolution and its superior signal to noise ratio. However, in most cases, its high cost will prevent it from being used for ongoing monitoring and study of wetlands. The lower cost per image acquisition of space platform sensors could make them much more viable for ongoing monitoring programs. Hyperion is the first generation of space based hyperspectral remote sensing. The modest success of this study can almost certainly be improved on as sensors improve and experience with hyperspectral remote sensing of wetlands grows. While species level remote sensing remains at the edge of remote sensing capability, its potential value to ecological studies makes further research imperative. The internally consistent, broad-scale data, which only remote sensing can provide will be essential to dealing with the global environmental changes taking place.

REFERENCES:

Ailstock, M.S., Norman, C.M., and Bushman, P.J. (2001), Common reed *Phragmites australis*: control and effects upon biodiversity in freshwater nontidal wetlands. *Restoration Ecology* 9:49-59.

Amsberry, L., Baker, M.A., Ewanchuk, P.J., and Bertness, M.D. (2000), Clonal intergration and the expansion of *Phragmites australis*. *Ecological Applications* 10:1110-1118.

Apan, A., Held, A., Phinn, S., and Markley, J. (2004), Detecting sugarcane 'orange rust' disease using EO-1 Hyperion hyperspectral imagery. *International Journal of Remote Sensing*, 25:489-498.

Artigas, F.J., and Yang. J. (2004), Hyperspectral Remote Sensing of Habitat Heterogeneity Between Tide-Restricted and Tide-Open Areas in the New Jersey Meadowlands. *Urban Habitats* 2:112-129.

Bachman, C.M., Donato, T.F., Lamela, G.M., Rhea, W.J., Bettenhausen, M.H., Fusina, R.A., Du Bois, K.R., Porter, J.H., and Truitt, B.R. (2002), Automatic classification of land cover on Smith Island, VA, Using HyMAP imagery. *IEEE Transactions on GeoScience and Remote Sensing* 40:2313-2330.

Benoit, L.K., and Askins., R.A. (1999), Impact of the spread of *Phragmites* on the distribution of birds in Connecticut tidal marshes. *Wetlands* 19:194-208.

Bernthal, T.W., and Willis, K.G. (2004), *Using Landsat 7 Imagery to Map Invasive Reed Canary Grass (Phalaris arundinacea): A Landscape Level Wetland Monitoring*

Methodology, Final Report to the U.S. Environmental Protection Agency Region V. Madison, Wisconsin: Wisconsin Department of Natural Resources.

Blossey, B. (1999), Before, during and after: the need for long-term monitoring in invasive plant species management. *Biological Invasions* 1:301-311.

Blossey, B., Schwarzlander, M., Hafliger, P., Casagrande, R., and Tewksbury, L. (2002), Common Reed. In *Biological Control of Invasive Plants in the Eastern United States* (R. Van Driesche, S. Lyon, B. Blossey, M. Hoddle and R. Reardon, Eds.) USDA Forest Service Publication FHTET-2002-04, USDA, Ft. Collins, CO, pp. 131-138.

Boardman, J.W., Kruse, K.A., and Green, R.O. (1995), Mapping target signatures via partial unmixing of AVIRIS data. in: *Summaries of the Fifth Annual JPL Airborne Geoscience Workshop*, Pasadena, CA.

Chambers, R.M., Meyerson, L.A., and Saltonstall, K. (1999), Expansion of *Phragmites australis* into tidal wetlands of North America. *Aquatic Botany* 64:261-273.

Cochrane, M., (2000), Using vegetation reflectance variability for species level classification of hyperspectral data. *International Journal of Remote Sensing* 21:2075-2087.

Congalton, R.G. (1991), A review of assessing the accuracy of classifications of remotely sensed data. *Remote Sensing of Environment* 37:35-46.

Dahl, T.E., and Allord, G.J., (1997), Technical aspects of wetlands, history of wetlands in the conterminous United States. Accessed on October 19, 2005 at: http://water.usgs.gov/nwsum/WSP2425/history.html

Datt, B., McVicar, T.R., Van Niel, T.G., Jupp, D.L.B., and Pearlman, J.S. (2003), Preprocessing EO-1 Hyperion hyperspectral data to support the application of agricultural indexes. *IEEE Transactions on Geoscience and Remote Sensing* 41:1246-1259.

de Lange, R., van Til, M., and Dury, S., (2004), The use of hyperspectral data in coastal zone vegetation monitoring. *EARSeL eProceedings* 3:143-153.

Edwards, T.C., Moisen, G.G., and Cutler, D.R. (1998) Assessing map accuracy in a remotely sensed ecoregion-scale cover map. *Remote Sensing of Environment* 63:73-83.

Eckert, S., Kneubühler, M., (2004), Application of Hyperion data to agricultural land classification and vegetation properties estimation in Switzerland. XXth ISPRS Congress, 12-23 July 2004 Istanbul, Turkey.

ERDAS Inc. (2002a), ERDAS Imagine v. 8.6. Field Guide.

ERDAS Inc. (2002b), ERDAS Imagine v. 8.6. Spectral Analysis User's Guide.

Ernst-Dottavio, C.L., Hoffer, R.M., and Mroczynski, R.P. (1981), Spectral characteristics of wetland habitats. *Photogrammetric Engineering and Remote Sensing* 47:223-227.

Galatowitsch, S.M., Anderson, N.O., and Ascher, P.D. (1999), Invasiveness in Wetland Plants in Temperate North America. *Wetlands* 19:733-755.

Goodenough, D.G., Bhogal, A.S., Dyk, A., Hollinger, A., Mah, Z., Niemann, K.O., Pearlman, J., Chen, H., Han, T., Love, J., and McDonald, S. (2002), *Monitoring Forests with Hyperion and ALI.*. IGARSS 2:882-885.

Hallett, J., Bosley, T.R., and Roznik, F.D. (1977), "Green Bay's coastal wetlands – a picture of dynamic change." In *Wetlands Ecology, Values and Impacts, Proceedings of the Waubesa Conference on Wetlands* (DeWitt, C.B., and Soloway, E. Eds.) Institute for Environmental Studies, Madison, Wisconsin.

Han, T., Goodenough, D.G., Dyk, A., and Love, L. (2002), *Detection and correction of abnormal pixels in Hyperion images*. IGARSS 2002, 3:1327-1330.

Haslam, S. (1969), The development of shoots in *Phragmites communis trin*. *Annals of Botany* 33:695-709.

Havens, K.J., Priest III, W.I., and Berquist, H. (1997), Investigation and long-term monitoring of *Phragmites australis* within Virginia's constructed wetland sites. *Environmental Management* 21:599-605.

Hawth's Analysis Tools. (2002), Hawth's Analysis Tools C 2002 Version 2.0. Programmer: Hawthorne Beyer. Accessed October 7, 2005 at: http://www.spatialecology.com/

Heywood, V.H. (1995), *The Global Biodiversity Assessment*. United Nations Environment Programme. Cambridge University Press, Cambridge.

Hirano, A., Madden, M., and Welch, R., (2003), Hyperspectral image data for mapping wetland vegetation. *Wetlands* 23:436-448.

Huguenin, R.L., Karaska, M.A., Van Blaricom, D., and Jensen, J.R. (1997), Subpixel classification of bald cypress and tupelo gum trees in thematic mapper imagery. *Photogrammetric Engineering and Remote Sensing* 63:717-725.

Johnston, C.A. (1984), Mapping Wisconsin's Wetlands. *Wisconsin Natural Resources* 8:4-6.

Johnston, C.A., and Meysembourg, P., (2002), Comparison of the Wisconsin and National Wetlands Inventories. *Wetlands* 22: 386-405.

Johnston, C.A., Bedford, B., Bourdaghs, M., Brown, T., Chang, J., C.B. Frieswyk, C.B., Tulbure, M., Vacarro, L., and Zedler, J.B. (in review), Plant species indicators of environmental condition in Great Lakes coastal marshes. *Wetlands*.

Jupp, D.L.B. and Datt, B. (2004), *Evaluation of the EO-1 Hyperion Hyperspectral Instrument and its Applications at Australian Validations Sites 2001-2003*. (pp.20-23). Canberra, Australia. CSIRO Earth Observation Centre.

Kruse, F.A., Lefkoff, A.B., Boardman, J.W., Heidebrect, K.B., Shapiro, A.T., Barloon, P.J., and Goetz, A.F.H. (1993), The Spectral Image Processing System (SIPS)—interactive visualization and analysis of imaging spectrometer data. *Remote Sensing of Environment* 44:145-163.

Kruse, F.A., Boardman, J.W., and Huntington, J.F., (2003), Comparison of airborne hyperspectral data and EO-1 Hyperion for mineral mapping. *IEEE Transactions on Geoscience and Remote Sensing* 41:1388-1400.

Kruse, F.A., Boardman, J.W., Huntington, J.F., Mason, P., and Quigley, M.A. (2002), Evaluation and validation of EO-1 Hyperion for geologic mapping. *IEEE International Geoscience and Remote Sensing Symposium* 1:593-595.

Lillesand, T.M. and Kiefer, R.W. (2000), *Remote Sensing and Image Interpretation*. New York, USA: John Wiley & Sons Inc.

Lopez, R.D., Edmonds, C.M., Neale, A.C., Slonecker, T.S., Jones, K.B., Heggem, D.T., Lyon, J.G., Jaworski, E., Garofalo, D., and Williams, D. (2004), Accuracy assessments of airborne hyperspectral data for mapping opportunistic plant species in freshwater coastal wetlands. In *Remote Sensing and GIS Accuracy Assessment* (R.S. Lunetta and J.G. Lyon, eds.) CRC Press, New York, pp. 253-267.

Lumme, J.H. (2004), Classification of vegetation and soil using imaging spectrometer data. XXth ISPRS Congress, Istanbul, Turkey.

Lynch, E.A., and Saltonstall, K., (2002), Paleoecological and genetic analyses provide evidence for recent colonization of native *Phragmites australis* populations in a Lake Superior wetland. *Wetlands* 22:637-646.

MacDonald, G.M. (2003), *Biogeography: Space, Time, and Life.* John Wiley & Sons, New York.

Malthus, T.J., and George, D.G., (1997), Airborne remote sensing of macrophytes in Cefni Reservoir, Anglesey, UK. *Aquatic Botany* 58:317-332.

Marks, M., Lapin, B., and Randall, J., (1994), *Phragmites australis (P. communis*): threats, management, and monitoring. *Natural Areas Journal* 14:285-294.

Martin, M.E., Newman, S.D., Aber, J.D., and Congalton, R.G. (1998), Determining forest species composition using high spectral resolution remote sensing data. *Remote Sensing of Environment* 65:249-254.

Meyerson, L.A., Saltonstall, K., Windham, L., Kiviat, E., and Findlay, S. (2000), A comparison of *Phragmites australis* in freshwater and brackish marsh environments in North America. *Wetlands Ecology and Management* 8:89-103.

Mooney, H.A., and Cleland, E.E. (2001), The evolutionary impact of invasive species. *Proceedings of the National Academy of Science* 98:5446-5451.

Mooney, H.A. and Hobbs, R.J. (2000), *Invasive Species in a Changing World*. Island Press, Washington.

Novacek, M.J., and Cleland, E.E. (2001), The current biodiversity extinction event: scenarios for mitigation and recovery. *Proceedings of the National Academy of Science* 98:5466-5470.

NOAA. (2005), National Oceanic and Atmospheric Administration-National Ocean Service. Website accessed September 7, 2005 at: http://co-ops.nos.noaa.gov/index.html

NOAA. (1992), NOAA's Medium Resolution Digital Vector Shorleline. Website accessed October 7, 2005 at: http://sposerver.nos.noaa.gov/projects/shoreline/shoreline.html

Oki, K., Oguma, H., and Sugita, M. (2002), Subpixel classification of alder trees using multitemporal Landsat Thematic Mapper imagery. *Photogrammetric Engineering and Remote Sensing* 68:77-82.

Ramsey, E.W., and Jensen, J.R. (1996), Remote sensing of mangrove wetlands: relating canopy spectra to site-specific data. *Photogrammetric Engineering and Remote Sensing* 62:939-948.

Reed, P.B., Jr. (1988), *National List of Plant Species that Occur in Wetlands: National Summary.* U.S. Fish and Wildlife Service Biological Report 88(24), pp. 98.

Rutchey, K., and Vilchek, L. (1999), Air photointerpretation and satellite imagery analysis techniques for mapping cattail coverage in a northern Everglades impoundment. *Photogrammetric Engineering and Remote Sensing* 65:185-191.

Pimentel, D., Lach, L., Zuniga, R., and Morrison, D., (2000), Environmental and economic costs of non-indigenous species in the United States. *BioScience* 50:53-65.

Pimm, S.L., Russell, G.J., Gittleman, J.L., and Brooks, T.M., (1995), The future of biodiversity. *Science*. 269:347-350.

Saltonstall, K. (2002), Cryptic invasion by a non-native genotype of common reed, *Phragmites australis*, into North America. *Proceedings of the National Academy of Science* 99:2445-2449.

Schmidt, K.S., and Skidmore, A.K. (2001), Exploring spectral discrimination of grass species in African rangelands. *International Journal of Remote Sensing* 22:3421-3434.

Schmidt, K.S., and Skidmore, A.K., (2003), Spectral discrimination of vegetation types in a coastal wetland. *Remote Sensing of Environment* 85:92-108.

Schwartz, M.W., Porter, D.J., Randall, J.M., and Lyons, K.E., (1996), Impact of Non-indigenous Plants. Sierra Nevada Ecosystem Project: Final report to Congress, vol. II., University of California Davis, Centers for Water and Wildland Resources.

Shigesada, N. and Kawasaki, K. (1997) *Biological Invasions: Theory and Practice* Oxford University Press, New York.

Spanglet, H.J., Ustin, S.L., and Rejmankova, E. (1998), Spectral reflectance characteristics of California subalpine marsh plant communities. *Wetlands* 18:307-319.

Stehman, V. and Czaplewski, R.L. (1998), Design and analysis for thematic map accuracy assessment: fundamental principles. *Remote Sensing of Environment* 64:331-344.

Thenkabail, P.S., Enclona, E.A., Ashton, M.S., Legg, C., and De Dieu, M.J. (2004), Hyperion, IKONOS, ALI and ETM+ sensors in the study of African rainforests. *Remote Sensing of Environment* 90:23-43.

Underood, E., Ustin, S., and DiPietro, D. (2003), Mapping nonnative plants using hyperspectral imagery. *Remote Sensing of Environment* 86:150-161.

USACE. (2005), United States Army Corps of Engineers, Great Lakes Water Levels. Accessed October 7, 2005 at: http://www.lre.usace.army.mil/greatlakes/hh/greatlakeswaterlevels/

USGS. (2001), Proceedings of the Hyperion and ALI Data Users Workshop. http://eo1.usgs.gov/userGuide/index.html

USGS. (2005), USGS EO-1 user's guide. Accessed August 3, 2005 at: http://eo1.usgs.gov/userGuide/hyp_prod.html

Ustin, S. L., DiPietro, D., Olmstead, K., Underwood, E., and Scheer, G.J. (2002), Hyperspectral remote sensing for invasive species detection and mapping. *International Geoscience and Remote Sensing Symposium* 3:1658–1660.

van Aardt, J.A.N., and Wynne, R.H. (2001), Spectral separability among six southern tree species. *Photogrammetric Engineering and Remote Sensing* 67:1367-1375.

Vitousek, P.M., D'Antonio, C.M., Loope, L.L., and Westbrooks, R. (1996), Biological invasions as global environmental change. *American Scientist* 84:468-479.

Vitousek, P.M., Mooney, H.A., Lubchenco, J., and Melillo, J.M. (1997), Human domination of Earth's ecosystems. *Science* 277:494-499.

Wilcove, D., Rothstein, D., Dubow, J., Phillips, A., and Losos, E. (1998), Quantifying threats to imperiled species in the United States. *BioScience* 48:607-615.

Wilcox, K. L., and Petrie, S.A. (2000), Monitoring *Phragmites australis* at Long Point, Ontario. In *Proceedings of the Leading Edge Conference* (S. Carty, S. Powell, M. Baran, and R. Murzin, eds.) Burlington, Ontario, Canada. ISBN # 0-77940039-9 CD ROM.

Williams, A.P., Hunt, E.R., Jr. (2002), Estimation of leafy spurge cover from hyperspectral imagery using mixture tuned matched filtering. *Remote Sensing of Environment* 82:446-456.

Windham, L. (2001), Comparison of biomass production and decomposition between *Phragmites australis* (common reed) and *Spartina patens* (salt hay grass) in brackish tidal marshes of New Jersey, USA. *Wetlands* 21:179-188.

Wisconsin DNR, (2005), A User's Guide to the Wisconsin Wetlands Inventory. Publication WZ022-92. Wisconsin Department of Natural Resources. Accessed August 30, 2005 at: http://dnr.wi.gov/org/water/fhp/wetlands/documents/WWI_Usersguide.pdf

Wolter, P. (2004) Environmental Remote Sensing Center, The Nelson Institute University of Wisconsin-Madison, ptwolter@wisc.edu.

Yamano, H., Chen, J., and Tamura, M. (2003), Hyperspectral identification of grassland vegetation in Xilinhot, Inner Mongolia, China. *International Journal of Remote Sensing* 24:3171-3178.

Zedler, J.B. and Kercher, S. (2004), Causes and consequences of invasive plants in wetlands: opportunities, opportunists, and outcomes. *Critical Reviews in Plant Sciences* 23:431-452.

Appendix A-1

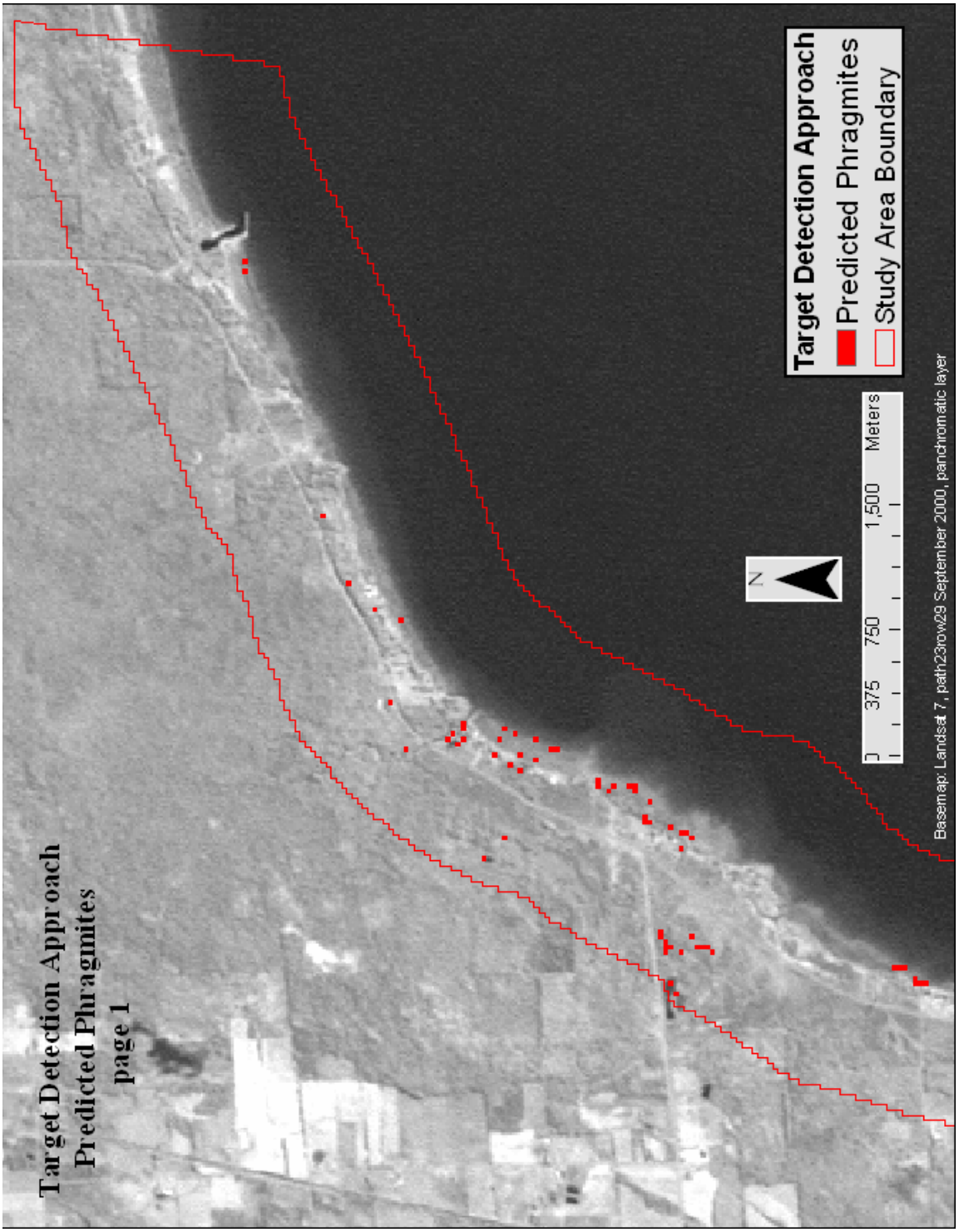
Target Detection Approach
Predicted Phragmites
page 1
Target Detection Approach
Predicted Phragmites
Study Area Boundary
N
0 375 750 1,500 Meters
Basemap: Landsat 7, path23row29 September 2000, panchromatic layer

Appendix A-2

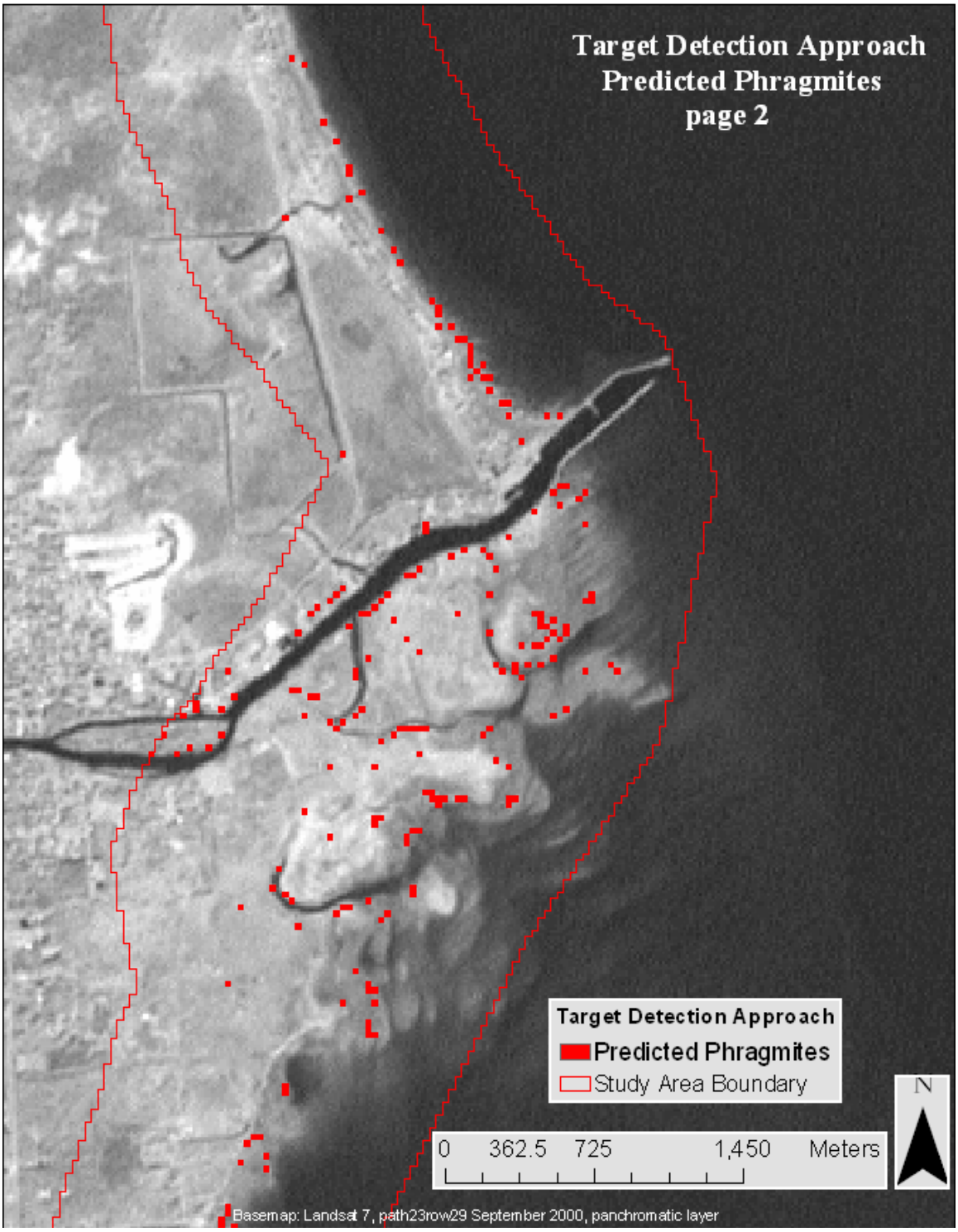
Target Detection Approach
Predicted Phragmites
page 2
Target Detection Approach
Predicted Phragmites
Study Area Boundary
0 362.5 725 1,450 Meters
N
Basemap: Landsat 7, path23row29 September 2000, panchromatic layer

Appendix A-3

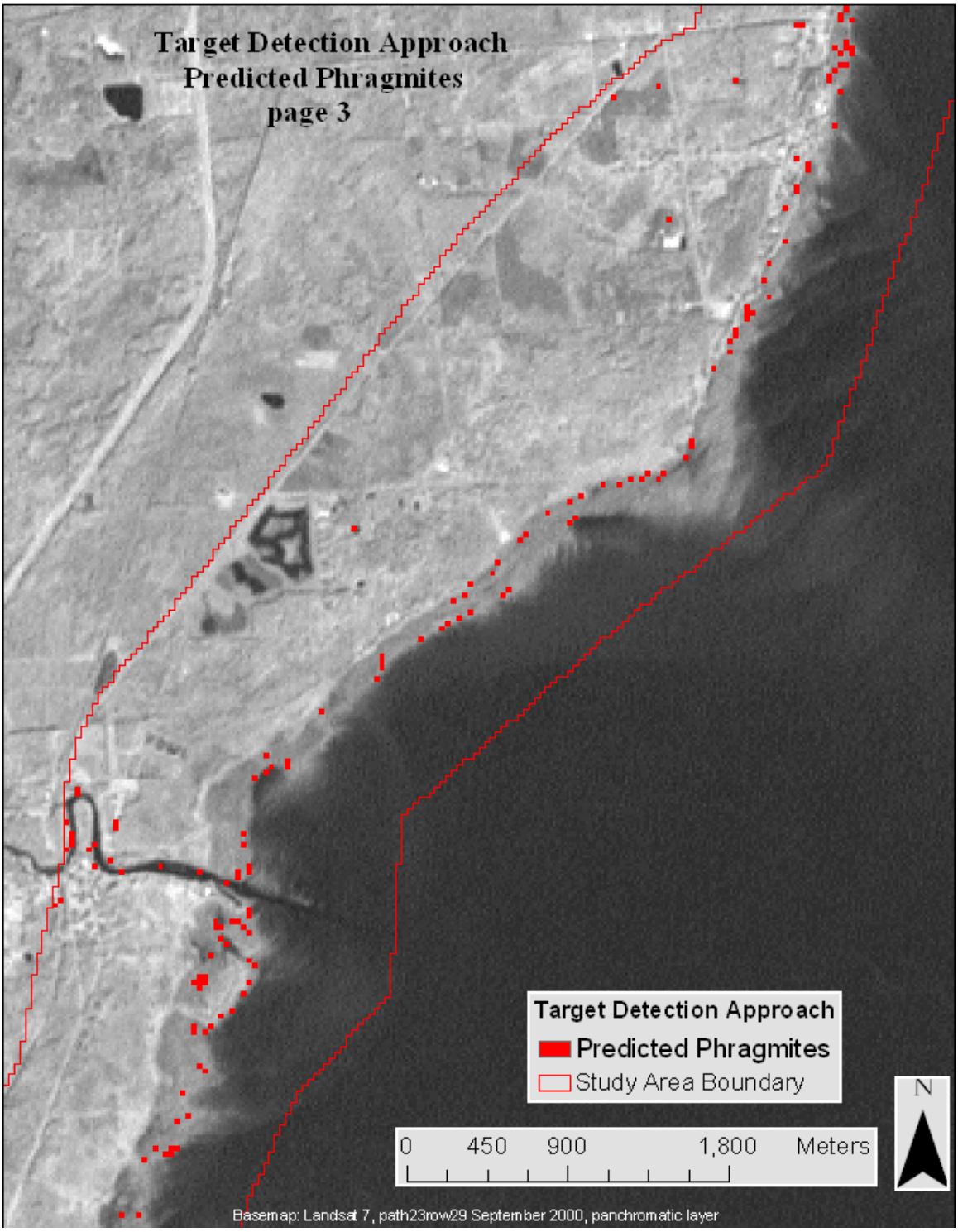
Target Detection Approach
Predicted Phragmites
page 3
Target Detection Approach
Predicted Phragmites
Study Area Boundary
0
450
900
1,800
Meters
N
Basemap: Landsat 7, path23row29 September 2000, panchromatic layer

Appendix A-4

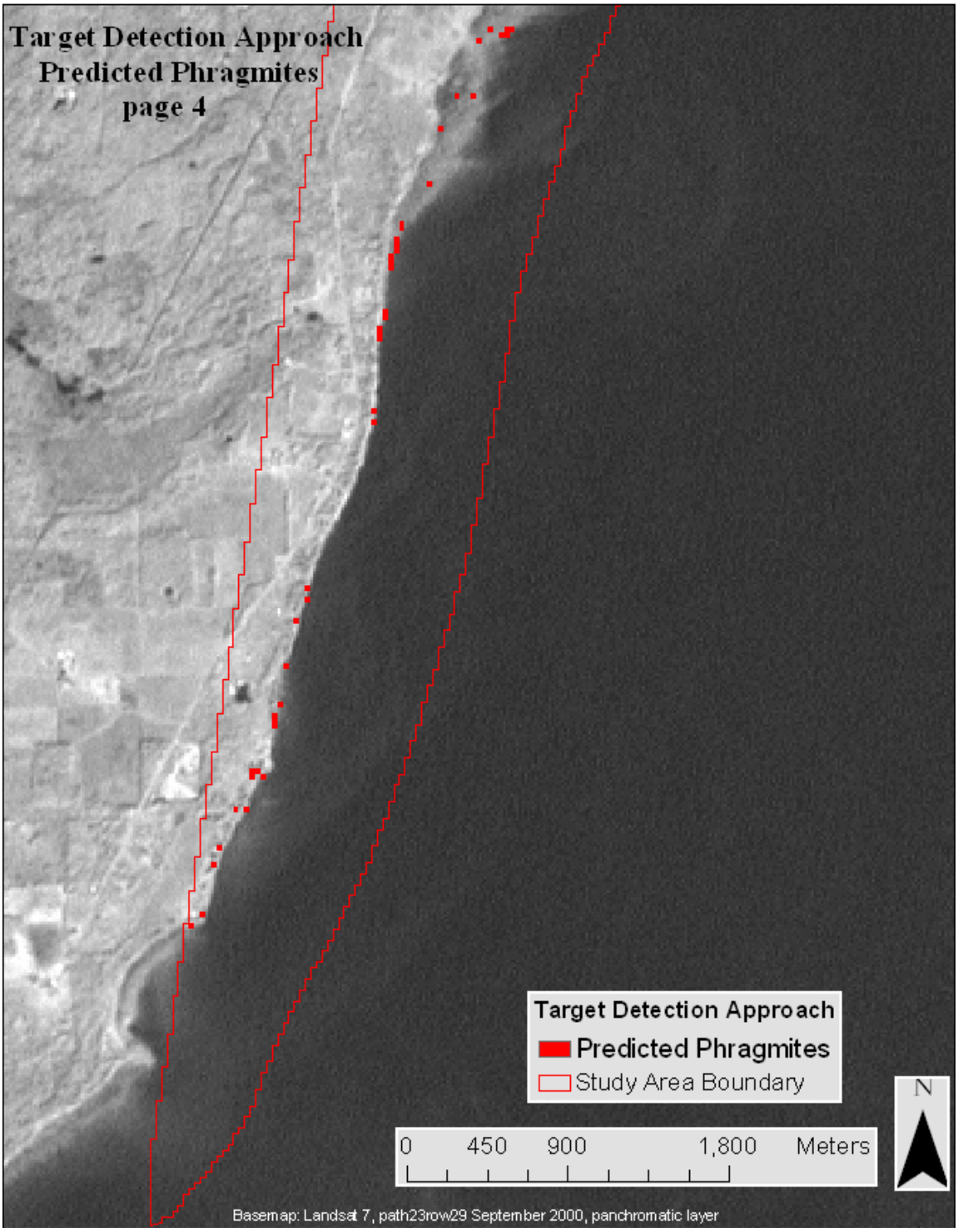
Target Detection Approach
Predicted Phragmites
page 4
Target Detection Approach
Predicted Phragmites
Study Area Boundary
0
450
900
1,800
Meters
N
Basemap: Landsat 7, path23row29 September 2000, panchromatic layer

Appendix B-1

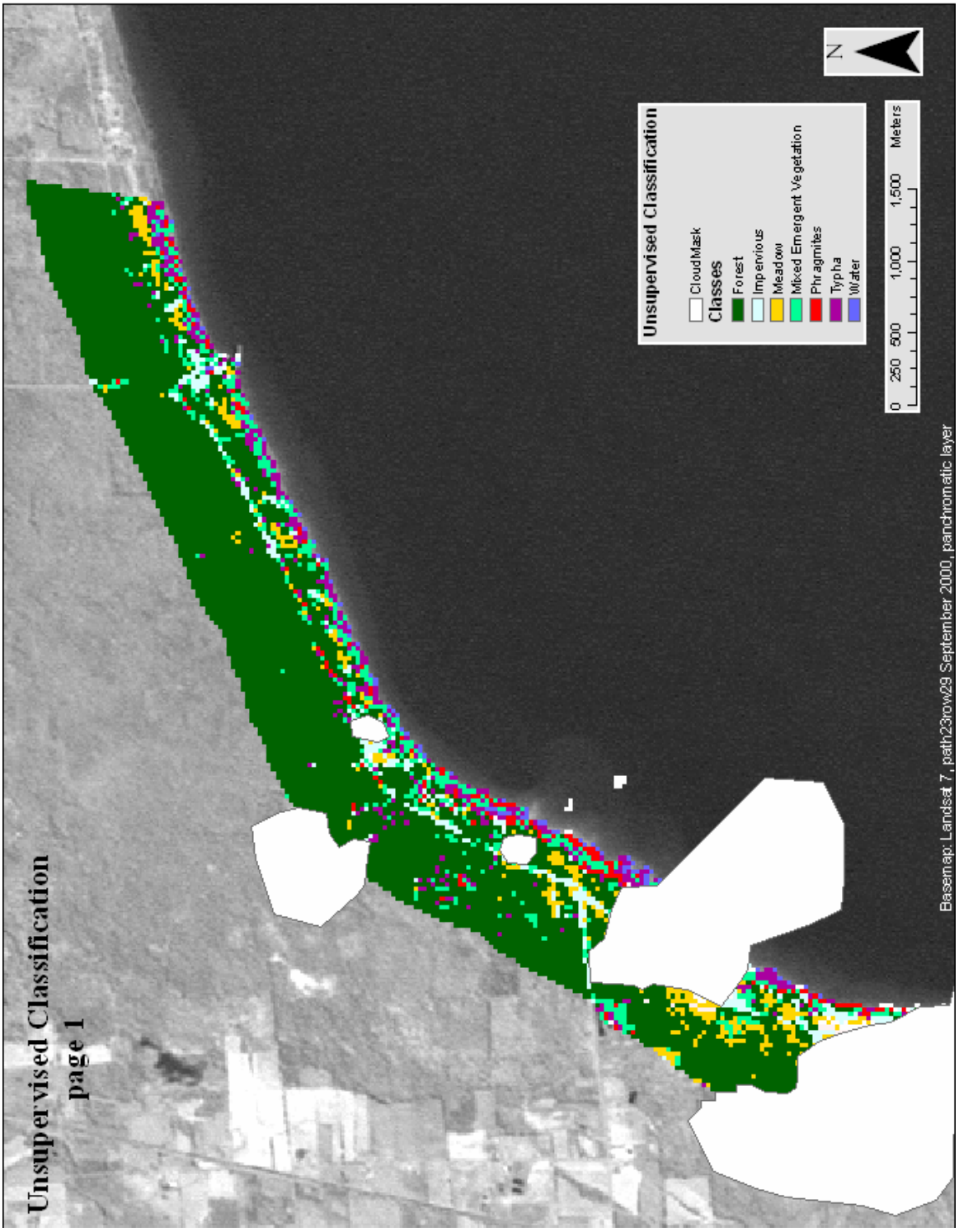
Unsupervised Classification
page 1
Unsupervised Classification
CloudMask
Classes
Forest
Impervious
Meadow
Mixed Emergent Vegetation
Phragmites
Typha
Water
0 250 500 1,000 1,500 Meters
N
Basemap: Landsat 7, path23row29 September 2000, panchromatic layer

Appendix B-2

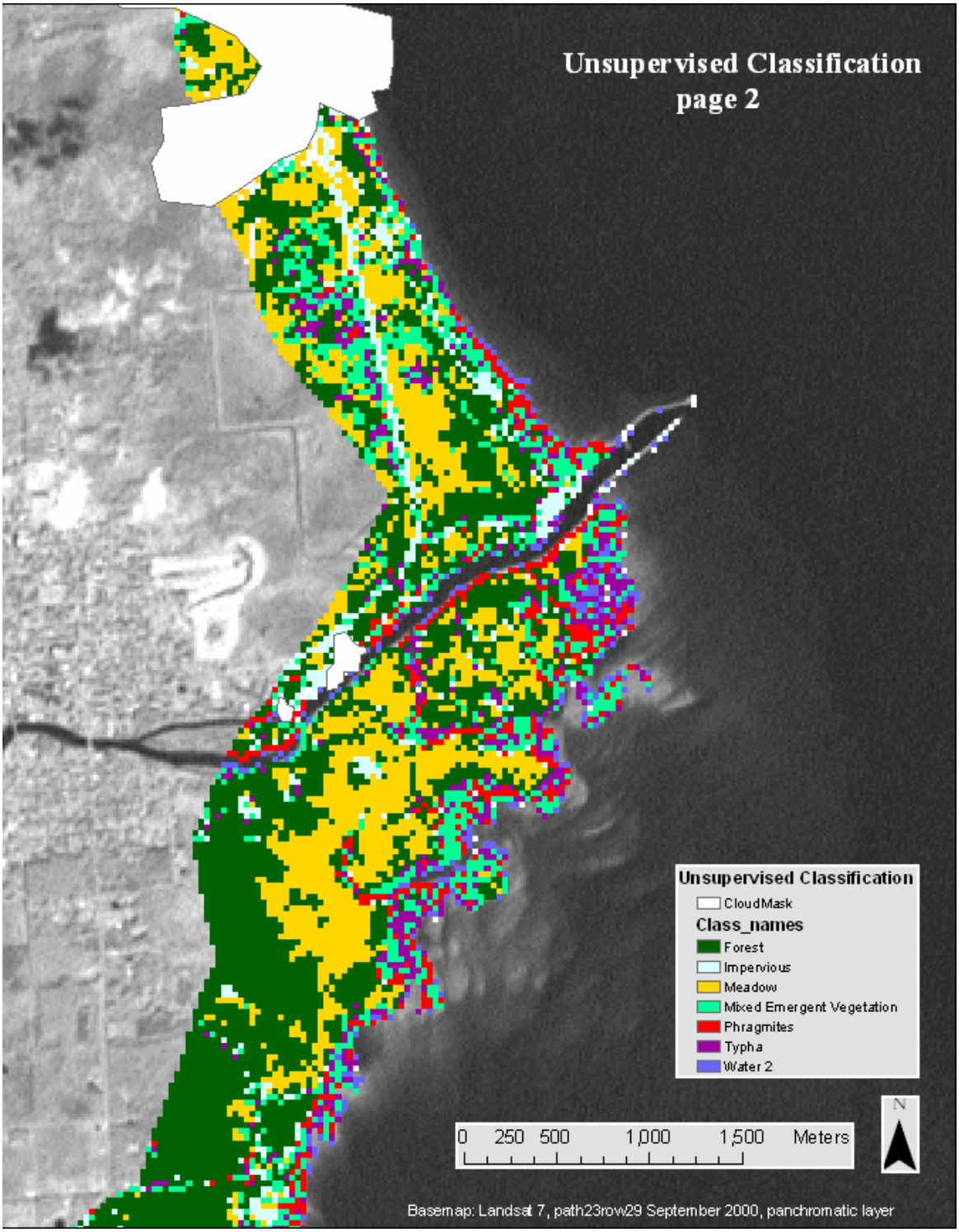
Unsupervised Classification
page 2
Unsupervised Classification
CloudMask
Class_names
Forest
Impervious
Meadow
Mixed Emergent Vegetation
Phragmites
Typha
Water 2
0 250 500 1,000 1,500 Meters
N
Basemap: Landsat 7, path23row29 September 2000, panchromatic layer

Appendix B-3

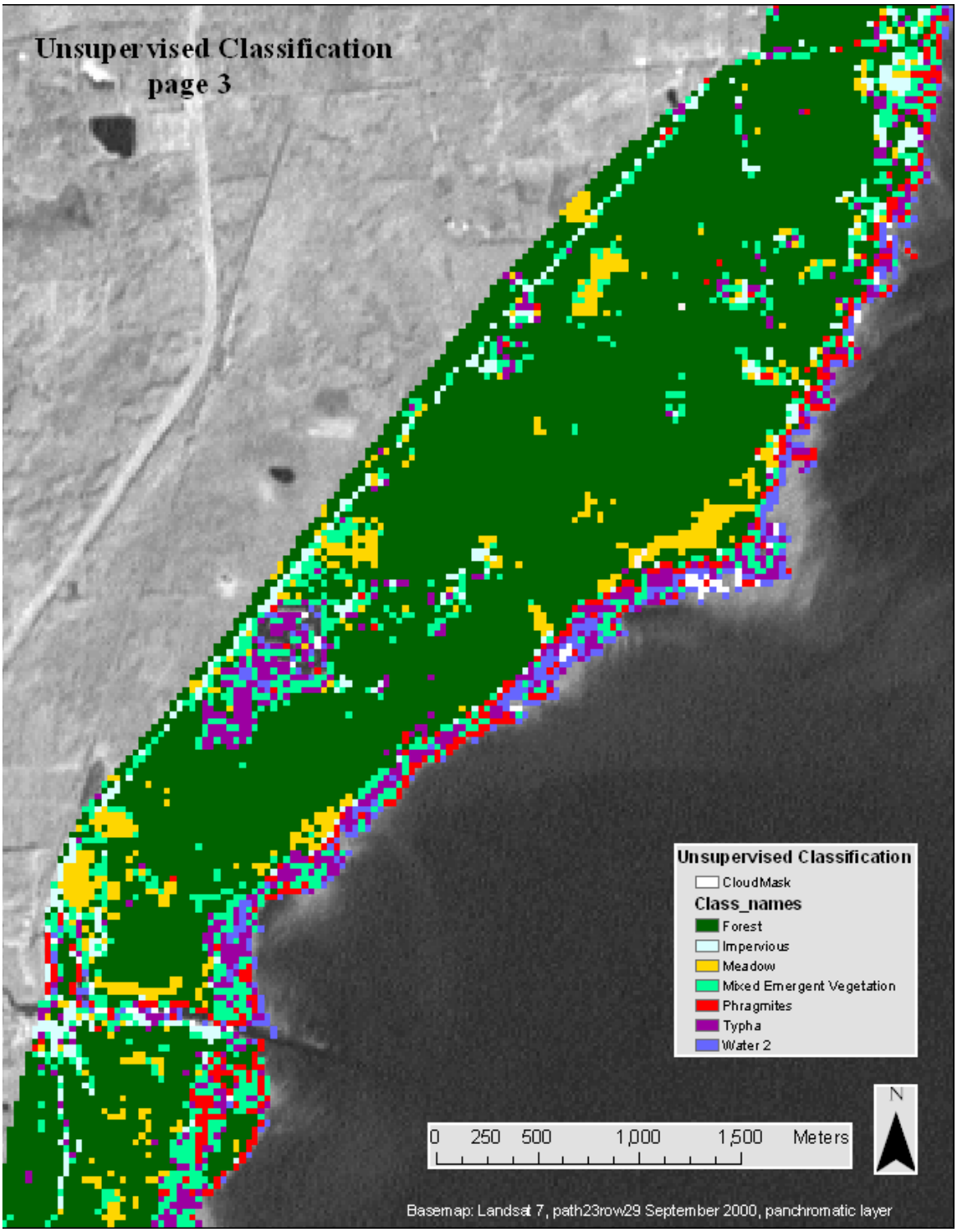
Unsupervised Classification
page 3
Unsupervised Classification
CloudMask
Class_names
Forest
Impervious
Meadow
Mixed Emergent Vegetation
Phragmites
Typha
Water 2
0 250 500 1,000 1,500 Meters
N
Basemap: Landsat 7, path23row29 September 2000, panchromatic layer

Appendix B-4

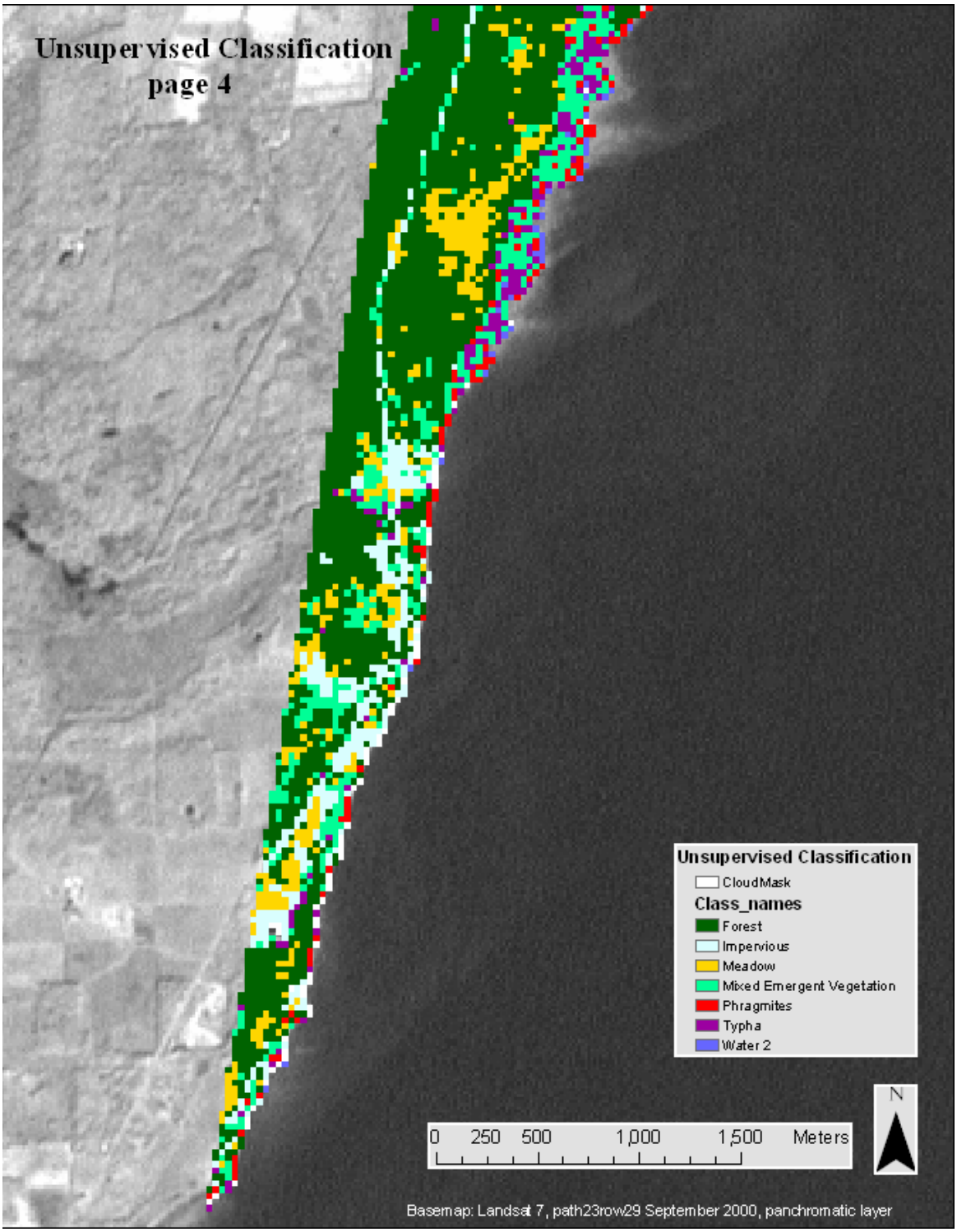
Unsupervised Classification
page 4
Unsupervised Classification
CloudMask
Class_names
Forest
Impervious
Meadow
Mixed Emergent Vegetation
Phragmites
Typha
Water 2
0 250 500 1,000 1,500 Meters
N
Basemap: Landsat 7, path23row29 September 2000, panchromatic layer

Appendix C-1

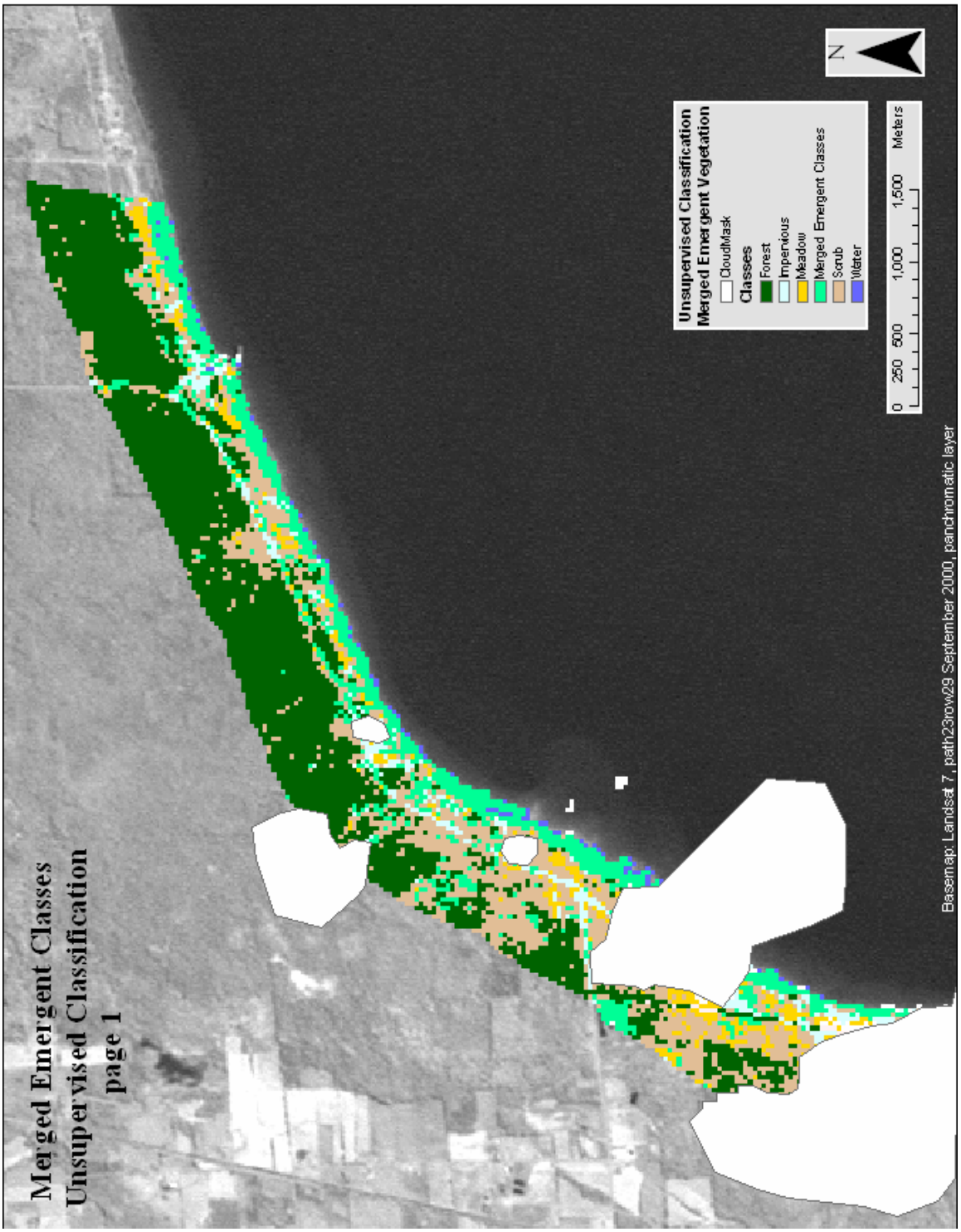
Merged Emergent Classes
Unsupervised Classification
page 1
Unsupervised Classification
Merged Emergent Vegetation
CloudMask
Classes
Forest
Impervious
Meadow
Merged Emergent Classes
Scrub
Water
0 250 500 1,000 1,500 Meters
N
Basemap: Landsat 7, path23row29 September 2000, panchromatic layer

Appendix C-2

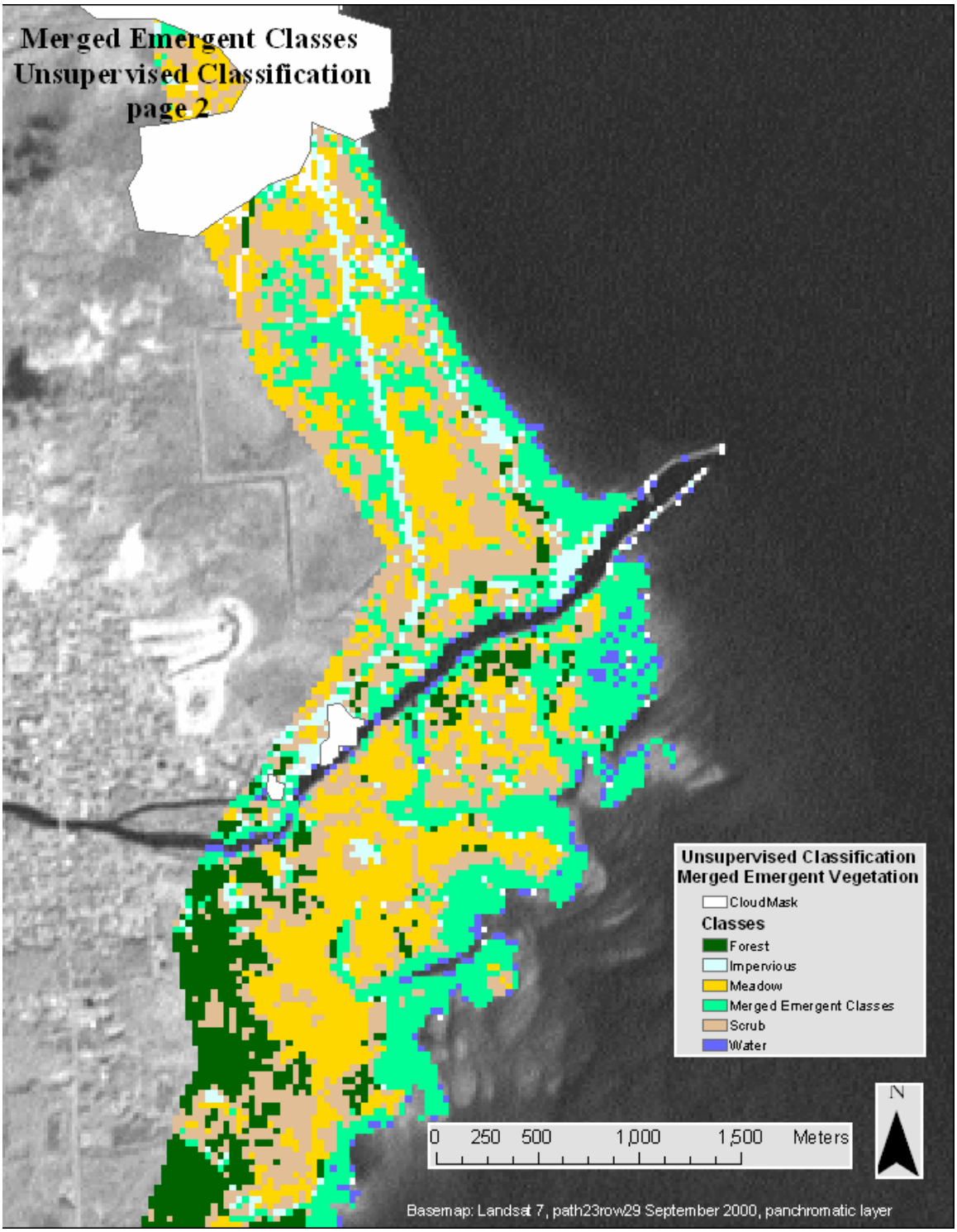
Merged Emergent Classes
Unsupervised Classification
page 2
Unsupervised Classification
Merged Emergent Vegetation
CloudMask
Classes
Forest
Impervious
Meadow
Merged Emergent Classes
Scrub
Water
N
0 250 500 1,000 1,500 Meters
Basemap: Landsat 7, path23row29 September 2000, panchromatic layer

Appendix C-3

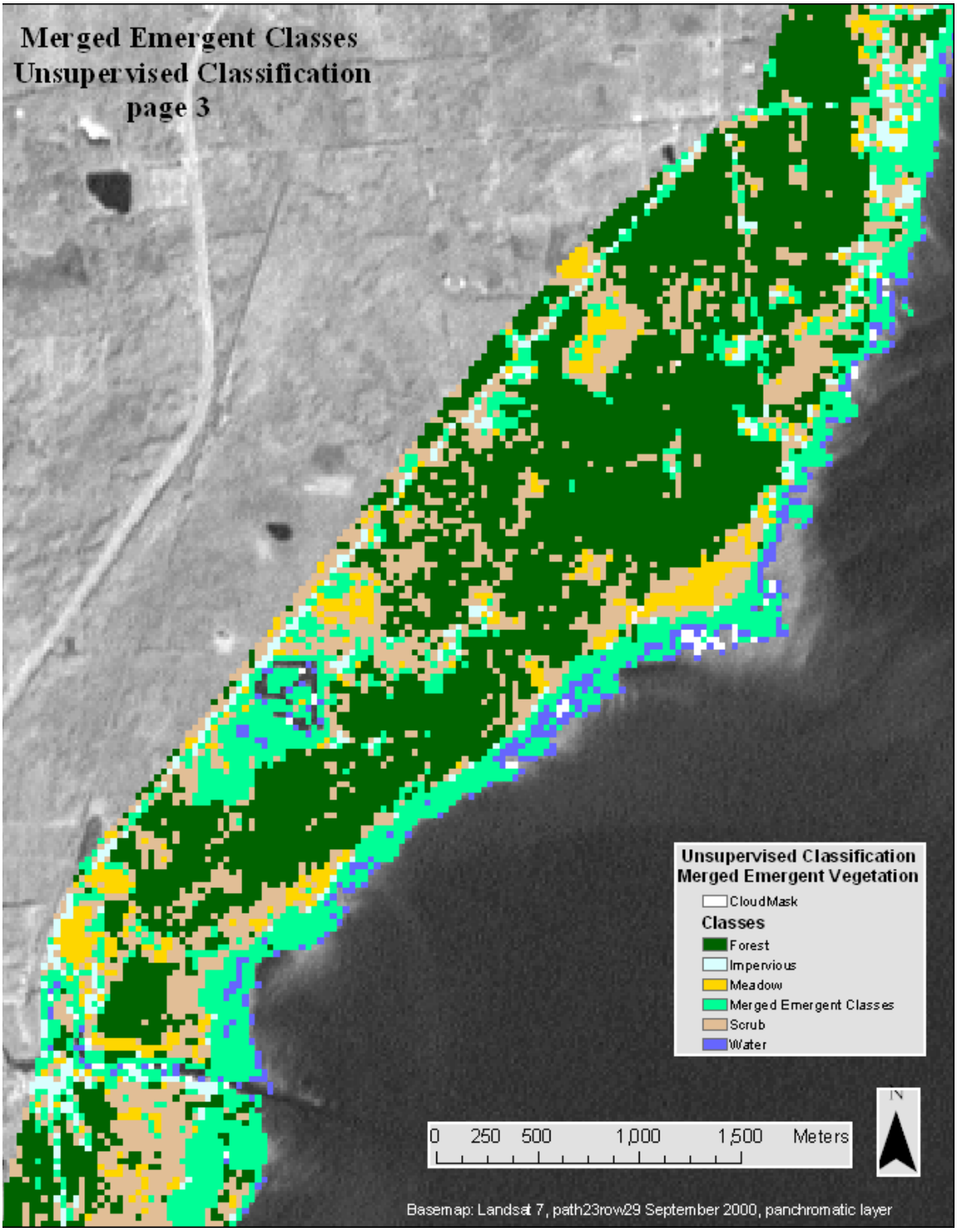
Merged Emergent Classes
Unsupervised Classification
page 3
Unsupervised Classification
Merged Emergent Vegetation
CloudMask
Classes
Forest
Impervious
Meadow
Merged Emergent Classes
Scrub
Water
0 250 500 1,000 1,500 Meters
N
Basemap: Landsat 7, path23row29 September 2000, panchromatic layer

Appendix C-4

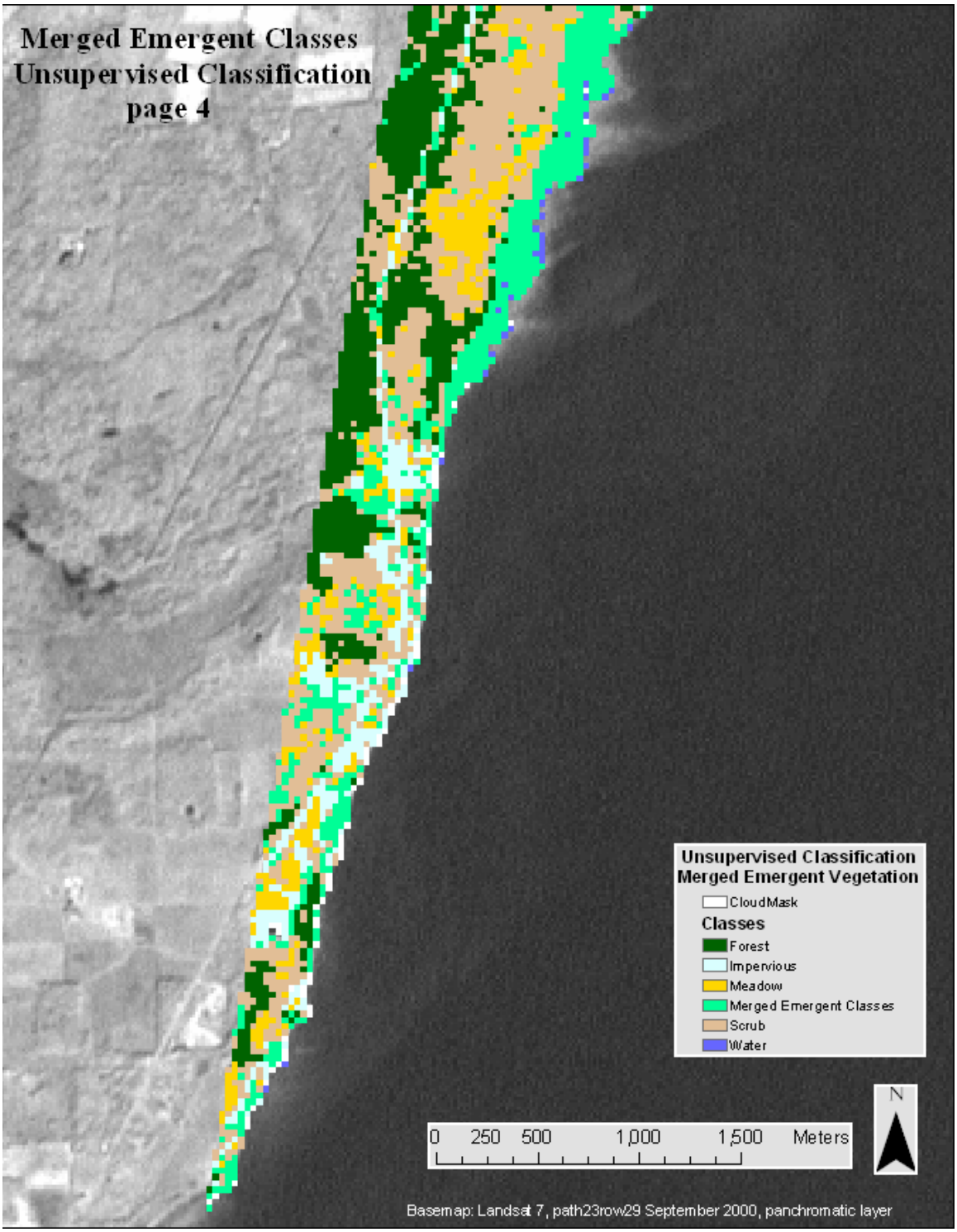
Merged Emergent Classes
Unsupervised Classification
page 4
Unsupervised Classification
Merged Emergent Vegetation
CloudMask
Classes
Forest
Impervious
Meadow
Merged Emergent Classes
Scrub
Water
0 250 500 1,000 1,500 Meters
N
Basemap: Landsat 7, path23row29 September 2000, panchromatic layer

Appendix D- 1: Accuracy assessment points

Reference Classification	Point ID	Unsupervised Classification	Target Detection Classification	Sample Point Notes
ForestD	A01	Scrub	not-*Phragmites*	1/4 grass and stumps; 3/4 open deciduous w/ understory of grasses & shorter trees
ForestD	A02	ForestD	not-*Phragmites*	Mown grass on the eastern 1/5; scrub and trees mixed for the remainder; picnic shelter at south east corner, no standing water or exposed soil
Phragmites	A03	x	*Phragmites*	Open water for southern 1/3; standing Phragmites to the north; Phragmites laying over in majority of pixel, maybe storm, ice or waves? Would assume dense & standing in Fall.
Phragmites	A04	x	*Phragmites*	Phragmites throughout; 2 to 3 m tall; 15 cm standing water
Phargmites	A05	Phrag	x	Phragmites moderate density with some shrubs and other; an area of meadow on the north edge; 5 cm of standing water
Phragmites	A06	Phrag	x	Open water on the south edge; Phragmites dominates with some typha mixed in, especially to the east 1/4; 40 cm standing water
Phragmites	A07	Phrag	x	Phragmites; fairly dense, shallow standing water
MixedEm	A08	MixedE	not-*Phragmites*	Mixed emergent veg including scirpus, moss, shrubs and phragmites; Phragmites dominant on the south 1/4
Phragmites	A09	Typha	not-*Phragmites*	Phragmites; open water in south-bay; open water on east edge-inlet; typha mixed in south 1/4 of pixel
ForestD	B01	ForestD	not-*Phragmites*	Forest based on air photos and observation from the road - area was posted
ForestD	B02	Scrub	not-*Phragmites*	Forest based on air photos and observation from the road - area was posted
MixedEm	C01	Phrag	x	mostly mixed emergent, western 3/5 mown; eastern edge stands of spartina & Phragmites open water
Typha	C02	Phrag	x	Center (1/2) of pixel Typha in 30+cm of water, med density phragmites in west&sw 1/3 of pixel; open water in east fraction
Phragmites	C03	Phrag	x	Phragmite through the center 1/2 of the pixel in 15 cm of standing water; mixed emergent to the west 1/5 and some open water on the east edge; sheared vegetation at the waters edge - probably typha
MixedEm	C04	MixedE	not-*Phragmites*	Mixed emergent with some phragmites; some standing water in the northeast 1/5
Phragmites	C05	Phrag	*Phragmites*	Phragmites to the north, west and south; center of pixel has 50 cm of standing water and typha, water to the east with sheared typha
Water2	C06	Phrag	*Phragmites*	center 1/5 of pixel typha in standing water, lots of severed typha, mostly open water, moderate to low density Phragmites to the west edge
Phragmites	C07	Phrag	*Phragmites*	Phragmites through the center in 30 cm standing water with mixedEm to the west and open water to the east;
Typha	C08	Phrag	x	Typha in standing water, lot of sheared off stems, nw 1/3 of pixel open water

Appendix D- 2

Reference Classification	Point ID	Unsupervised Classification	Target Detection Classification	Sample Point Notes
Phragmites	C09	x	*Phragmites*	Phragmites to the south; grades into mixedEm to the west and north; denser stand to the extreme east edge
Phragmites	C10	Phrag	x	Phragmites throughout but grades into mixed emergent from just west of pixel center to west edge; 10 cm standing water
Phragmites	C11	Phrag	*Phragmites*	Phragmites moderate density to north west and south, some typha mixed in; standing water at the east edge and more typha in the mix; some bare soil in the southeast corner
Phragmites	C12	Phrag	x	Phragmites throughout but not very dense; some mown area; some open water where veg is gone from dragging in dock; some bare soil there as well; shallow standing water throughout
Phragmites	C13	Phrag	x	Eastern 1/3 sheared typha and open water; phargmites throughout the rest; mixed with typha in most areas; some phragmites matted and litter;
Phragmites	C14	Phrag	*Phragmites*	East to west swath about 20 m mown and now has quite a bit of standing water; dominant Phragmites throughout rest of pixel
Typha	C15	x	*Phragmites*	typha in standing water at edge of shore, lots of severed typha, data sheet shows phragmites to north, south and east
Phragmites	C16	Phrag	x	Phragmites throughout dense; very little standing water if any
Phragmites	C17	x	*Phragmites*	Bay in east 1/5 of pixel; Phragmites in 15 cm standing water moderate density with some typha and litter
Phragmites	C18	x	*Phragmites*	Phragmites north, south and west; some typha in deeper water to the east; a small area of mixed veg just south of center
Phragmites	C19	Phrag	*Phragmites*	Phragmites grades into mixed emergent to the west; water at extreme eastern edge; no standing water in most of area
MixedEm	C20	Phrag	x	mixed emergents including Phrag, Typha, and sedges; Large stand of Phragmites at the eastern edge
Phragmites	C21	x	*Phragmites*	Phragmites throughout with some typha mixed in the east and some small salix in the understory to the west
Water2	C22	x	*Phragmites*	about 1/3 of the pixel is phragmites in standing water, about 1/2 open water, remainder is typha
Phragmites	C23	x	*Phragmites*	Dense phragmites throughout, no standing water
Phragmites	C24	x	*Phragmites*	Phragmites throughout; density-5; no standing water or exposed soil
MixedEm	C25	x	*Phragmites*	center of pixel scirpus, typha, and sedges. / phragmites to the north, sparse phrag to the southeast, sparse phrag to the sw

Appendix D- 3

Reference Classification	Point ID	Unsupervised Classification	Target Detection Classification	Sample Point Notes
MixedEm	C26	Phrag	x	southern 1/2 is a backyard with large broadleaf trees; northern 1/2 is mown emergents
Impervious	C27	Scrub	not-*Phragmites*	Yard, house, road, trees, mown emergent veg at north edge
Impervious	C28	Imperv	not-*Phragmites*	Yard, house, road, trees, mown emergent veg North half
Scrub	C29	Scrub	not-*Phragmites*	Shrubs and grasses to the west; yard, outbuildings and house to the east
ForestD	D01	x	*Phragmites*	Quite mixed pixel at the end of line of trees, also area of grasses, forbs, emergent & shrubs and some open water
Water2	D02	Typha	not-*Phragmites*	Point in the middle of a shallow inlet about 25m wide; vegetation at the edges; some rushes
MixedEm	D03	Phrag	*Phragmites*	few phragmites, typha, sedges, mixed emergent, about 1/2 open water
Meadow	D04	Phrag	*Phragmites*	2/3 mixed calamagrostis, ?phalaris, very sparse typha; remaining 1/3 grasses, goldenrod, Phragmites & open water
MixedEm	D05	Meadow	not-*Phragmites*	Very mixed pixel; marginal call to mixed em; includes shallow open water to the east; meadow to the west and a mixed emergent band in the middle-each about equal proportions
Water2	D06	Phrag	x	western 3/5 of pixel shallow open water, narrow band of scirpus at waters edge and 1/5 of pixel grasses
Meadow	D07	x	*Phragmites*	dominated by calamagrostis, some typha no standing water, typha litter
Meadow	D08	Meadow	not-*Phragmites*	North half grasses, south half includes some typha; no standing water or exposed soil
Meadow	D09	x	*Phragmites*	predominantly grasses, meadow, with some typha mixed in a the center of the sampling unit, soggy ground
Meadow	D10	x	*Phragmites*	equally divided between grasses with a few goldenrod and typha, no standing water or bare soil
Typha	D11	ForestD	not-*Phragmites*	Typha except for eastern 1/8 meadow ; soggy throughout but no standing water
Meadow	D12	x	*Phragmites*	more than 1/2 grasses, typha area and mixed emergant areas make up rest of pixel
Typha	D13	ForestD	not-*Phragmites*	Typha throughout; wet but no standing water;
ForestD	D14	x	*Phragmites*	Deciduous canopy, semi open, shrub understory sparse, river at edge of pixel
Scrub	D15	Phrag	*Phragmites*	mixed pixel with meadow with shrubs at center, water at north edge and trees at edges east and west
Water2	D16	Water2	not-*Phragmites*	center was in water of Oconto river; south third emergent veg including salix and phragmites
Scrub	D17	Phrag	*Phragmites*	Sparse phragmites in north third, shrubs in center and trees to the south, water at north edge

Appendix D- 4

Reference Classification	Point ID	Unsupervised Classification	Target Detection Classification	Sample Point Notes
Scrub	D18	Phrag	*Phragmites*	shrubs, water at very north edge
MixedEm	D19	Phrag	*Phragmites*	mixed emergent with only edges of open water on one side and shrubs/trees on the other
Meadow	E01	Scrub	not-*Phragmites*	some wild rice, some typha stems; some burned area; some sparse phragmites and some Calamagrostis and Phalaris; standing water in some areas
Meadow	E02	x	*Phragmites*	grassy meadow mix, plowed land at edge, trees, and some sparse phragmites, originally called "other"
Meadow	E03	Meadow	not-*Phragmites*	Calamagrostis, (all dried stems) wet but no standing water; a few large trees to the north
Meadow	E04	Meadow	not-*Phragmites*	Calamagrostis(?), a stand of typha to the north east; wet but no standing water
Meadow	E05	Meadow	not-*Phragmites*	Mixture of Calamagrostis (?) Phalaris and rice grass; some typha to the far north and south east; a small area of corn to the south west
Meadow	E06	x	*Phragmites*	predominantly grasses with isolated areas of typha, phrag, and corn, soggy throughout
Meadow	E07	Meadow	not-*Phragmites*	mixed grasses (?Phalaris and Calamagrostis) throughout with typha mixed in the east half
Scrub	F01	ForestD	not-*Phragmites*	Shrubs throughout; up to 4 m tall; a few trees
Scrub	F02	Scrub	not-*Phragmites*	Scrub/shrub except for nw corner tussock sedge, soggy in the area of the sedges
Scrub	F03	Scrub	not-*Phragmites*	Scrub with a small area of grasses; shallow standing water or soggy throughout
Meadow	F04	Scrub	not-*Phragmites*	tough call between shrub and meadow; a few big trees
Scrub	G01	Scrub	not-*Phragmites*	broadleaf shrubs pretty dense with a few taller trees
ForestC	G02	x	*Phragmites*	Tree farm, tall pines with very little understory vegetation, small area of short (<5M) deciduous
ForestD	G03	ForestD	not-*Phragmites*	deciduous canopy shrubby underbrush; no standing water or exposed soil
ForestC	G04	ForestD	not-*Phragmites*	Conifer tree farm for bottom 3/5 ; mixed forest elsewhere
ForestC	G05	ForestD	not-*Phragmites*	Conifer tree farm for bottom 3/5 ; mixed forest elsewhere
other	G06	Phrag	x	1/3 road & gravelly sholder, 1/3 ditch with some water, 1/3 shrubs at edge of trees, shadows from trees
other	G07	Phrag	*Phragmites*	1/3 road & gravelly sholder, 1/3 ditch with some water, 1/3 shrubs at edge of trees, tree shadows
Meadow	G08	MixedE	not-*Phragmites*	mown grasses, large yard with a pond conifer tree farm to the east
ForestD	H01	ForestD	not-*Phragmites*	Deciduous with scrub understory
Scrub	H02	Scrub	not-*Phragmites*	tough call between shrub and d forest,
Scrub	H03	MixedE	not-*Phragmites*	Scrub and conifer to the north ; otherwise shrubs
ForestC	H04	x	*Phragmites*	Tree farm, tall pines with very little understory vegetation, somewhat open canopy

Appendix D- 5

Reference Classification	Point ID	Unsupervised Classification	Target Detection Classification	Sample Point Notes
Scrub	I01	ForestD	not-*Phragmites*	Salix and dogwood; some standing water, 10 cm standing water
ForestC	I02	ForestC	not-*Phragmites*	Conifer with fairly open canopy
Scrub	I03	ForestD	not-*Phragmites*	scrub mixed with trees
Meadow	I04	Meadow	not-*Phragmites*	tough call, someone's large yard with pond; shrubs to the east;
ForestD	J01	Scrub	not-*Phragmites*	Deciduous forest pretty open moss and litter undertory with a few shrubs
Phragmites	J02	x	*Phragmites*	very center mixed emergent; and just to the northwest of center grasses; otherwise Phragmites
Phragmites	J03	Phrag	*Phragmites*	Phragmites, not very dense, soggy to shallow standing water
MixedEm	J04	x	*Phragmites*	mixed emergent with a sparse mix of phragmites to the northwest
MixedEm	J05	Meadow	not-*Phragmites*	Carex stricta, some wetland grasses, some shrubs to the south east corner
MixedEm	J06	x	*Phragmites*	mixed emergent with a lot of exposed soil 3 or 4 cm of water, sparse phragmites shoots and litter from last year
MixedEm	J07	Phrag	x	mixed emergent vegetation including Scirpus, Carex and very sparse Phragmites
MixedEm	J08	Phrag	x	mixed emergent including Scirpus, other sedges, also Salix and some very sparse Phragmites
Meadow	J09	Imperv	not-*Phragmites*	Grasses throughout the center of the pixel with dense phragmites stands to the south and west edges,
Phragmites	J10	x	*Phragmites*	northwest 2/3 phragmites; grades into mixed emergent to the southeast
MixedEM	K01	Typha	not-*Phragmites*	mixed emergent including sparse typha and phrag, more phrag to the southeast and some typha w/o seed heads to the south
MixedEm	K02	Typha	not-*Phragmites*	generally mixed emergent with more typha to the north and some sparse phragmites to the east
Meadow	K03	Typha	not-*Phragmites*	Meadow with mixed emergents and some bare soil to the east 1/5; no standing water
Meadow	K04	Imperv	not-*Phragmites*	Meadow with some mixed emergent mixed no standing water
Phragmites	K05	Phrag	x	mixed throughout with 35% phrag 30% scrub and 30% typha
Phragmites	K06	Phrag	*Phragmites*	Phragmites in the western 2/3 typha and open water to the east
Typha	K07	Phrag	x	2/3 typha in standing water, far right edge open water, Phragmites to nw just less than 1/4 of pixel, to west and south edges of pixel
Typha	K08	Phrag	*Phragmites*	very mixed pixel, typha dominant in at least the center 1/2 of the pixel, dense Phragmites to the west, open water to east

Appendix D- 6

Reference Classification	Point ID	Unsupervised Classification	Target Detection Classification	Sample Point Notes
Phragmites	K09	Phrag	x	West edge Salix and sparse phrag., then a band of shallow water north to south with some phragmites Salix and emerg. veg., east 2/3 of pixel phragmites
MixedEm	K10	MixedE	not-*Phragmites*	Typha, Salix and other, wet but no standing water
Phragmites	K11	Phrag	x	Phragmites and typha mixed throughout most; very tall phragmites to the northeast corner
Typha	K12	Phrag	x	Typha, open water to the ne edge
Typha	K13	Phrag	*Phragmites*	typha dominant in center of pixel some open water the east, an area of phragmites to the north center of the pixel
Typha	K14	x	*Phragmites*	typha dominant, open water to the northeast corner of pixel, phragmites to the northwest, probably out of the pixel
Phragmites	K15	x	*Phragmites*	Tall phragmites throughout most with an understory of salix, some typha mixed in the south edge
Phragmites	K16	x	*Phragmites*	Generally tall phragmites with typha to the east and west central areas.
Water2	L01	Phrag	*Phragmites*	open water in the middle of the Pensaukee river
Water2	L02	Phrag	x	open water
Water2	L03	Phrag	x	open water with sliver of bank (Salix, trees, shrubs, some reeds)
Water2	L04	Phrag	x	open water with 1/5 pixel bank (Salix, sparse Phragmites)
Water2	L05	Phrag	x	1/2 open water, 1/2 someone's yard and house, road at so. Edge
Water2	L06	Phrag	*Phragmites*	open water in the middle of the Pensaukee river
Water2	L07	Phrag	x	open water with tree and rocks in nw corner
Water2	L08	Phrag	x	open water
Water2	L09	Water2	not-*Phragmites*	generally open water with a point of land with trees, bareground and some misc sparse veg.
Water2	L10	x	*Phragmites*	open water in the middle of the Pensaukee river
Phragmites	L11	ForestD	not-*Phragmites*	Phragmites for bottom 60% of pixel with 20 cm standing water, a band of typha to the north of that 10 m wide and then trees at the north edge of the pixel
Typha	L12	Scrub	not-*Phragmites*	Typha throughout with some of it laying down, Phragmites in the extreme southeast corner
Typha	L13	Phrag	x	Typha and typha litter, shallow standing water 10cm+/-
Typha	L14	Phrag	*Phragmites*	typha and open water, standing water 30 cm, Phragmites at extreme sw edge of sample
Phragmites	L15	x	*Phragmites*	Pretty dense stand of phragmties surrounded by water, some typha
Phragmites	L16	Phrag	*Phragmites*	Phragmites esp. to the south and west; typha with some phrag to the northeast and open shallow water to the east; phragmites again at the east edge
MixedEm	L17	Phrag	x	mixed emergent including Scirpus, sparse typha and salix, stand of Phragmites at north edge
MixedEm	L18	Scrub	not-*Phragmites*	Carex stricta with 10 cm standing water with a few scattered shrubs, concentration of shrubs to the northwest corner
MixedEm	L19	Scrub	not-*Phragmites*	Carex st., some shrubs scattered esp to the sw and se corners, tree in the far se corner